CAPITAL UNIVERSITY OF SCIENCE AND TECHNOLOGY, ISLAMABAD

Nanofluid Flow through Porous Medium over Stretching Sheet in the Presence of Joule Heating and Inclined Magnetic Field

by

Sajid Ali

A thesis submitted in partial fulfillment for the degree of Master of Philosophy

in the

Faculty of Computing
Department of Mathematics

2021

I am dedicating this heartfelt effort to my beloved family who supported me to conduct this research study and the respected teachers for helping and guiding me to make a final output.

CERTIFICATE OF APPROVAL

Nanofluid Flow through Porous Medium over Stretching Sheet in the Presence of Joule Heating and Inclined Magnetic Field

by

Sajid Ali

(MMT 173008)

THESIS EXAMINING COMMITTEE

S. No.	Examiner	Name	Organization
(a)	External Examiner	Dr. Khadija Maqbool	IIU, Islamabad
(b)	Internal Examiner	Dr. Shafqat Hussain	CUST, Islamabad
(c)	Supervisor	Dr. Dur-e-Shehwar Sagheer	CUST, Islamabad

Dr. Dur-e-Shehwar Sagheer
Thesis Supervisor
December, 2021

Dr. Muhammad Sagheer
Head
Dept. of Mathematics
December, 2021

Dr. Muhammad Abdul Qadir
Dean
Faculty of Computing
December, 2021

Author's Declaration

I, **Sajid Ali** hereby state that my M.Phil thesis titled "**Nanofluid Flow through Porous Medium over Stretching Sheet in the Presence of Joule Heating and Inclined Magnetic Field**" is my own work and has not been submitted previously by me for taking any degree from Capital University of Science and Technology, Islamabad or anywhere else in the country/abroad.

At any time if my statement is found to be incorrect even after my graduation, the University has the right to withdraw my M.Phil degree.

(Sajid Ali)

Registration No: MMT173008

Plagiarism Undertaking

I solemnly declare that research work presented in this thesis titled "**Nanofluid Flow through Porous Medium over Stretching Sheet in the Presence of Joule Heating and Inclined Magnetic Field**" is solely my research work with no significant contribution from any other person. Small contribution/help wherever taken has been duly acknowledged and that complete thesis has been written by me.

I understand the zero tolerance policy of the HEC and Capital University of Science and Technology towards plagiarism. Therefore, I as an author of the above titled thesis declare that no portion of my thesis has been plagiarized and any material used as reference is properly referred/cited.

I undertake that if I am found guilty of any formal plagiarism in the above titled thesis even after award of M.Phil Degree and the University reserves the right to withdraw/revoke my M.Phil degree and that HEC and the University have the right to publish my name on the HEC/University website on which names of students are placed who submitted plagiarized work.

(Sajid Ali)

Registration No: MMT173008

Acknowledgement

First, I would like to thank Almighty Allah for blessing me with knowledge and making it easier for me to pursue M.Phil study.

I am most sincerely and heartily grateful to my honorable supervisor, and my mentor **Dr. Dur-e-Shehwar Sagheer**, for her support throughout this research. I would like to express my deepest appreciation to her for the suggestions she has made to enhance the quality of this thesis. By working under her supervision, I have not just acquired technical knowledge but also learnet about being a good human. I also wish to thank her for always being there for discussions on this thesis despite her extremely busy schedule. I owe my profound gratitude to **Dr. Muhammad Sagheer** for his superb guidance and inexhaustible inspiration throughout this thesis. Without his tireless help, I would have not been able to commence this current research study. I am truly thankful to my teachers at Capital University of Science and Technology, **Dr. Rashid Ali**, **Dr. Abdul Rehman Kashif**, **Dr. Muhammad Afzal**, **Dr. Samina Rashid** and **Dr. Shafqat Hussain**. They are excellent teachers and I learnt a lot from them throughout the course of my M. Phil study. My most sincere and warm wishes to my friends especially university fellows **Raja Bilal Javed**, Qasim Mahmood, Haseeb Chohan and Faisal Mahmood who were always there as a source of encouragement for me. I am extremely grateful to my beloved parents, sisters, brother, wife and nephews for their love and prayers that always give me spiritual and moral support where I needed. The acknowledgement will surely remain incomplete if I don't express my deep indebtedness and cordial thanks to my friends for their valuable suggestions, guidance during my thesis.

(Sajid Ali)

Abstract

The main objective of this thesis is to examine the unsteady two-dimensional nanofluid flow over a vertical stretching permeable surface in the presence of an inclined magnetic field and non-uniform heat source/sink with Joule heating, viscous dissipation and porous medium. Four different types of nanoparticles, namely silver Ag, copper Cu, alumina Al_2O_3, and Titania TiO_2, are considered by using water as a base fluid with the Prandtl number. The governing partial differential equations are transformed to coupled non-linear ordinary differential equations by appropriate similarity transformation. Furthermore, the similarity equations are solved numerically by using the fourth-order Runge-Kutta integration scheme shooting method. A comparison of obtained numerical results is made with previously published results in some special cases, and excellent agreement is noted. Numerical results for velocity and temperature profiles and for various nanoparticles are discussed for various values of physical parameters.

Contents

List of Figures

List of Tables

Abbreviations

BC	Boundary Condition
BVP	Boundary Value Problem
Cu	Copper
IMF	Inclined Magnetic Field
IVP	Initial Value Problem
MHD	Magneto-hydrodynamic
NU	Non-Uniform
ODEs	Ordinary Differential Equations
PDEs	Partial Differential Equations
RK	Runge-Kutta

Symbols

A, B	The coefficient of space and temperature dependent heat source/sink
a, b, c	Constants
B_0	Magnetic field
C_p	Heat capacity at constant pressure
D_1, D_2, D_3	Constants
d	Permeability parameter
E_c	Eckert number
f	Similarity function
f_w	Mass transfer parameter, positive for suction/negative for injection
g	Acceleration due to gravity
k	The effective thermal conductivity
M	Magnetic parameter
P_r	Prandtl number
q'''	Non-uniform heat source/sink
S	Unsteadiness parameter
T	Temperature of the nanofluid
T_w	Surface temperature
T_∞	Ambient temperature
t	Time
u, v	Velocity components along x and y direction
U_w	Stretching velocity
V_w	Mass flux velocity
x, y	Cartesian coordinates

θ	Dimensionless temperature
ϕ	Nanoparticle volume fraction
η	Dimensionless similarity varible
ψ	Stream function
γ	Inclined angle of magnetic field
ν_f	Kinematic viscosity of fluid
λ	Buoyancy or convection parameter
β	Thermal expansion coefficient

Chapter 1

Introduction

The analysis of hydrodynamic flow and heat transfer over a stretching sheet has gained substantial attention owing to its extensive applications in industry and its influence to some technological processes. Sakiadis [1] laid foundation for such a problem by exploring the boundary layer fluid flow over a steady solid surface moving with a constant velocity. The study of thermal reaction was investigated by Erickson et al. [2] and analytically manifested by Tsou et al. [3]. Cran [4] augmented the work of Sakiadis [1] to the flow caused by an elastic sheet moving in its own plane with a velocity changing linearly with interval from an established point. Afterwords, a number of researchers [5–8] investigated the steady or unsteady boundary layer flow of Newtonian and non-Newtonian fluids over linear and nonlinear stretching planes.

The word "nano" anteceds to 1915 in the book "The World of Neglected Dimensions" by Oswald [9]. A distinct characteristic of the matter at nano-scale makes nanotechnology a novel research domain in the twenty-first century. In the last few decades, scientists and researchers all over the globe made effort to continuously work on various aspects of nanotechnology. A nanofluid is a fluid in which solid nanoparticles with length scales of 1-100 nm are contained in a basic heat transfer fluid. Thermal conductivity is strengthened by these nanoarticlesis and the base fluid's convective heat transfer coefficient considerably [10–12]. Oil, ethylene glycol, and water mixtures, for example, are poor heat transfer fluids

because their thermal conductivity affects the heat transfer coefficient between the heat transfer surface and the heat transfer medium. In 1995, Choi [13] came forth as a first person who used the term "nanofluid" to represent a fluid containing nanoparticles. Choi et al. [14] described that the addition of a mini amount (less than 1 percent by volume) of nanoparticles to conventional heat transfer liquids enlarged the thermal conductivity of the fluid up to two times approximately. Over the past twenty years, many research scholars studied various characteristics of heat transfer behavior of nanofluid and fluid flow [15–17] and established that enhanced heat transfer coefficient were attained with nanofluids.

Experimental studies [18, 19] exhibited that even with a minute volumetric fraction of nanoparticles (usually less than 5 percent), with an exceptional improvement in the convective heat transfer coefficient, the thermal conductivity of the base fluid is enhanced by 10-15 percent.In physics, chemistry, and engineering, the study of magnetic field effects is crucial. Many industrial types of equipment, such as the magneto hydrodynamic (MHD) generator, pumps, bearings, and boundary layer control, are affected by the interaction between the electrically conducting fluid and a magnetic field. Many researchers have recently investigated the impact of electrically conducting nanofluids in the presence of magnetic fields. Physics, chemistry, biomedical engineering, biosciences, and nuclear power plants all benefit from these investigations.

The unstable magnetic nanofluid behaviour of boundary layers along stationary or moving stretched permeable surfaces are one of the most fundamental and essential issues in this field. Daniel et al. [20] discussed the effects of twofold stratification on unsteady electrical MHD mixed convection nanofluid flow with viscous dissipation and Joule heating.

The flow of a nanofluid over an inclined vertical porous plate with radiation and heat generation/absorption was examined using MHD heat and mass transfer by Reddy et al. [21]. Prabhavathi et al. [22] and Sreedevi et al. [23] investigated the flow of MHD boundary layer heat and mass transfer around a vertical cone embedded in porous media filled with nanofluid. Hayat et al. [24] provided a numerical simulation of melting heat transfer and radiation effects in a

carbon-water nanofluid stagnation point flow. All of these investigations were focused on Newtonian fluid flows, whereas only the MHD non-Newtonian nanofluid flow caused by a stretched sheet was investigated by Madhu et al. [25], Hayat et al. [26], and Hsiao [27]. Eldabe and Abou-Zeid [28] developed a homotopy perturbation approach for MHD pulsatile non-Newtonian nanofluid flow with heat transfer via a non-Darcy porous medium with heat transfer through a non-Darcy porous medium. Sreedevi et al. [29] studied the effects of thermal radiation, chemical reaction and mass transmission of nanofluid through a linear and non-linear stretching surface. The same scientists recently performed magneto-hydrodynamic heat and mass transfer study of single and multi-wall carbon nanotubes along a vertical cone with convection [30]. Jyothi et al. [31] investigated the effect of a magnetic field and thermal radiation on the convective flow of SWCNTs-water and MWCNTs-water nanofluid between spinning stretchable discs under convective boundary conditions. The activation energy of a nanofluid flow in the presence of a chemical reaction and convective boundary conditions was investigated by Zeeshan et al. [32]. In the light of aforementioned investigations, it is clear that not a attempts has been made to explore inclined magnetohydrodynamic nanofluid transport with non-uniform heat source/sink, to the best of the authors' knowledge. The purpose of this research is to investigate the effects of nanoparticles on the heat transfer properties of a permeable unstable stretched sheet. In addition, the extra effects of a non-uniform heat source/sink and an inclined magnetic field are taken into account in this model. In the present study, the nanofluid model proposed by Tiwari and Das [33] was used, as this model successfully applied in several papers [34–36]. The governing partial differential equations are reduced to ordinary differential equations using an appropriate similarity transformation, and then numerically solved using the fourth-order Runge-Kutta integration scheme and the shooting method with the help of symbolic computational software MATLAB. In several situations, the derived numerical findings are compared to previously published data [37–39], and there is excellent agreement. The results are visually displayed, and the physical components of the problem are explored. The skin friction coefficient and the local Nusselt number at the stretched surface are also provided and explained in tabular form.

1.1 Thesis Contribution

In this thesis, a detailed review of Elgazery [40] is conducted and the results have been imitated by considering the additional effects of viscous dissipation, Joule's heating and porous medium.

1.2 Thesis Outline

A brief overview of the content of the thesis is provided as:

In Chapter 2, we explain few basic definitions and terminologies. Furthermore, some basic laws and dimensionless physical parameters are also included.

In Chapter 3 Elgazery [40], which considers a 2-dimensional unstable stretched surface with non-uniform heat source/sink in the presence of an angled magnetic field, is reviewed in detail.

In Chapter 4, we extend the model given in Elgazery [40] by considering the additional impact of viscous dissipation, Joule's heating and porous medium fluid in the momentum and energy equation. The obtained system of dimensionless ODEs is solved numerically by shooting method. The behavior of different physical parameters is explained through tables and graphs.

In Chapter 5, we recapitulate the thesis and give the conclusion from the whole work.

All the references used in this research work are listed in Bibliography.

Chapter 2

Basic Definitions and Governing Equations

This chapter addresses some basic concepts, definitions and governing laws related to the fluid dynamics. Dimensionless quantities are also discussed which seem to be helpful in the subsequent chapters. Moreover, a brief discussion has been done for the numerical methodology adopted for the solution of governing equations. A simple two-dimensional Poisson problem is also solved here to explain the numerical procedure for the achievement of results.

2.1 Basic Definitions

This section covers some fundamental fluid dynamics definitions. These concepts are used to describe the flow, heat transfer and influence of thermophysical properties that are used in next chapter.

Definition 2.1.1. (**Fluid**)
"Fluid is a substance that shows continuous deformation under the effect of shear stress." [41]

Definition 2.1.2. (**Fluid Mechanics**)
"Fluid mechanics is the study of fluids either in motion or at rest."[41]

Definition 2.1.3. (**Fluid Statics**)

"Fluid statics is that branch of fluid dynamics which focuses on the study of fluids at rest."[41]

Definition 2.1.4. (**Fluid Dynamics**)

"The branch of fluid mechanics that is concerned with motion of fluids from one place to another."[41]

Definition 2.1.5. (**Pressure**)

"The continuous physical force exerted on the unit area of surface is said to be pressure. It is expressed by P and mathematically, it can be written as

$$P = \frac{F}{A},$$

where F and A denote the applied physical force and area of the surface."[42]

Definition 2.1.6. (**Density**)

"Density is defined as mass per unit volume. It is represented by Greek letter ρ and mathematically, it is defined as

$$\rho = \frac{m}{V},$$

where m and V are the mass and volume of the substance, respectively."[42]

Definition 2.1.7. (**Viscosity**)

"Viscosity of a fluid is defined as the measure of resistance to steady distortion by shear/tensile stress. A notation used for viscosity is μ and its mathematical expression is,

$$\text{Viscosity}(\mu) = \frac{\text{Shear stress}}{\text{Rate of shear strain}},$$

where μ is called the coefficient of absolute viscosity/dynamics viscosity or simple viscosity. The dimension of viscosity is $\left[\frac{M}{LT}\right]$."[42]

Definition 2.1.8. (**Kinematic Viscosity**)

"It is defined as the ratio of the dynamic viscosity μ to the density ρ of the fluid. It is also referred as momentum diffusivity. It is denoted by Greek letter ν. Mathematically,

$$\nu = \frac{\mu}{\rho},$$

In SI system of units the unit of kinematic viscosity is $\frac{m^2}{s}$ and dimension is $[L^2T^{-1}]$." [42]

Definition 2.1.9. (**Nanofluids**)

"The nanofluid is defined as the homogeneous mixture of the base fluid and nanoparticles. The nanoparticles used in nanofluids are typically made of metals, oxides, copper, carbides or carbon nanotubes." [42]

2.2 Classification of Fluids

Fluids are basically divided into two main classes. These classes can be defined as follows.

Definition 2.2.1. (**Compressible and Incompressible Fluids**)

"A flow is incompressible in which the density remains constant within the fluid. Therefore, the volume of every portion of the fluid remain unchanged. Mathematically,

$$\frac{D\rho}{Dt} = 0,$$

where, ρ is the fluids density and $\frac{D}{Dt}$ is the material derivative. Mathematically, material derivative is given by

$$\frac{D}{Dt} = \frac{\partial}{\partial t} + V.\nabla, \tag{2.1}$$

In (2.1),V indicates the fluid's velocity and ∇ is the differential operator. In Cartesian coordinate system ∇ can be written as

$$\nabla = \frac{\partial}{\partial x}\widehat{i} + \frac{\partial}{\partial y}\widehat{j} + \frac{\partial}{\partial z}\widehat{k},$$

the flow is known to be incompressible if the fluid's density remains constant. Liquids are treated as incompressible." [43]

Definition 2.2.2. (**Newtonian and Non-Newtonian Fluids**)

"The fluids, which fulfill Newton's law of viscosity are known as Newtonian fluid. Newton's law is described mathematically as follows;

$$\tau_{yx} = \mu(\frac{du}{dx}), \tag{2.2}$$

where τ_{yx} is the shear stress and μ is called the constant of proportionality. The most common example of Newtonian fluids is water. Those fluids, which do not obey the Newton's law of viscosity are known as non-Newtonian fluids. For Non-Newtonian fluids,

$$\tau_{yx} = k(\frac{du}{dx})^n, \tag{2.3}$$

where $n \neq 1$ is flow behavior index. For $n = 1$ with $k = \mu$, the above equation reduce to the Newton's law of viscosity. Paints, blood, biological fluids and polymer melts, are good examples of non-Newtonian fluids."[43]

Definition 2.2.3. (**Real Fluid**)
"The fluids, which have non-zero viscosity are called real fluids. These fluids may be compressible or in-compressible. It depends upon the relationship between the shear stress and rate of shear strain."[43]

Definition 2.2.4. (**Flow**)
"It is the deformation of material under the influence of different forces. If this deformation increase continuously without any limit, then this process is known as flow."[43]

2.3 Types of Flows

Following are different types of fluid's flow depending upon its physics and status of channel.

Definition 2.3.1. (**Uniform and Non-Uniform Flows**)
"The flow, in which magnitude as well as the direction of the fluid velocity is the same at each points of the flow. In case of non-uniform flow, the velocity is not same at each point of the flow at any given instant."[43]

Definition 2.3.2. (**Steady and Unsteady Flows**)
"Fluid flows can be classified as steady or unsteady on the basis of fluid properties. The flow is said to be steady, if the fluid properties such as velocity and density

do not vary with time. Water flow with consistent release through a pipeline is an example of steady flow. Mathematically,

$$\frac{\partial B}{\partial t} = 0,$$

where B denotes any fluid property. On the other hand flow in which fluid properties change with time is known as unsteady flow. Water flow with varying release through a pipe is an example of unsteady flow. Mathematically, In this case,[43]

$$\frac{\partial B}{\partial t} \neq 0."$$

Definition 2.3.3. (**Laminar and Turbulent Flows**)
"A flow in which the particles of the fluid have specific path and individual particle does not intersect each other is known as laminar flow. In such flow, the particles move along well-defined path. The flow in which fluid particles have no specific paths and they move randomly is called turbulent flow."[43]

Definition 2.3.4. (**Internal Flow**)
"Internal flows are those where fluids flow through confined spaces, e.g., flow in pipe."[43]

Definition 2.3.5. (**External Flow**)
"The flow which is not confined by the solid surface, is known as external flow. The flow of water in the river is an example of the external flow."[43]

2.4 Mechanism of Heat Transfer

Heat is an important form of energy. It always transfers from hot region to cold region with or without the involvement of material medium. The ways through which it transfers from one body to another body are called "modes of heat transfer ". The common means for heat transfer are conduction, convection and radiation.These can be defined as given below:

Definition 2.4.1. (**Conduction**)
"Due to collision of molecules in contact form, heat is transferred from one objects

to another objects is called conduction. Such types of heat transfer occurs in the solid."[42]

For examples:

Picking up a hot cup of tea,

When a car is started, the engine heats up,

Conduction can be seen in a radiator.

Definition 2.4.2. (**Convection**)

"It is a mechanism in which heat transfer occurs due to the motion of molecules within the fluid such as air and water. A mathematical expression for convection phenomena is

$$q = hA(T_s - T_\infty), \tag{2.4}$$

where h, A, T_s and T_∞ denote the heat transfer coefficient, the area, the temperature of the surface and the temperature away from the surface respectively. Further, it is subdivided into the following three categories."[42] For examples:

Macaroni rising and falling in a pot of boiling water,

I'm drinking a steaming cup of tea. The steam demonstrates heat transfer into the atmosphere.

Definition 2.4.3. (**Natural Convection**)

"It is the process, in which heat transfer is caused by the temperature differences. It effects the density of the fluids and the fluid motion is not developed by an external source. It occurs only in the presence of gravitational force and also known as free convection."[42]

For examples:

- Sea breeze: This occurrence happens during the day. The light warms both the sea and the land,
- Land Breeze: This occurrence happens during the night when the situation reverses.

Definition 2.4.4. (**Forced Convection**)

"It is a type of heat transfer in which an external source is used to produce motion of the fluid. e.g. fan or a pump."[42]

For example on a hot summer day, using water heaters or geysers for quick water heating and using a fan.

Definition 2.4.5. (**Mixed Convection**)

"It is the combination of both forced convection and natural convection and both occur simultaneously."[42]

For example on a heated plate, a fan blows upward. Because heat rises naturally, The heat transfer is aided by the air being forced upward over the plate.

Definition 2.4.6. (**Radiation**)

"In radiation process, heat is transferred through electromagnetic rays and waves. It takes place in liquids and gasses.

An example of radiation would be atmosphere, the atmosphere is heated by the radiation of the sun."[42]

For examples:

Your stereo's sound waves,

A microwave oven produces microwaves,

Your cell phone emits electromagnetic radiation.

Definition 2.4.7. (**Thermal Conductivity**)

"It is the property of a substance which measures the ability to transfer heat. Fourier's law of conduction which relates the flow rate of heat by conduction to the temperature gradient is

$$\frac{dQ}{dt} = -kA\frac{dT}{dx},$$

where A, k, $\frac{dT}{dx}$ and $\frac{dQ}{dt}$ are the area, the thermal conductivity, the gradient and the rate of heat transfer, respectively. The SI unit of thermal conductivity is $\frac{Kgm}{s^3}$ and the dimension of thermal conductivity is $\left[\frac{ML}{T^3}\right]$."[42]

Definition 2.4.8. (**Thermal Diffusivity**)

"The ratio of the unsteady heat conduction k, of a substance to the product of specific heat capacity C_p and density ρ is called thermal diffusivity. It quantify the ability of a substance to transfer heat rather to store it. Mathematically, it can be written as

$$\alpha = \frac{k}{\rho C_p},$$

The unit and dimension of thermal diffusivity in SI system are $m^2 s^{-1}$ and $[LT^{-1}]$ respectively."[42]

Definition 2.4.9. (**Joule Heating**)

"It is the procedure in which heat is generated by passing an electric current through a conductor. It is also known as ohmic heating and resistive heating."[42]

Definition 2.4.10. (**Viscous Dissipation**)

"In viscous fluid flow, the viscosity of the fluid will take energy from the kinetic energy and transform it into internal energy of the fluids. This process is called viscous dissipation."[42]

Definition 2.4.11. (**Thermal Radiation**)

"The ejection of electromagnetic waves from the matters that have temperature higher than absolute zero is called thermal radiation."[42]

For example: Daily weather

Definition 2.4.12. (**Porous Medium**)

"A material containing the pores in it is called porous material or a porous medium. Pores are usually filled with fluid, i.e., liquid or gases. A porous medium is often considered by its porosity.

Many natural materials such as soil, rocks (e.g., aquifers, petroleum, zeo-lites), biological tissues (e.g., wood, bones, cork) and hand made substances such as ceramics and cements can be characterized as porous media."[42]

2.5 Dimensionless Numbers

In this section we will define some dimensionless numbers which are of significant importance for the problems discussed in chapter 3 and chapter 4.

Definition 2.5.1. (**Reynolds Number**)

"It is the ratio of inertial forces to viscous forces. The behavior of the different

kinds of flow will be identify like laminar or turbulent flow. Mathematically,

$$Re = \frac{\frac{\rho U^2}{L}}{\frac{\mu U}{L^2}}, \qquad \Rightarrow \qquad Re = \frac{LU}{\nu},$$

where U denotes the free stream velocity, L is the characteristics length and μ stands for kinematic viscosity."[44]

Definition 2.5.2. (**Prandtl Number**)

"The ratio of kinematic diffusivity to heat diffusivity is said to be prandtle number. It is denoted by P_r. Mathematically it can be written as

$$P_r = \frac{\nu}{\alpha} \quad \Rightarrow \quad \frac{\frac{\mu}{\rho}}{\frac{k}{C_p}} \quad \Rightarrow \quad \frac{\mu C_p}{k\rho},$$

where μ and α denote the momentum diffusivity or kinetic diffusivity and thermal diffusivity respectively. Here C_p denotes the specific heat and k stands for thermal conductivity. The Prandtl number named after the German physicist Ludwig Prandtl is used characteristics the regime of convection. "[44]

Definition 2.5.3. (**Nusselt Number**)

"It is the relationship between the convective to the conductive heat transfer through the boundary of the surface. It is a dimensionless number which was first introduced by the German mathematician Nusselt. Mathematically, it is defined as:

$$N_u = \frac{hL}{k},$$

where h stands for convective heat transfer, L stands for characteristics length and k stands for thermal conductivity. A large Nusselt number means very efficient. For example turbulent pipe flow yields No of order 100 to 1000 and Nusselt number of value one represent heat transfer by pure conduction."[44]

Definition 2.5.4. (**Schmidt Number**)

"Schmidt number (S_c) is a dimensionless number after Ernst Wilhelm Schmidt and characterized as the proportion of momentum diffusivity (viscosity) to mass diffusivity and is utilized to describe fluid flows in which there are simultaneous momentum and mass diffusion convection."[44]

Definition 2.5.5. (**Eckert Number**)

"It is the proportion of the kinetic energy dissipated in the flow to the thermal energy conducted into or away from the fluid."[44]

Definition 2.5.6. (**Skin Friction Coefficient**)

"Skin friction coefficient represents the value of friction which occurs when fluid moves across the surface. Mathematically

$$C_f = \frac{2T_{yx}}{\rho U_e^2},$$

where T_{yx} is the shear stress at the wall, ρ the density and U_e the free-stream velocity."[44]

Definition 2.5.7. (**Darcy Number**)

"The Darcy number D_a represents the effect of the permeability of medium according to its cross sectional area

$$Da = \frac{\kappa}{H^2},$$

where κ shows the permeability of porus medium and H is the length of prescribed geometry. It was first introduced by Henry Darcy. It is transformed by the non dimensionalizing the differential form of Darcy's law."[44]

2.6 Continuity Equation

"Continuity equation is derived from the law of conservation of mass and mathematically [45], it is expressed by

$$\frac{\partial \rho}{\partial t} + \nabla.(\rho V) = 0, \tag{2.5}$$

where t is the time. If fluid is an incompressible then the continuity equation is expressed by

$$\nabla.V = 0." \tag{2.6}$$

2.7 Law of Conservation of Momentum

"Each particle of fluid obeys Newtons second law of motion which is at rest or in steady state or accelerated motion. This law states that the combination of all applied external forces acting on a body is equal to the time rate of change of linear momentum of the body. In vector notation this law can be written as [46]

$$\rho\frac{dV}{dt} = \text{div}\tau + \rho\mathbf{b}, \tag{2.7}$$

for Navier-Stokes equation

$$\tau = -pI + \mu A_1, \tag{2.8}$$

where A_1 is the tensor and first time it was produced by Rivlin-Erickson.

$$A_1 = \text{gradV} + (\text{gradV})^t, \tag{2.9}$$

In the above equations, $\dfrac{d}{dt}$ denote material time derivative or total derivative, ρ denote density, V denote velocity field, τ the Cauchy stress tensor, b the body forces, p the pressure, μ the dynamic viscosity. The Cauchy stress tensor is expressed in the matrix form

$$\tau = \begin{bmatrix} \sigma_{xx} & \tau_{yx} & \tau_{zx} \\ \tau_{xy} & \sigma_{yy} & \tau_{zy} \\ \tau_{xz} & \tau_{yz} & \sigma_{zz} \end{bmatrix}, \tag{2.10}$$

where σ_{xx}, σ_{yy} and σ_{zz} are normal stresses, others wise the shear stresses. For two-dimensional flow, we have $V = [u(x, y, 0), v(x, y, 0), 0]$ and thus

$$\text{gradV} = \begin{bmatrix} \frac{\partial u}{\partial x} & \frac{\partial u}{\partial y} & 0 \\ \frac{\partial v}{\partial x} & \frac{\partial v}{\partial y} & 0 \\ 0 & 0 & 0 \end{bmatrix}, \tag{2.11}$$

$$\frac{\partial u}{\partial t} + u\frac{\partial u}{\partial x} + v\frac{\partial u}{\partial y} = -\frac{1}{\rho}\frac{\partial p}{\partial x} + v\left(\frac{\partial^2 u}{\partial x^2} + \frac{\partial^2 u}{\partial y^2}\right), \tag{2.12}$$

Similarly, we repeat the above process for Y component as follows:

$$\frac{\partial u}{\partial t} + u\frac{\partial u}{\partial x} + v\frac{\partial u}{\partial y} = -\frac{1}{\rho}\frac{\partial p}{\partial y} + v\left(\frac{\partial^2 u}{\partial x^2} + \frac{\partial^2 u}{\partial y^2}\right)." \tag{2.13}$$

2.8 Law of Conservation of Energy

"The law of conservation of energy states that the time rate of change of the total energy is equal to the sum of the rate of work done by the applied forces and change of heat content per unit time.

$$\frac{\partial \rho}{\partial t} + \nabla.\rho u = -\nabla.q + Q + \phi$$

where ϕ is a dissipation function."[45]

2.9 Solution Methodology

Shooting method [35] is used to solve the higher order nonlinear ordinary differential equations. To implement this technique, first convert the higher order ODEs to the system of first order ODEs. In the shooting method, first we assume the missing initial conditions and the differential equations are then integrated numerically through Runge-Kutta method as an initial value problem. The accuracy of the assumed missing initial condition is then checked by comparing the calculated values of the dependent variables at the terminal point with their given value there. If the boundary conditions are not fulfilled upto the required accuracy, with the new set of initial conditions, which are modified by Newton's method. The method is repeated again until the required accuracy is achieved. To explain the shooting method, we consider a general second order boundary value problem,

$$y'' = f(x, y, y'(x)), \tag{2.14}$$

subject to the boundary conditions

$$y(0) = 0, \qquad y(L) = A, \tag{2.15}$$

By denoting y by y_1 and y_1' by y_2, Eq. (2.14) can be written in the form of following system of first order equations

$$y_1' = y_2, \qquad y_1(0) = 0, \qquad y_2' = f(x, y_1.y_2), \qquad y_1(L) = A. \tag{2.16}$$

Denote the missing initial condition $y_2(0)$ by s, to have

$$y_1^{'} = y_2, \qquad y_1(0) = 0, \qquad y_2^{'} = f(x, y_1.y_2), \qquad y_2(0) = s. \tag{2.17}$$

Now the problem is to find s such that the solution of the IVP (2.17) satiates the boundary condition $y(L) = A$.

In other words, if the solutions of the initial value problem (2.17) are denoted by $y_1(x, s)$ and $y_2(x, s)$, one should search for that value of s which is an approximate root the equation.

$$y_1(L, s) - A = \phi(s) = 0, \tag{2.18}$$

To find an approximate root of the Eq. (2.18) by the Newton's method, the iteration formula is given by

$$s_{n+1} = s_n - \frac{\phi(s_n)}{\frac{d\phi(s_n)}{ds}}, \qquad n = 0, 1, 2, 3, ... \tag{2.19}$$

$$s_{n+1} = s_n - \frac{y_1(L, s_n) - A}{\frac{dy_1(L, s_n)}{ds}}, \tag{2.20}$$

To find the derivative of y_1 with respect of s, differentiate (2.17) with respect to s. For simplification, use the following notations

$$\frac{dy_1}{ds} = y_3, \qquad \frac{dy_2}{ds} = y_4, \tag{2.21}$$

This process results in the following IVP.

$$y_3^{'} = y_4, \qquad y_3(0) = 0, \qquad y_4^{'} = \frac{\partial f}{\partial y_1} y_3 + \frac{\partial f}{\partial y_2} y_4, \qquad y_4(0) = 1, \tag{2.22}$$

Now, solving the IVP Eq. (2.22), the value of y_3 at L can be computed. This value is actually the derivative of y_1 with respect to s computed at L. Setting the value of $y_3(L, s)$ in Eq. (2.20), the modified value of s can be achieved. This new value of s is used to solve the Eq. (2.17) and the process is repeated until the value of s is within a described degree of accuracy.

Chapter 3

Study of Nanofluid Flow over a Stretching Sheet with Inclined Magnetic Field and Non-Uniform Heat Source/Sink

3.1 Introduction

A detailed review of the work done by Elgazery [40] is presented here. The flow of nanofluids over a permeable unstable stretched surface with a non uniform heat source/sink in the presence of a magnetic field has been studied in this chapter.

Transformations of similarity are used to reduce the partial differential equation that governs into set of non-linear ordinary differential equation. These equations are then numerically solved using the shooting method, followed by the RK-4 and Newton methods using the MATLAB tool.

Finally, the numerical outcomes are discussed for different physical parameters causing impact on the heat. Graphs are represented to show the physical significance of distinct dimensionless quantities.

3.2 Mathematical Modeling

In this chapter, we suppose that the boundary layer flow is unsteady, laminar, incompressible, two-dimensional, and electrically conducting owing to a permeable stretching sheet that is vertical in the x direction. The flow is subjected to a uniform inclined magnetic field B_0 [47]. Along the x-axis, the application of an inclined magnetic field with an acute angle γ. The created magnetic field and viscous dissipation are also expected to have minimal effects. Convectional heat transfer is taken into consideration. The sheet's linear stretching as it moves in its own plane at the surface velocity creates the flow.

$$U_w\left(x,t\right)=\frac{xa}{1-ct}\ ,$$

where the constants a and c are both positive having dimension t^{-1} with $ct\leq 1$ and $c\geq 0$ [48].

$T_w\left(x,t\right)$ is the temperature at the sheet surface as a function of distance x and

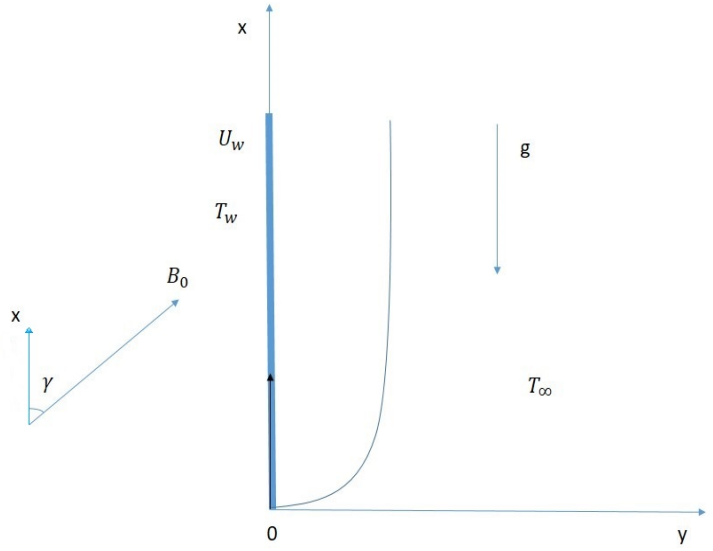

FIGURE 3.1: The coordinate system and physical model

time t, and its temperature T_∞ is higher than that of the surrounding fluid. Thermal equilibrium is also expected for the base fluid (water) and the nanoparticles, with no slide between them [48]. The thermophysical characteristics of water and

nanoparticles are listed in the table below.

TABLE 3.1: Thermophysical properties of water and nanoparticles

	$\rho(kg/m^3)$	$C_p(j/kgK)$	$k(W/mK)$	$\beta \times 10^{-5}(K^{-1})$
Pure water	997.1	4179	0.613	21
Copper(Cu)	8933	385	401	1.67
Silver(Ag)	10500	235	429	1.89
Alumina(Al_2O_3)	3970	765	40	0.85
Titanium oxide(TiO_2)	4250	686.2	8.9538	0.9

3.3 Governing Equations

The current flow and heat transfer for a nanofluid in the presence of an inclined magnetic field, as well as internal heat generation/absorption due to the Boussinesq approximations, can be described as:

Continuity equation:

$$\frac{\partial u}{\partial x} + \frac{\partial v}{\partial y} = 0 \tag{3.1}$$

Momentum equation:

$$\frac{\partial u}{\partial t} + u\frac{\partial u}{\partial x} + v\frac{\partial u}{\partial y} = \frac{\mu_{nf}}{\rho_{nf}}\frac{\partial^2 u}{\partial y^2} + g\frac{(\rho\beta)_{nf}}{\rho_{nf}}(T - T_\infty) - \frac{\sigma_{nf}}{\rho_{nf}}B_0^2 \sin^2\gamma u \tag{3.2}$$

Energy equation:

$$\frac{\partial T}{\partial t} + u\frac{\partial T}{\partial x} + v\frac{\partial T}{\partial y} = \alpha_{nf}\frac{\partial^2 T}{\partial y^2} + \frac{q'''}{(\rho C_P)_{nf}} \tag{3.3}$$

along with the initial and boundary conditions

$$\left.\begin{aligned} u &= u_w(x,t) = \frac{ax}{1-ct}, \\ v &= v_w(t) = -\sqrt{\frac{av_f}{1-ct}}f_w, \\ T &= T_\infty + \frac{bx}{(1-ct)^2} = T_{w(x,t)}, \quad \text{at} \quad y = 0, \\ u &= 0, \qquad T = T_\infty, \qquad\qquad \text{as} \quad y \to \infty \end{aligned}\right\} \tag{3.4}$$

where u represents velocity components in the x direction and v represents velocity components in the y directions. $f_w > 0$ and $f_w < 0$ are injection and suction parameters, respectively, while b is constant with a temperature/length dimension. Assisting and opposing flow is aspect field by the value $b > 0$ and $b < 0$ respectively. The dimension of b is temperature/length, In the absence of buoyancy force, $b = 0$ denotes the forced convection limit. Whereas ν_f is the kinematic viscosity of fluid.

3.4 Similarity Transformation

The following similarity variables are used to transform the partial differential equations into ordinary differential equations [40].

$$\psi(x,y,t) = \sqrt{\frac{a\nu_f}{(1-ct)}}xf(\eta), \qquad \eta = \sqrt{\frac{a}{\nu_f(1-ct)}}y,$$
$$\theta(\eta) = \frac{T-T_\infty}{T_w-T_\infty}, \qquad u = \frac{\partial\psi}{\partial y} = \frac{ax}{(1-ct)}f'(\eta),$$
$$v = -\frac{\partial\psi}{\partial x} = -\sqrt{\frac{a\nu_f}{1-ct}}f(\eta).$$

Some significant derivatives are calculated as follows:

- $\dfrac{\partial u}{\partial x} = \left(\dfrac{a}{1-ct}\right)f'$,
- $\dfrac{\partial v}{\partial y} = -\sqrt{\dfrac{a\nu_f}{1-ct}}f'(\eta)\dfrac{\partial}{\partial y}(\eta),$
$= -\sqrt{\dfrac{a\nu_f}{1-ct}}f'(\eta)\left(\sqrt{\dfrac{a}{\nu_f(1-ct)}}\right),$
$= -\sqrt{\dfrac{a}{1-ct}}f'(\eta)\left(\sqrt{\dfrac{a}{(1-ct)}}\right),$
$= -\dfrac{a}{1-ct}f'(\eta).$

The heat source/sink with non-uniform heat distribution is modeled [49] as $\left[q'''\right]$ as follow:

$$q''' = \frac{u_w(x)k_{nf}}{x\nu_{nf}}\left[A(T_w-T_\infty)f' + B(T-T_\infty)\right],$$

where A and B are the heat source/sink coefficients that are space and temperature dependent. Internal heat generation is represented by $A > 0$ and $B > 0$, internal heat absorption is represented by $A < 0$ and $B < 0$, respectively.

Continuity equation is trivially satisfied as follows:

- $$\frac{\partial u}{\partial x} + \frac{\partial v}{\partial y} = \frac{a}{1-ct} f^{'} + \left(-\frac{a}{1-ct} f^{'} \right),$$
$$\frac{\partial u}{\partial x} + \frac{\partial v}{\partial y} = \frac{a}{1-ct} f^{'} - \frac{a}{1-ct} f^{'},$$
$$\frac{\partial u}{\partial x} + \frac{\partial v}{\partial y} = 0.$$

For the conversion of momentum Eqs. (3.2), we proceed as follows:

- $$\frac{\partial u}{\partial t} = ax \frac{\partial}{\partial t} f^{'}(1-ct)^{-1},$$
$$= -axf^{'}(1-ct)^{-2}(-c) + ax(1-ct)^{-1} f^{''} \frac{\partial}{\partial t} \left(\sqrt{\frac{a}{\nu_f}} (1-ct)^{-\frac{1}{2}} \right) y,$$
$$= \frac{acxf^{'}}{(1-ct)^2} + \frac{axy}{(1-ct)} f^{''} \sqrt{\frac{a}{\nu_f}} \left((-\frac{1}{2})(1-ct)^{-\frac{3}{2}}(-c) \right),$$
$$= \frac{acxf^{'}}{(1-ct)^2} + \frac{acxy}{2(1-ct)^{\frac{5}{2}}} f^{''} \sqrt{\frac{a}{\nu_f}}.$$
- $$\frac{\partial u}{\partial x} = \frac{a}{1-ct} f^{'}.$$
- $$\frac{\partial u}{\partial y} = \frac{\partial}{\partial y} \left(\frac{ax}{(1-ct)} f^{'} \right),$$
$$= \frac{ax}{(1-ct)} f^{''} \frac{\partial}{\partial y} \left(\sqrt{\frac{a}{\nu_f(1-ct)}} y \right),$$
$$= \frac{ax}{(1-ct)} \sqrt{\frac{a}{\nu_f(1-ct)}} f^{''}.$$
- $$\frac{\partial^2 u}{\partial y^2} = \frac{ax}{(1-ct)} \sqrt{\frac{a}{\nu_f(1-ct)}} \frac{\partial}{\partial y} \left(f^{''} \right),$$
$$= \frac{ax}{(1-ct)} \sqrt{\frac{a}{\nu_f(1-ct)}} f^{'''} \frac{\partial}{\partial y} \left(\sqrt{\frac{a}{\nu_f(1-ct)}} y \right),$$
$$= \frac{ax}{(1-ct)} \sqrt{\frac{a}{\nu_f(1-ct)}} f^{'''} \sqrt{\frac{a}{\nu_f(1-ct)}},$$

$$= \frac{ax}{(1-ct)}\left(\frac{a}{\nu_f(1-ct)}\right) f''',$$
$$= \frac{a^2x}{\nu_f(1-ct)^2} f'''.$$

- $$\frac{\partial u}{\partial x} = \left(\frac{a}{(1-ct)} x f'\right)\left(\frac{a}{1-ct} f'\right),$$
$$= \frac{a^2}{(1-ct)^2} x\,(f')^2.$$

$$v\frac{\partial u}{\partial y} = \left(-\sqrt{\frac{a\nu_f}{1-ct}} f\right)\left(\frac{ax}{(1-ct)}\sqrt{\frac{a}{\nu_f(1-ct)}} f''\right),$$

- $$v\frac{\partial u}{\partial y} = -\frac{xa^2}{(1-ct)^2} f f''.$$

By using above derivatives, the dimensionless form of the L.H.S of (3.2) becomes:

- $$\frac{\partial u}{\partial t} + u\frac{\partial u}{\partial x} + v\frac{\partial u}{\partial y} = \frac{acx}{(1-ct)^2} f' + \frac{acxy}{2(1-ct)^{\frac{5}{2}}} f''\sqrt{\frac{a}{\nu_f}}$$
$$+ \frac{a^2x}{(1-ct)^2}(f')^2 - \frac{xa^2}{(1-ct)^2} f f'',$$

$$\frac{\partial u}{\partial t} + u\frac{\partial u}{\partial x} + v\frac{\partial u}{\partial y} = \frac{xa}{(1-ct)^2}\left[c\left(f' + \frac{\eta}{2} f''\right) + a\left((f')^2 - f f''\right)\right]. \quad (3.5)$$

Likewise the R.H.S is as follow:

- $$\frac{\mu_{nf}}{\rho_{nf}}\frac{\partial^2 u}{\partial y^2} + g\frac{(\rho\beta)_{nf}}{\rho_{nf}}(T - T_\infty) - \frac{\sigma_{nf}}{\rho_{nf}} B_0^2 u \sin^2\gamma = \frac{\mu_{nf}}{\rho_{nf}}\frac{a^2x}{\nu_f(1-ct)^2} f'''$$
$$+ g\frac{(\rho\beta)_{nf}}{\rho_{nf}}\theta(T - T_\infty) - \frac{\sigma_{nf}}{\rho_{nf}} B_0^2 \sin^2\gamma \frac{ax}{(1-ct)} f',$$

$$= \frac{a^2x\mu_{nf}}{\rho_{nf}\nu_f(1-ct)^2} f''' + \frac{bxg(\rho\beta)_{nf}}{(1-ct)^2\rho_{nf}}\theta - \frac{axB_0^2\sigma_{nf}}{(1-ct)\rho_{nf}} \sin^2\gamma f'. \quad (3.6)$$

From (3.5) and (3.6) we get:

- $$\frac{a^2x}{(1-ct)^2}\left[\frac{\mu_{nf}}{\rho_{nf}\nu_f} f''' + \frac{(\rho\beta)_{nf}}{a^2\rho_{nf}} gb\theta - \frac{\sigma_{nf}}{a\rho_{nf}} B_0^2(1-ct) f' \sin^2\gamma\right]$$
$$= \frac{ax}{(1-ct)^2}\left[cf' + \frac{c}{2}\eta f'' + a(f')^2 - a f f''\right]$$

$$\Rightarrow \quad \frac{c}{a}(f' + \frac{\eta}{2} f'') + (f')^2 - f f'' = \frac{\mu_{nf}}{\rho_{nf}\nu_f} f''' + \frac{(\rho\beta)_{nf}}{a^2\rho_{nf}} gb\theta$$
$$- \frac{\sigma_{nf}}{a\rho_{nf}} B_0^2(1-ct) f' \sin^2\gamma,$$

$$\Rightarrow \quad \frac{\rho_{nf}\nu_f}{\mu_{nf}}\left[s(f'+\frac{\eta}{2}f'')+(f')^2-ff''\right]=f'''+\frac{(\rho\beta)_{nf}\nu_f}{a^2\mu_{nf}}gb\theta - \frac{\sigma_{nf}\nu_f}{a\mu_{nf}}B_0^2(1-ct)f'\sin^2\gamma,$$

$$\Rightarrow \quad f'''+\frac{\rho_{nf}\nu_f}{\mu_{nf}}ff''-\frac{\rho_{nf}\nu_f}{\mu_{nf}}(f')^2-\frac{\rho_{nf}\nu_f}{\mu_{nf}}s(f'+\frac{\eta}{2}f'')+\frac{(\rho\beta)_{nf}\nu_f}{a^2\mu_{nf}}gb\theta - \frac{\sigma_{nf}\nu_f}{a\mu_{nf}}B_0^2(1-ct)f'\sin^2\gamma=0,$$

$$\Rightarrow \quad f'''+\frac{(1-\phi)^{2.5}}{\mu_f}\left[\left((1-\phi)\rho_f+\phi\rho_p\right)\nu_f ff''-\left((1-\phi)\rho_f+\phi\rho_p\right)\nu_f(f')^2 - \left((1-\phi)\rho_f+\phi\rho_p\right)\nu_f s(f'+\frac{\eta}{2}f'')+\frac{\left((1-\phi)(\rho\beta)_f+\phi(\rho\beta)_p\right)gb\nu_f}{a^2}\theta - \frac{((1-\phi)\sigma_f+\phi\sigma_p)\nu_f}{a}B_0^2(1-ct)f'\sin^2\gamma\right]=0,$$

$$\Rightarrow \quad f'''+(1-\phi)^{2.5}\left((1-\phi)+\phi\frac{\rho_p}{\rho_f}\right)ff''-\left((1-\phi)+\phi\frac{\rho_p}{\rho_f}\right)(f')^2 - s\left((1-\phi)+\phi\frac{\rho_p}{\rho_f}\right)\left(f'+\frac{\eta}{2}f''\right)+\frac{(1-\phi)(\rho\beta)_f+\phi(\rho\beta)_p}{a^2\rho_f}gb\theta - \frac{\sigma_{nf}}{a\rho_f}B_0^2(1-ct)f'\sin^2\gamma=0,$$

$$\Rightarrow \quad f'''+(1-\phi)^{2.5}\left[D_1ff''-D_1(f')^2-D_1s\left(f'+\frac{\eta}{2}f''\right) + (\rho\beta)_f\left((1-\phi)+\phi\frac{(\rho\beta)_p}{(\rho\beta)_f}\right)\frac{gb\theta}{a_2\rho_f}-\frac{\sigma_{nf}}{a\rho_f}B_0^2(1-ct)f'\sin^2\gamma\right]=0.$$

Now finally the dimensionless form of (3.2) is:

$$f'''+(1-\phi)^{2.5}\left[D_1\left(ff''-\left(f'\right)^2-s\left(f'+\frac{\eta}{2}f''\right)\right)+\lambda D_2\theta-Mf'\sin^2\gamma\right]=0,$$

To convert the energy equation (3.3) into an ordinary differential equation, we first calculate the following derivative [45]:

- $\theta(\eta)=\dfrac{T-T_\infty}{T_w-T_\infty}$,
  $\Rightarrow \quad T=T_\infty+(T_w-T_\infty)\theta$
  $\Rightarrow \quad T=T_\infty+\dfrac{bx}{(1-ct)^2}\theta.$
- $\dfrac{\partial T}{\partial x}=\dfrac{b}{(1-ct)^2}\theta.$
- $\dfrac{\partial T}{\partial y}=\dfrac{bx}{(1-ct)^2}\theta'\sqrt{\dfrac{a}{(1-ct)\nu_f}}.$
- $\dfrac{\partial^2 T}{\partial y^2}=\dfrac{abx}{\nu_f(1-ct)^3}\theta''.$
- $\dfrac{\partial T}{\partial t}=\dfrac{\partial}{\partial t}\left(\dfrac{bx}{(1-ct)^2}\theta\right),$
  $=\dfrac{2bcx}{(1-ct)^3}\theta+\dfrac{bxy}{(1-ct)^2}\theta'\dfrac{\partial}{\partial t}\sqrt{\dfrac{a}{\nu_f(1-ct)}}y,$

$$= \frac{2bcx}{(1-ct)^3}\theta + \frac{bcxy}{2(1-ct)^{\frac{7}{2}}}\theta'\sqrt{\frac{a}{\nu_f}},$$
$$= \frac{bcx}{(1-ct)^2}\left(2\theta + \frac{y}{2}\theta'\sqrt{\frac{a}{\nu_f(1-ct)}}\right).$$

- $\frac{\partial T}{\partial x} = \frac{\partial}{\partial x}\left(\frac{bx}{(1-ct)^2}\theta\right),$
$= \frac{b\theta}{(1-ct)^2}.$

- $\frac{\partial T}{\partial y} = \frac{\partial}{\partial y}\left(\frac{bx}{(1-ct)^2}\theta\right),$
$= \frac{bx}{(1-ct)^2}\theta'\frac{\partial}{\partial y}\sqrt{\frac{a}{\nu_f(1-ct)}}y,$
$= \frac{bx}{(1-ct)^2}\theta'\sqrt{\frac{a}{\nu_f(1-ct)}}.$

- $\frac{\partial^2 T}{\partial y^2} = \frac{bx}{(1-ct)^2}\theta''\sqrt{\frac{a}{\nu_f(1-ct)}}\frac{\partial}{\partial y}\left(\sqrt{\frac{a}{\nu_f(1-ct)}}y\right),$
$= \frac{abx}{\nu_f(1-ct)^3}\theta''.$

- $\frac{\mu_{nf}}{\nu_{nf}} = \rho_{nf},$
$\frac{1}{\nu_{nf}} = \frac{\rho_{nf}}{\mu_{nf}},$
$\frac{\nu_f}{\nu_{nf}} = \frac{\nu_f\rho_{nf}}{\mu_{nf}},$
$= \frac{\nu_f\left[(1-\phi)\rho_f + \phi\rho_p\right](1-\phi)^{2.5}}{\mu_f},$
$= \frac{\nu_f(1-\phi)^{2.5}}{\mu_f}\rho_f\left[(1-\phi) + \phi\frac{\rho_p}{\rho_f}\right],$
$= \frac{\mu_f(1-\phi)^{2.5}\rho_f}{\rho_f\mu_f}D_1,$
$= D_1(1-\phi)^{2.5}.$

- $\frac{\nu_f}{\alpha_{nf}} = \nu_f\frac{(\rho C_p)_{nf}}{k_{nf}}$
$= \nu_f\frac{(\rho C_p)_{nf}}{D_3k_f},$
$= \frac{\nu_f}{D_3k_{nf}}\left[(1-\phi)(\rho C_p)_f + \phi(\rho C_p)_p\right],$
$= \frac{\nu_f}{D_3k_f}(\rho C_p)_f\left[(1-\phi) + \phi\frac{(\rho C_p)_p}{(\rho C_p)_f}\right],$
$= \frac{P_rD_2}{D_3}.$

Hence dimensionless form of (3.3) becomes:

- $$\frac{\partial T}{\partial t}+u\frac{\partial T}{\partial x}+v\frac{\partial T}{\partial y}=\frac{bcx}{(1-ct)^3}\left(2\theta+\frac{y}{2}\theta^{'}\sqrt{\frac{a}{\nu_f(1-ct)}}\right)$$
$$+\left(\frac{ax}{1-ct}\right)\left(\frac{b\theta}{(1-ct)^2}\right)f^{'}-\left(\sqrt{\frac{a\nu_f}{(1-ct)}}f\right)\left(\frac{bx\theta^{'}}{(1-ct)^2}\sqrt{\frac{a}{\nu_f(1-ct)}}\right),$$
$$\Rightarrow\ \frac{\partial T}{\partial t}+u\frac{\partial T}{\partial x}+v\frac{\partial T}{\partial y}=\frac{bx}{(1-ct)^3}\left[c\left(2\theta+\frac{\eta}{2}\theta^{'}\right)+af^{'}\theta-af\theta^{'}\right] \quad (3.7)$$

Similarly R.H.S of (3.3), can be formulated as

$$\frac{abx\alpha_{nf}\theta^{''}}{\nu_f(1-ct)^3}+\frac{axk_{nf}}{x\nu_{nf}(\rho C_p)_{nf}(1-ct)}\left[A(T_w-T_\infty)f^{'}+B(T-T_\infty)\right] \quad (3.8)$$

From (3.7) and (3.8) we get:

- $$\frac{abx\alpha_{nf}}{\nu_f(1-ct)^3}\left[\theta^{''}+\frac{k_{nf}(T_w-T_\infty)}{x\nu_{nf}}(Af^{'}+B\theta)\frac{(1-ct)^2\nu_f}{b\alpha_{nf}(\rho C_p)_{nf}}\right]$$
$$=\frac{bx}{(1-ct)^3}\left[c(2\theta+\frac{\eta}{2}\theta^{'})+af^{'}\theta-af\theta^{'}\right],$$
$$\Rightarrow\quad\frac{a\alpha_{nf}}{\nu_f}\left[\theta^{''}+\frac{(1-ct)^2bxk_{nf}}{x(1-ct)^2\nu_{nf}}(Af^{'}+B\theta)\frac{\nu_f}{b\alpha_{nf}(\rho C_p)_{nf}}\right]$$
$$=c\left(2\theta+\frac{\eta}{2}\theta^{'}\right)+a\left(f^{'}\theta-f\theta^{'}\right),$$
$$\Rightarrow\quad\theta^{''}+\frac{k_{nf}}{\nu_{nf}}(Af^{'}+B\theta)\frac{\nu_f}{\alpha_{nf}(\rho C_p)_{nf}}=\frac{\nu_f}{\alpha_{nf}}\left[\frac{c}{a}(2\theta+\frac{\eta}{2}\theta^{'})+\theta f^{'}-\theta^{'}f\right],$$
$$\Rightarrow\quad\theta^{''}+(Af^{'}+B\theta)\frac{\nu_f\alpha_{nf}(\rho C_p)_{nf}}{\alpha_{nf}(\rho C_p)_{nf}\nu_{nf}}=\frac{\nu_f}{\alpha_{nf}}\left[\frac{c}{a}(2\theta+\frac{\eta}{2}\theta^{'})+\theta f^{'}-\theta^{'}f\right],$$
$$\Rightarrow\quad\theta^{''}+\frac{\nu_f}{\nu_{nf}}(Af^{'}+B\theta)=\frac{\nu_f}{\alpha_{nf}}\left[\frac{c}{a}(2\theta+\frac{\eta}{2}\theta^{'})+\theta f^{'}-\theta^{'}f\right],$$
$$\Rightarrow\quad\theta^{''}+D_1(1-\phi)^{2.5}(Af^{'}+B\theta)+\frac{P_rD_2}{D_3}\left[f\theta^{'}-f^{'}\theta-s(2\theta+\frac{\eta}{2}\theta^{'})\right]=0.$$

The procedure of converting boundary conditions into dimensionless form has been discussed below:

- $u=U_w(x,t)=\frac{ax}{1-ct},\quad$ at $\quad y=0$
$u=\frac{ax}{1-ct}f^{'}(\eta),$
$\Rightarrow\quad\frac{ax}{1-ct}f^{'}(\eta)=\frac{ax}{1-ct},$
$\Rightarrow\quad f^{'}(\eta)=1,\quad$ at $\quad\eta=0$
- $T=T_w=T_\infty+\frac{bx}{(1-ct)^2},\quad$ at $\quad y=0$
$\theta(\eta)=\frac{T-T_\infty}{T_w-T_\infty},$
$\Rightarrow\quad T-T_\infty=\frac{bx}{(1-ct)^2},$
$\Rightarrow\quad\theta(\eta)\,(T_w-T_\infty)=T-T_\infty,$

$$\Rightarrow \quad \theta(\eta)\,(T_w - T_\infty) = \frac{bx}{(1-ct)^2},$$
$$\Rightarrow \quad \theta(\eta)(\frac{bx}{(1-ct)^2}) = \frac{bx}{(1-ct)^2},$$
$$\Rightarrow \quad \theta(\eta) = 1, \quad \text{at} \quad \eta = 0$$

- $\nu = \nu_w(t) = -\sqrt{\frac{a\nu_f}{1-ct}} f_w, \quad \text{at} \quad y = 0$
  $\nu = -\frac{\partial \psi}{\partial x} = -\sqrt{\frac{a\nu_f}{1-ct}} f(\eta),$
  $\Rightarrow \quad -\sqrt{\frac{a\nu_f}{1-ct}} f(\eta) = -\sqrt{\frac{a\nu_f}{1-ct}} f_w,$
  $\Rightarrow \quad f(\eta) = f_w, \quad \text{at} \quad \eta = 0$

- $u = 0, \quad \text{at} \quad y = \infty$
  $\Rightarrow \quad \frac{ax}{1-ct} f'(\eta) = 0,$
  $\Rightarrow \quad f' = 0 \quad \text{at} \quad \eta = \infty$

- $T = T_\infty, \quad \text{at} \quad y = \infty$
  $\Rightarrow \quad \theta(\eta) = \frac{T_\infty - T_\infty}{T_w - T_\infty},$
  $\Rightarrow \quad \theta(\eta) = 0, \quad \text{at} \quad y = \infty$

Finally, the following ordinary differential equations is obtained:

$$f''' + (1-\phi)^{2.5}\left[D_1(ff'' - (f')^2 - s(f' + \frac{\eta}{2}f'')) + \lambda D_2\theta - Mf' \sin^2\gamma\right] = 0. \quad (3.9)$$

$$\theta'' + D_1(1-\phi)^{2.5}(Af' + B\theta) + \frac{P_r D_2}{D_3}\left[f\theta' - f'\theta - s(2\theta + \frac{\eta}{2}\theta')\right] = 0, \quad (3.10)$$

with the boundary conditions:

$$\left.\begin{aligned} f' = 1, \quad f = f_w, \quad \theta = 1, \quad \text{at} \quad \eta = 0, \\ f' = 0, \quad \theta = 0, \quad \text{at} \quad \eta \to \infty. \end{aligned}\right\} \quad (3.11)$$

The following expression refers to different parameters used in the above equations [40]:

$$P_r = \frac{(\rho C_p)_f \nu_f}{k_f}, \qquad M = \frac{\sigma_{nf} B_0^2}{a\rho_f}(1-ct),$$
$$S = \frac{c}{a}, \qquad \lambda = \frac{gb(\rho\beta)_f}{a^2\rho_f}.$$

Here, M is the magnetic field parameter, P_r is the prandtl number, S is the unsteadiness parameter and λ is the buoyancy or convection parameter. Also, $\lambda > 0$ and $\lambda < 0$ correspond to assisting and opposing flow while $\lambda = 0$ is for forced convection flow situation.

D_1, D_2 and D_3 are constants given by:

$$D_1 = (1-\phi) + \frac{\rho_p}{\rho_f}\phi, \qquad D_2 = (1-\phi) + \frac{(\rho C_p)_p}{(\rho C_p)_f}\phi,$$
$$D_3 = \frac{k_{nf}}{k_f}.$$

3.5 Thermophysical Properties of Nanofluid

The heat capacity of the nanofluid C_p , electrical conductivity σ_{nf}, density of the nanofluid ρ_{nf}, thermal diffusivity α_{nf} and the thermal expansion coefficient β are presented as follows, respectively [40]

$$\rho_{nf} = (1-\phi)\rho_f + \phi\rho_p, \qquad \sigma_{nf} = (1-\phi)\sigma_f + \phi\sigma_p,$$
$$(\rho C_p)_{nf} = (1-\phi)(\rho C_p)_f + \phi(\rho C_p)_p, \qquad \alpha_{nf} = \frac{k_{nf}}{(\rho C_p)_{nf}},$$
$$(\rho\beta)_{nf} = (1-\phi)(\rho\beta)_f + \phi(\rho\beta)_p,$$
$$\mu_{nf} = \frac{\mu_f}{(1-\phi)^{2.5}}, \qquad \nu_f = \frac{\mu_f}{\rho_f}.$$

3.6 Solution Methodology

To find the numerical solution (3.9) and (3.10) equations are first converted into first order differential equations with corresponding boundary conditions and can be solution obtained by shooting technique. We must choose a suitably finite value of η in this method. Two convert (3.9) and (3.10) into system of first order ODE's the following notations are opted:

$$f = y_1, \quad f' = y_1', \quad f''' = y_3', \quad \theta = y_4, \quad \theta'' = y_5',$$

Further denote

$$f = y_1, \quad y_1^{'} = y_2, \quad y_2^{'} = y_3, \quad f^{'''} = y_3^{'}, \quad \theta = y_4, \quad y_4^{'} = y_5, \quad \theta^{''} = y_5^{'}.$$

As consequence of above notations the following system of ODE,s is acquired:

$$\left.\begin{aligned}
y_1^{'} &= y_2, && y_1(0) = f_w,\\
y_2^{'} &= y_3, && y_2(0) = 1,\\
y_3^{'} &= -(1-\phi)^{2.5}\left[D_1(y_1y_3 - y_2^2 - s(y_2 + \frac{\eta}{2}y_3))\right.\\
&\quad \left. + D_2\lambda y_4 - M\sin^2\gamma y_2\right], && y_3(0) = p,\\
y_4^{'} &= y_5, && y_4(0) = 1,\\
y_5^{'} &= -(1-\phi)^{2.5}D_1(Ay_2 + By_4) - \frac{P_rD_2}{D_3}\left[y_1y_5\right.\\
&\quad \left. - y_2y_4 - s(\frac{\eta}{2}y_5 + 2y_4)\right], && y_5(0) = q,
\end{aligned}\right\} \tag{3.12}$$

In order to achieve approximate numerical results, (3.12) is solved by RK-4 method. The domain of our problem is considered to be bounded $[0, \eta_\infty]$,

where η_∞ is a positive number for which the variation in the behavior of flow is negligible after $\eta = \eta_\infty$. p and q are assumed as missing conditions for the solution of (3.12) such that:

$$\left.\begin{aligned} y_2(\eta_\infty, p, q) &= 0\\ y_4(\eta_\infty, p, q) &= 0. \end{aligned}\right\} \tag{3.13}$$

To update the values of p and q, Newton's iterative scheme has been used which has the following formula:

$$\begin{bmatrix} p_{n+1}\\ q_{n+1}\end{bmatrix} = \begin{bmatrix} p_n\\ q_n\end{bmatrix} - \begin{bmatrix} \frac{\partial y_2}{\partial p} & \frac{\partial y_2}{\partial q}\\ \frac{\partial y_4}{\partial p} & \frac{\partial y_4}{\partial q}\end{bmatrix}^{-1}_{(p_n,q_n)} \begin{bmatrix} y_2(\eta_\infty, p_n, q_n)\\ y_4(\eta_\infty, p_n, q_n)\end{bmatrix}, \qquad n = 0, 1, 2... \tag{3.14}$$

to start the iterative process, choose $p = p_0$, $q = q_0$.

To incorporate Newton's method, we further use the following notations:

$$\left.\begin{array}{lll} \dfrac{\partial y_1}{\partial p} = y_6, & \dfrac{\partial y_2}{\partial p} = y_7, & \dfrac{\partial y_3}{\partial p} = y_8, \\ \dfrac{\partial y_4}{\partial p} = y_9, & \dfrac{\partial y_5}{\partial p} = y_{10}, & \\ \dfrac{\partial y_1}{\partial q} = y_{11}, & \dfrac{\partial y_2}{\partial q} = y_{12}, & \dfrac{\partial y_3}{\partial q} = y_{13}, \\ \dfrac{\partial y_4}{\partial q} = y_{14}, & \dfrac{\partial y_5}{\partial q} = y_{15}, & \end{array}\right\} \tag{3.15}$$

Newton's formula takes the following form after using the new notation:

$$\begin{bmatrix} p_{n+1} \\ q_{n+1} \end{bmatrix} = \begin{bmatrix} p_n \\ q_n \end{bmatrix} - \begin{bmatrix} y_7 & y_{12} \\ y_9 & y_{14} \end{bmatrix}^{-1}_{(p_n, q_n)} \begin{bmatrix} y_2(\eta_\infty, p_n, q_n) \\ y_4(\eta_\infty, p_n, q_n) \end{bmatrix} \tag{3.16}$$

Differentiating equations (3.12), first w.r.t. p and then w.r.t. q, we get the following ten first order ODEs along with the associated initial conditions.

$$\begin{aligned}
y_6^{'} &= y_7, && y_6(0) = 0, \\
y_7^{'} &= y_8, && y_7(0) = 0 \\
y_8^{'} &= -(1-\phi)^{2.5}\,[D_1\,(y_1 y_8 + y_3 y_6 - 2y_2 y_7 \\
&\quad -s(y_7 + \frac{\eta}{2} y_8)\Big) + D_2 \lambda y_9 - M \sin^2\gamma y_7\Big], && y_8(0) = 1, \\
y_9^{'} &= y_{10}, && y_9(0) = 0, \\
y_{10}^{'} &= -(1-\phi)^{2.5} D_1 (A y_7 + B y_9) - \frac{P_r D_2}{D_3}\,[y_1 y_{10} \\
&\quad + y_5 y_6 - y_2 y_9 - y_4 y_7 - s\left(2y_9 + \frac{\eta}{2} y_{10}\right)\Big], && y_{10}(0) = 0, \\
y_{11}^{'} &= y_{12}, && y_{11}(0) = 0, \\
y_{12}^{'} &= y_{13}, && y_{12}(0) = 0, \\
y_{13}^{'} &= -(1-\phi)^{2.5}\,[D_1 (y_1 y_{13} + y_3 y_{11} - 2y_2 y_{12} \\
&\quad -s(y_{12} + \frac{\eta}{2} y_{13})) + D_2 \lambda y_{14} - M \sin^2\gamma y_{12}\Big], && y_{13}(0) = 0, \\
y_{14}^{'} &= y_{15}, && y_{14}(0) = 0, \\
y_{15}^{'} &= -(1-\phi)^{2.5} D_1 (A y_{12} + B y_{14}) - \frac{P_r D_2}{D_3}\,[y_1 y_{15} \\
&\quad + y_5 y_{11} - y_2 y_{14} - y_4 y_{12} - s(2y_{14} + \frac{\eta}{2} y_{15})\Big], && y_{15}(0) = 1.
\end{aligned}$$

The iterative process is repeated until the criteria listed below are met:

$$\max\{|y_2(\eta_\infty, p_n, q_n)|, |y_4(\eta_\infty, p_n, q_n)|\} < \varepsilon^*$$

where ε^* is an arbitrarily small positive number. Here ε^* is taken as 10^{-10}.

3.7 Validation of Code

For validation of the numerical code Tables 3.2 and 3.3 have been presented and the result are compared with the results of Brinkman model [50]. In Tables 3.2 and 3.3 shows, an excellent agreement between the compared results and those of already published in the literature:

TABLE 3.2: Value of $-f''(0)$ for various A, B, and ϕ with $P_r = 6.785$, $\gamma = \frac{\pi}{3}$, $\lambda = 0.5$, and $f_w = S = M = 0.1$.

A	**B**	ϕ	**Cu**		**Current Cu**	**Current** Al_2O_3
-0.5	-0.5	0.05	1.13901	1.02053	1.15455	1.03772
-0.5	-0.5	0.15	1.26227	1.00119	1.27560	1.01758
-0.5	0.0	0.05	1.13772	1.01947	1.15364	1.03687
-0.5	0.0	0.15	1.26009	0.99979	1.27431	1.01655
-0.5	0.5	0.05	1.13637	1.01838	1.15294	1.03611
-0.5	0.5	0.15	1.25767	0.99834	1.27371	1.01566
0.0	-0.5	0.05	1.12971	1.01175	1.15015	1.03435
0.0	-0.5	0.15	1.25236	0.992261	1.27087	1.01443
0.0	0.0	0.05	1.12769	1.01013	1.14813	1.03272
0.0	0.0	0.15	1.24869	0.989996	1.26789	1.01258
0.0	0.5	0.05	1.12549	1.0084	1.14592	1.03098
0.0	0.5	0.15	1.24412	0.987451	1.26434	1.01053
0.5	-0.5	0.05	1.12028	1.00285	1.15269	1.03734
0.5	-0.5	0.15	1.24223	0.983153	1.27236	1.01676
0.5	0.0	0.05	1.11753	1.00065	1.15097	1.03595
0.5	0.0	0.15	1.23698	0.979972	1.26990	1.01520
0.5	0.5	0.05	1.11447	0.998258	1.14910	1.03448
0.5	0.5	0.15	1.23015	0.97628	1.26705	1.01351

3.8 Results and Discussion

This section contains the numerical results have been displayed in graphical format. For numerical calculations, different physical properties of water, copper Cu and alumina Al_2O_3 are considered. The effects of various parameters such as nanoparticles volume fraction ϕ, Prandtal number P_r, chemical reaction γ, Magnetic parameter M, unsteadiness parameter S, bouyancy or convection parameter λ, on

TABLE 3.3: Value of $-\theta^{'}(0)$ for various A, B, and ϕ with $P_r = 6.785$, $\gamma = \frac{\pi}{3}$, $\lambda = 0.5$, and $f_w = S = M = 0.1$

A	**B**	ϕ	**Cu**	Al_2O_3	**Current Cu**	**Current** Al_2O_3
-0.5	-0.5	0.05	3.47169	3.45288	2.59682	2.56815
-0.5	-0.5	0.15	2.84113	2.78241	2.26934	2.19463
-0.5	0.0	0.05	3.37271	3.37184	2.48062	2.47153
-0.5	0.0	0.15	2.69323	2.68589	2.10664	2.08563
-0.5	0.5	0.05	3.27066	3.2888	2.36431	2.37408
-0.5	0.5	0.15	2.53558	2.5857	1.94786	1.97532
0.0	-0.5	0.05	3.27349	3.2836	3.20272	3.21015
0.0	-0.5	0.15	2.5905	2.54533	2.71891	2.72300
0.0	0.0	0.05	3.16522	3.19592	3.09143	3.12003
0.0	0.0	0.15	2.42212	2.49284	2.55864	2.62108
0.0	0.5	0.05	3.05233	3.10533	2.97520	3.02681
0.0	0.5	0.15	2.23725	2.38041	2.38441	2.51424
0.5	-0.5	0.05	3.07389	3.1132	3.81307	3.83940
0.5	-0.5	0.15	2.33646	2.41486	3.19729	3.24948
0.5	0.0	0.05	2.95612	3.01872	3.72156	3.76518
0.5	0.0	0.15	2.14762	2.29781	3.06671	3.16601
0.5	0.5	0.05	2.83218	2.92044	3.62723	3.68918
0.5	0.5	0.15	1.93409	2.17266	2.92889	3.07979

velocity and temperature have been analyzed.

FIGURE 3.2 and 3.3 show how different types of nanofluids behave in terms of velocity and temperature. It has been noted that the thickness of both the momentum and thermal boundary layers changes as the type of nanoparticle changes. Ag-water nanofluid shows the lower velocity than other nanofluids while titanium dioxide nanofluid shows the lowest temperature profile.

In FIGURE 3.4, 3.5, 3.6 and 3.7 the effect of magnetic field parameter$M$ on the temperature profile and velocity profile for the copper water and Alumina water of the nanofluid can be seen. It has been noted that when the magnetic parameter M is increased, the velocity profile in the boundary layer decreases and the temperature profile increases by increasing the magnetic parameter M. This is due to the Lorentz force, which is created when a transverse magnetic field is applied to an electrically conducting fluid. This force slows down the motion of the fluid and increases the temperature.

FIGURE 3.8, 3.9, 3.10 and 3.11 depict the influence of suction/injection parameter on velocity distribution $f(x)$ and temperature distribution $\theta(\eta)$, for both

cases of Cu-water and Al_2O_3-water. It has been noted that by increasing the suction parameter f_w, the velocity and temperature distribution are reduced. On the other hand, figures exhibits the opposite behavior for $f_w < 0$ (injection). Increase in f_w leads to speeding up and cooling down of the fluid flow. As an output the decreases in heat flux is seen in boundary layer domain.

FIGURE 3.12, 3.13, 3.14, 3.15, 3.16, 3.17, 3.18 and 3.19 show how different values of heat generation source ($A > 0$ and $B > 0$) and heat absorption sink ($A < 0$) and ($B < 0$) affect nanofluid velocity and temperature distribution across the boundary layer. The heat source increases the boundary layer thickness. On the other hand the opposite result occurs with heat sink as shown Figures 3.12, 3.13 and 3.16, 3.17. The pure fluid's velocity is higher than Cu-water's velocity, whereas the opposite results occur for Al_2O_3-water. Furthermore, it is obvious from Figures 3.14, 3.15 and 3.18, 3.19 that the thermal boundary layer decreases for ($A < 0$and $B < 0$), The interior heat sink can be used to successfully cool the regime physically. The heat sources $A > 0$ and $B > 0$, on the other hand, show the reverse pattern. It's worth noting that in the nanofluid scenario, the impacts of heat source/sink parameters (A and B) on the velocity and temperature profile are stronger than in the pure fluid case.

FIGURE 3.20, 3.21, 3.22 and 3.23 the effect of the convection parameter λ on the velocity and temperature profile of copper water and Alumina water is discussed. Convection is the mechanism of heat transfer through a fluid in the presence of bulk of fluid motion. In the case of forced convection the fluid is forced to flow over a surface. Due to this reason it is observed that the thickness of velocity profile of the hydrodynamic boundary layer increase when the convection parameter λ is increased.

FIGURE 3.24, 3.25, 3.26 and 3.27 demonstrate the magnetic field inclination angle γ on the velocity distributions. It is obvious that increasing the inclination angle γ decreases the velocity profile and increases the temperature profile of the nanofluids. The reason for this is that as the angle of inclination increases, the magnetic field becomes stronger. Because of the stronger magnetic fields, It creates a force that opposes the flow (Lorentz force). The thickness of the momentum boundary layer is reduced as a result of this force. Due to the fact that

M is directly proportional to the $\sin 2\gamma$ hence for $\gamma = 0$ has no consequence on velocity while magnetic field effects when $\gamma = 90^o$

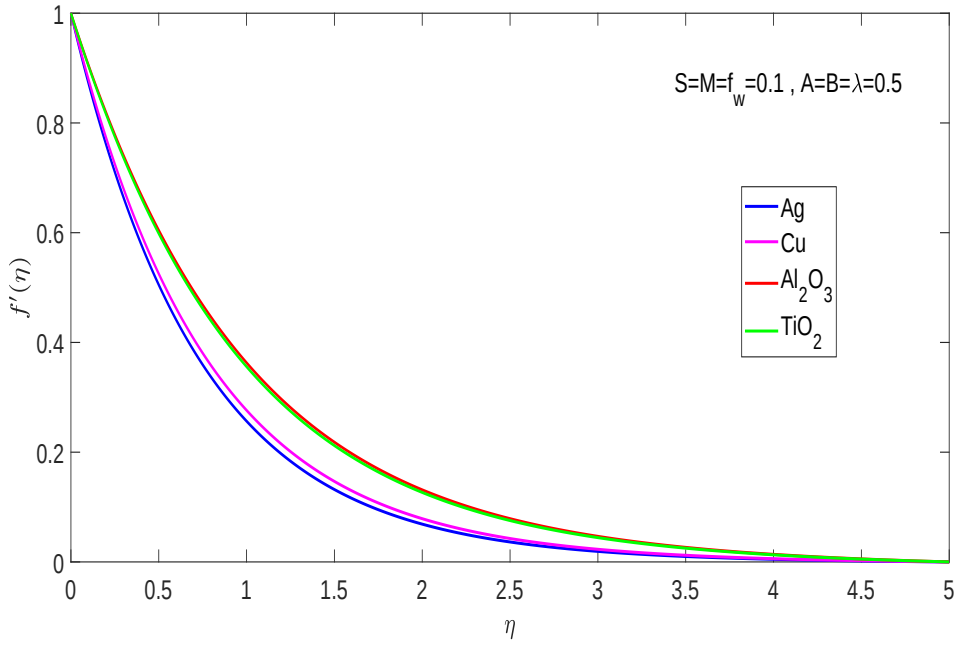

FIGURE 3.2: Velocity profile for different types of nanofluids

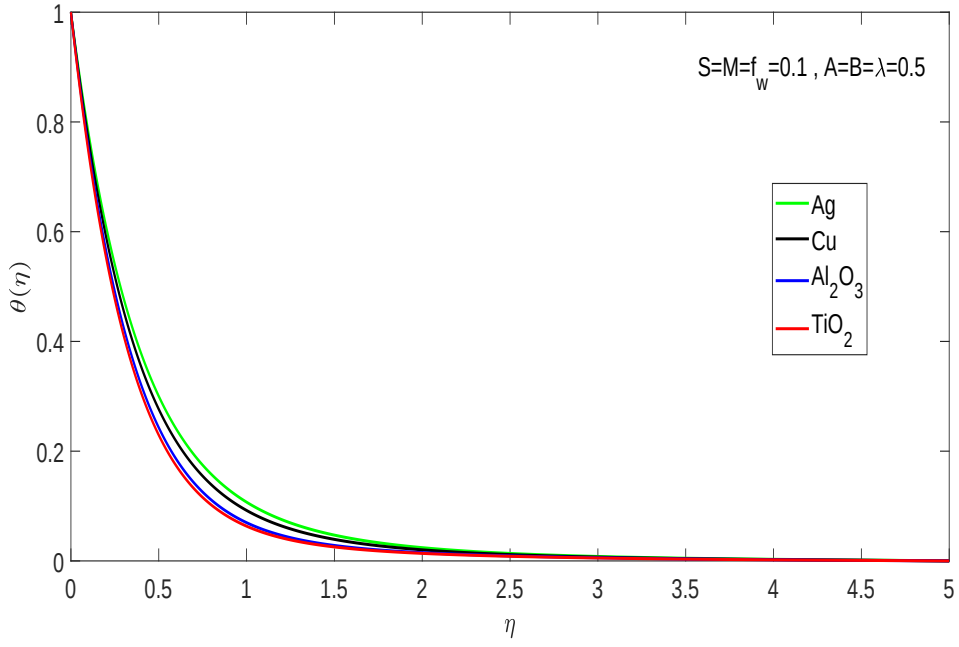

FIGURE 3.3: Temperature profile for different types of nanofluids

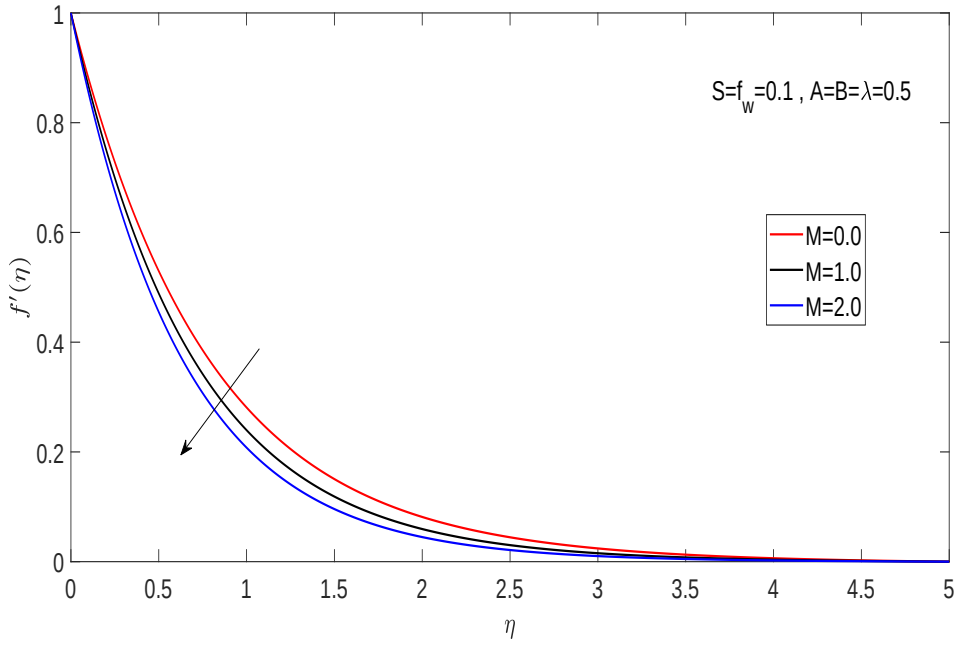

FIGURE 3.4: Effects of M on velocity distribution for Cu-water

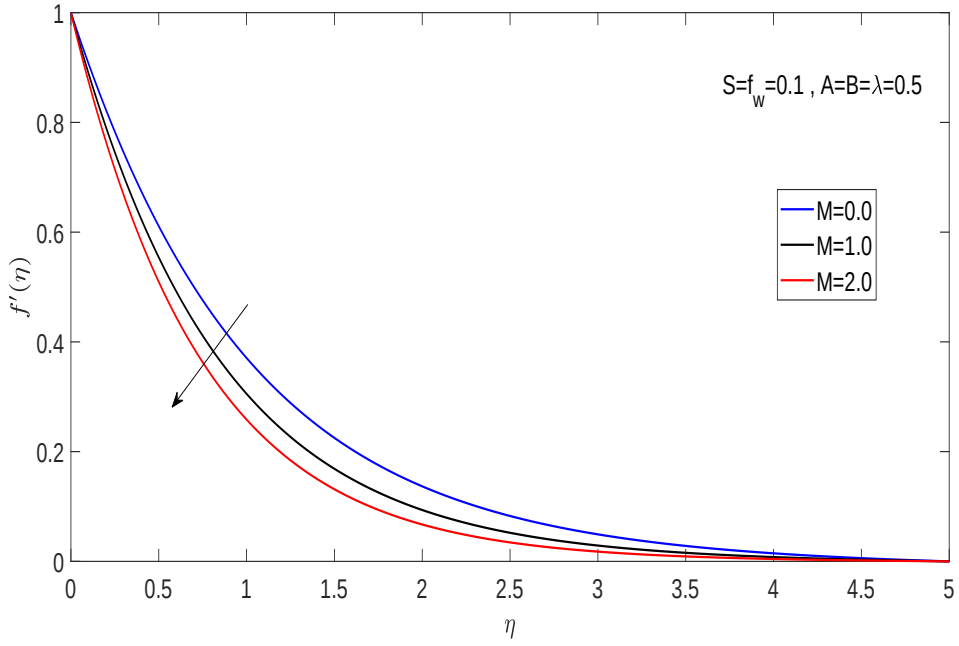

FIGURE 3.5: Effects of M on velocity profile for Alumina-water

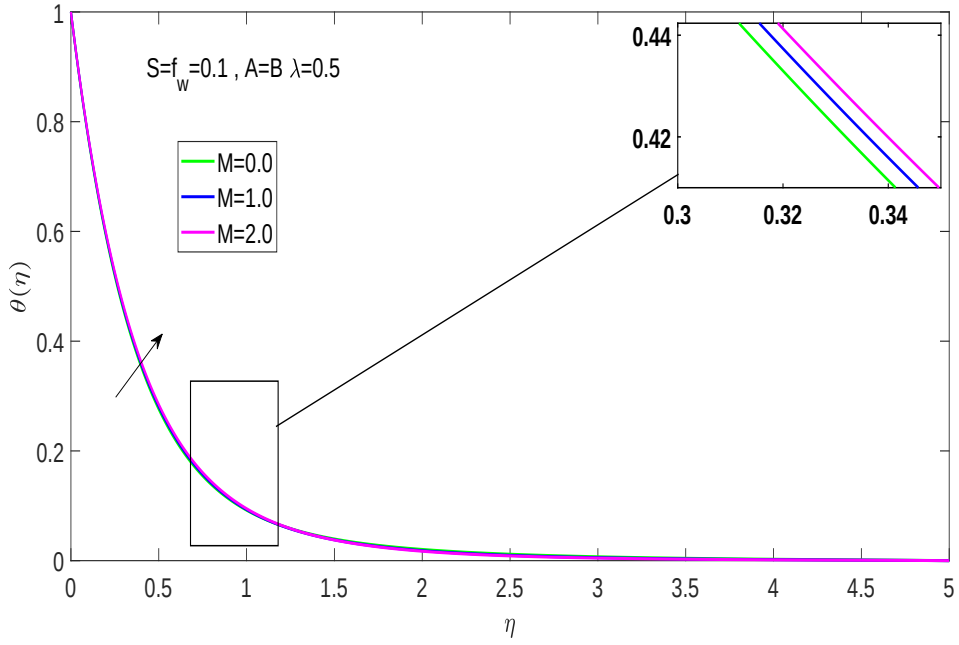

FIGURE 3.6: Effects of M on temperature profile for Cu-water

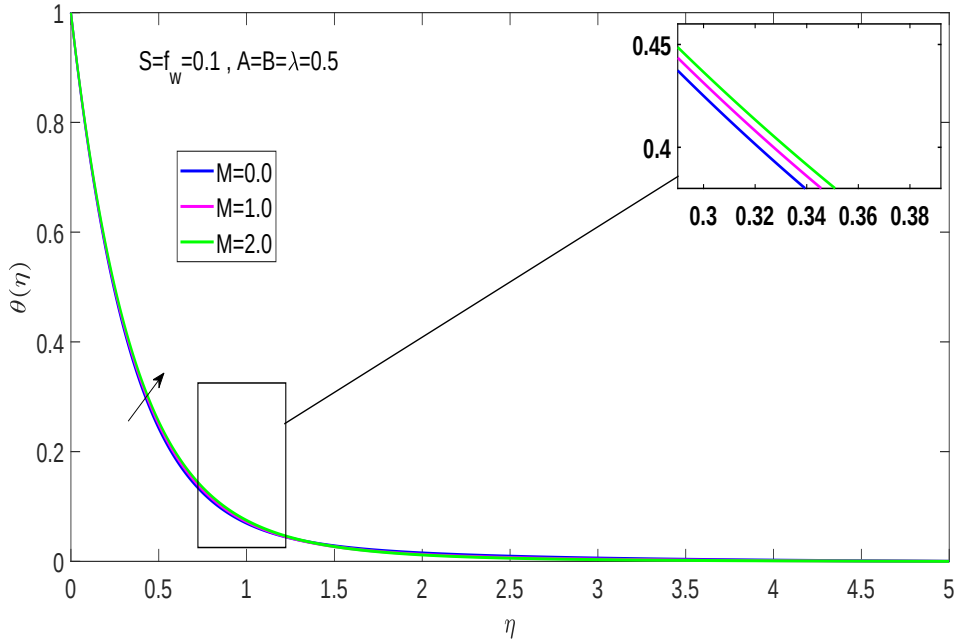

FIGURE 3.7: Effects of M on temperature distribution for Al_2O_3-water

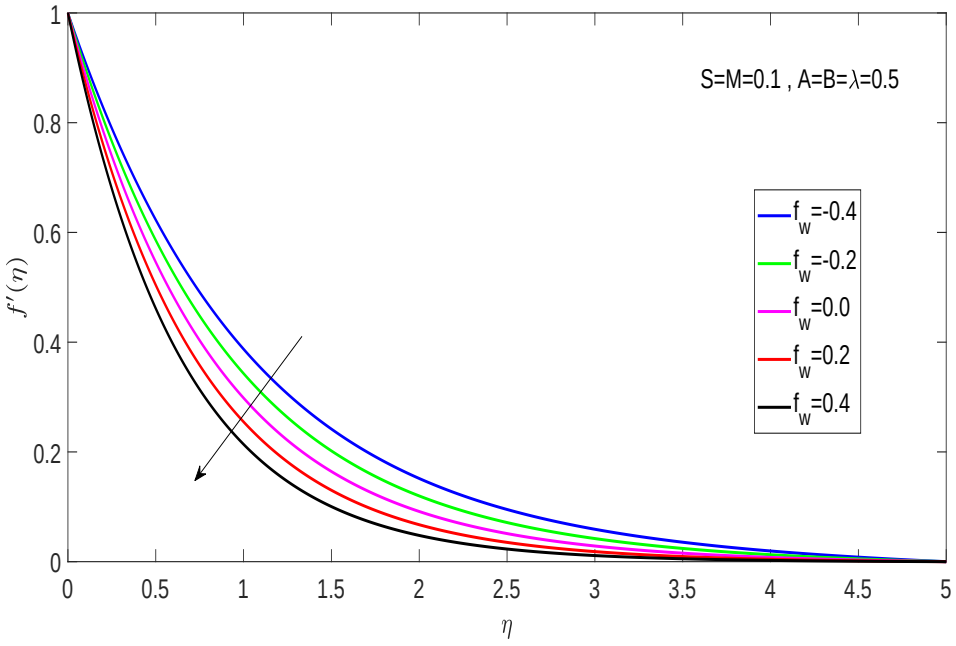

FIGURE 3.8: Effects of f_w on velocity profile for Cu-water

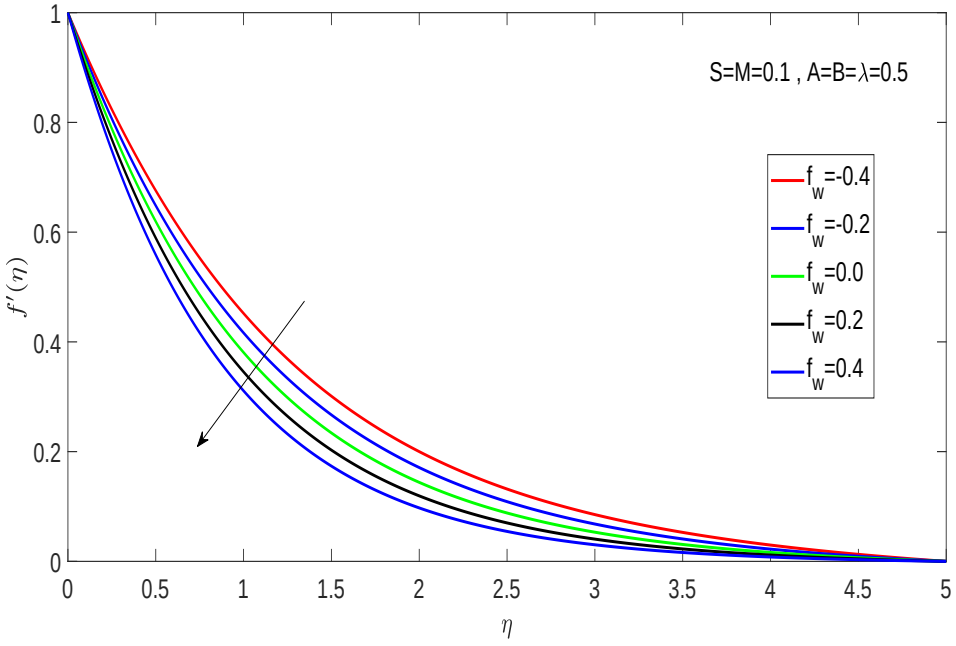

FIGURE 3.9: Effects of f_w on velocity distribution for Al_2O_3-water

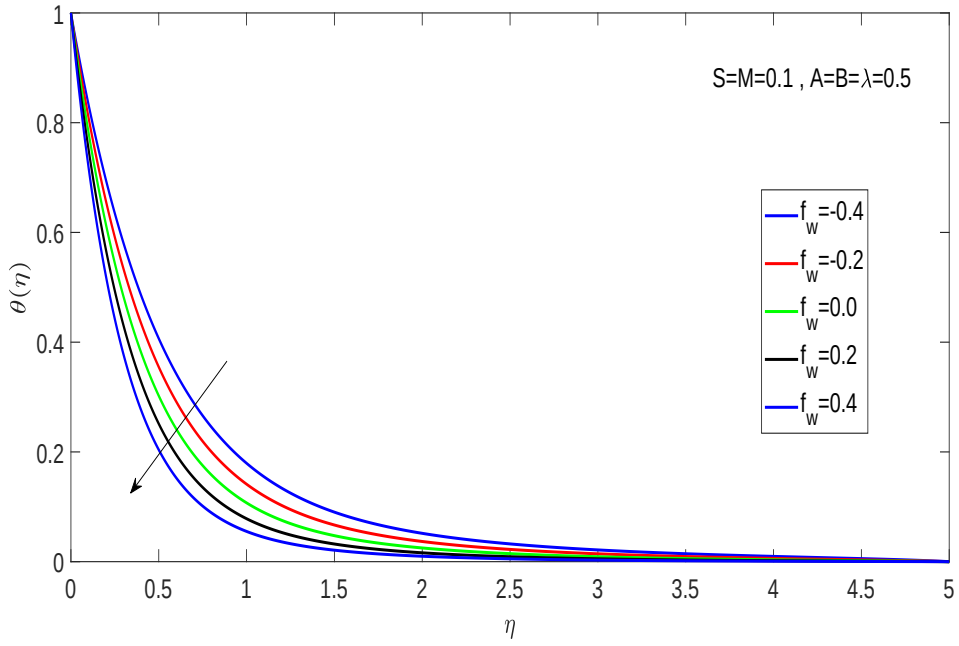

FIGURE 3.10: Effects of f_w on temperature distribution for Cu-water

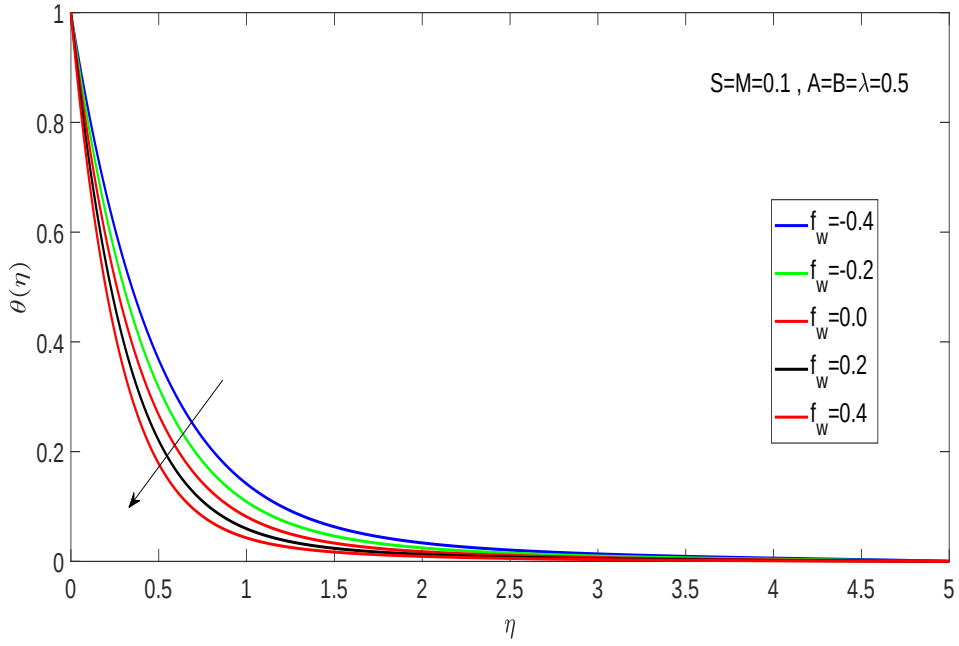

FIGURE 3.11: Effects of f_w on temperature distribution for Al_2O_3-water

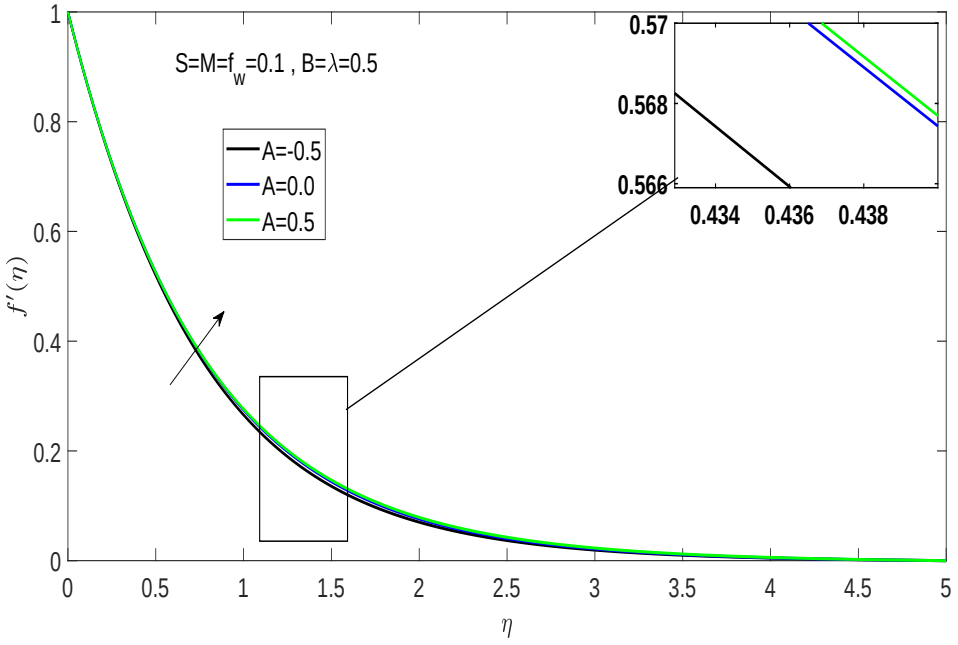

FIGURE 3.12: Effects of A on velocity distribution for Cu-water

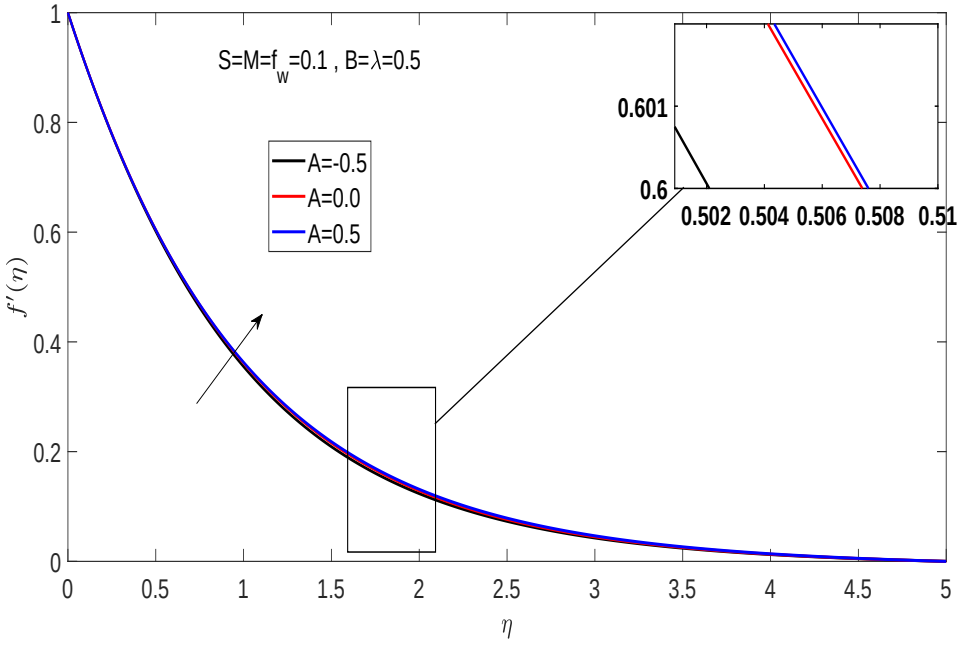

FIGURE 3.13: Effects of A on velocity distribution for Al_2O_3-water

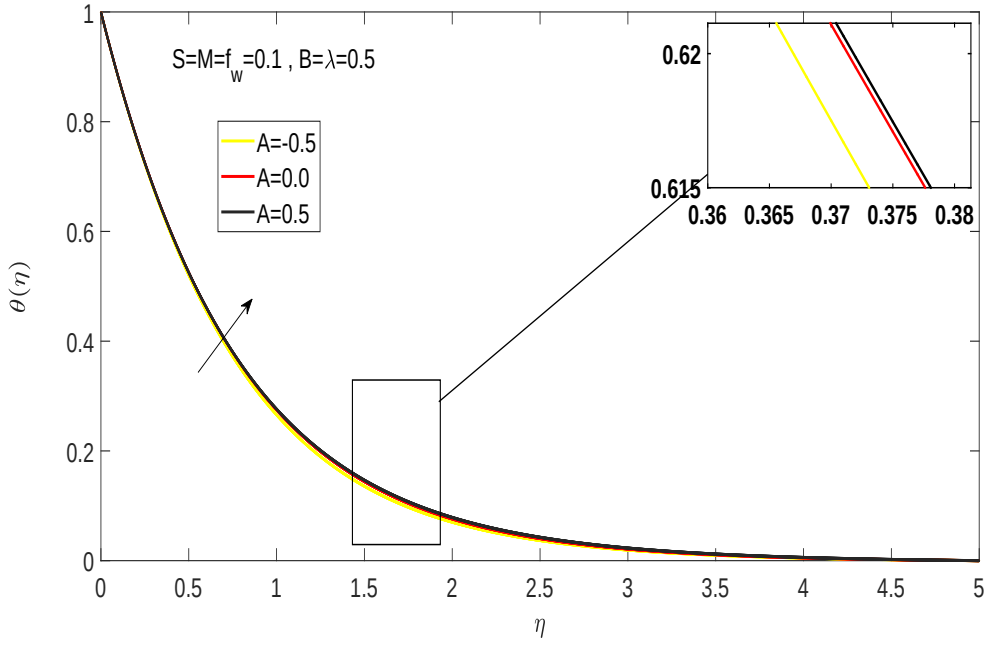

FIGURE 3.14: Effects of A on temperature distribution for Cu-water

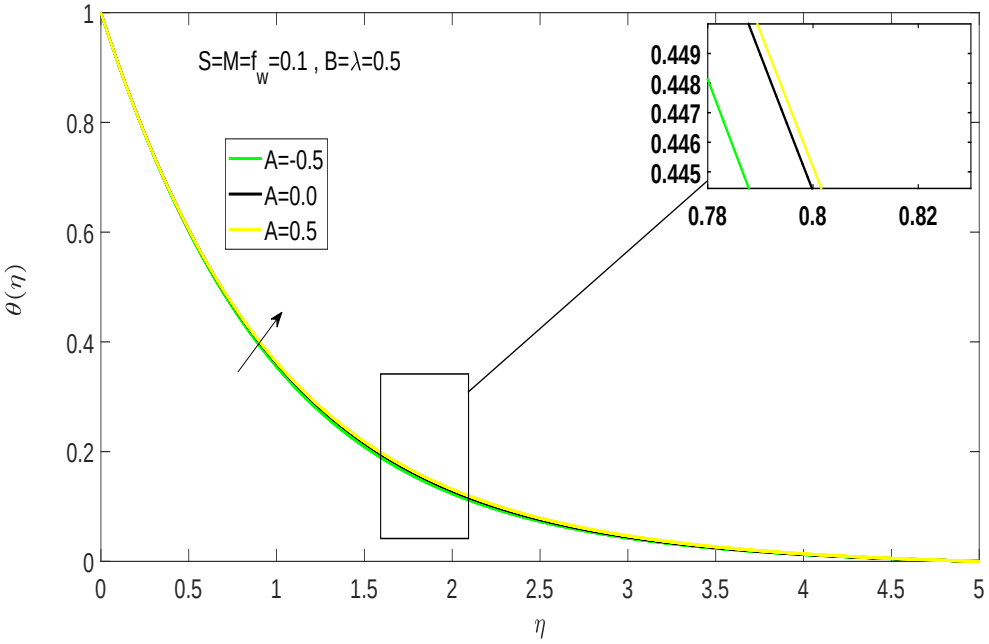

FIGURE 3.15: Effects of A on temperature distribution for Al_2O_3-water

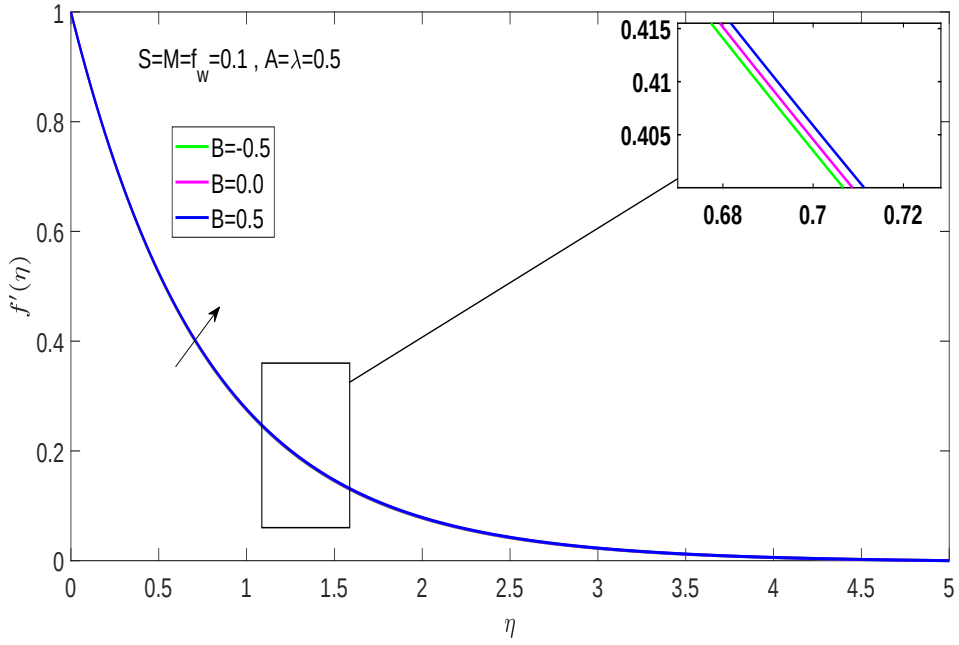

FIGURE 3.16: Effects of B on velocity distribution for Cu-water

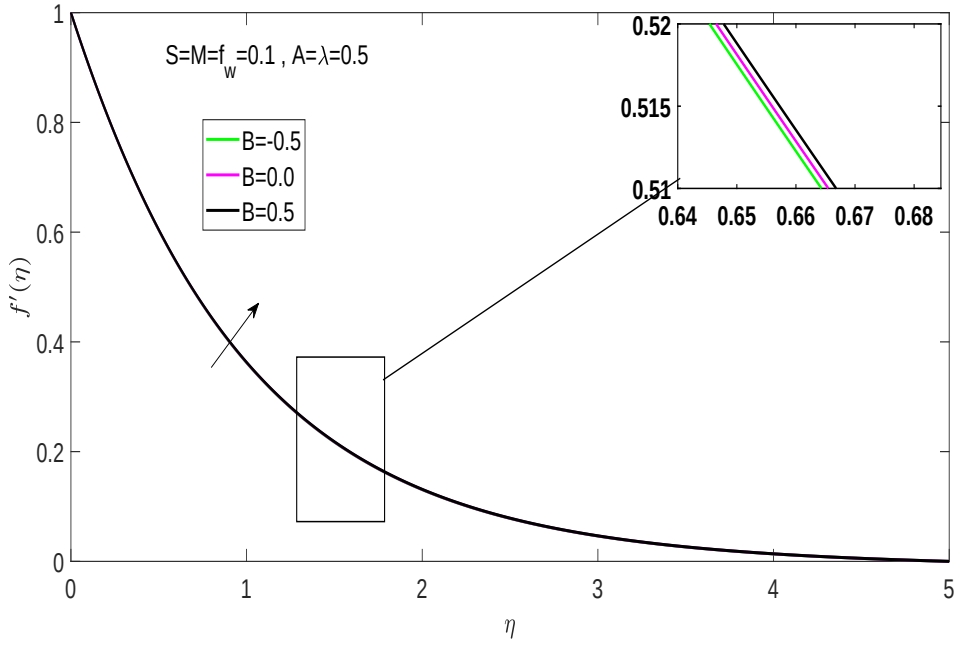

FIGURE 3.17: Effects of B on velocity distribution for Al_2O_3-water

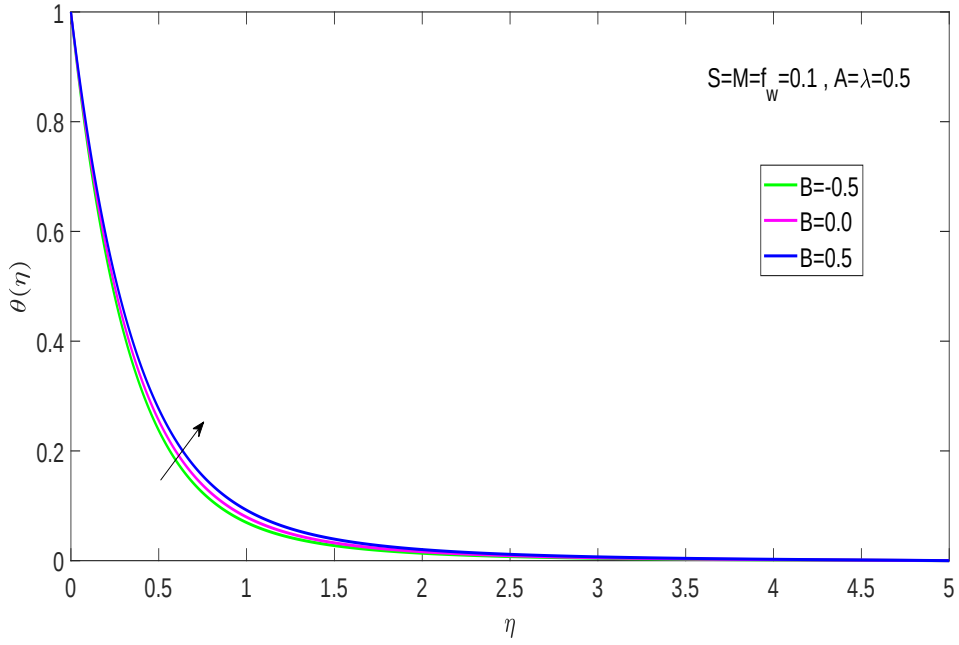

FIGURE 3.18: Effects of B on temperature distribution for Cu-water

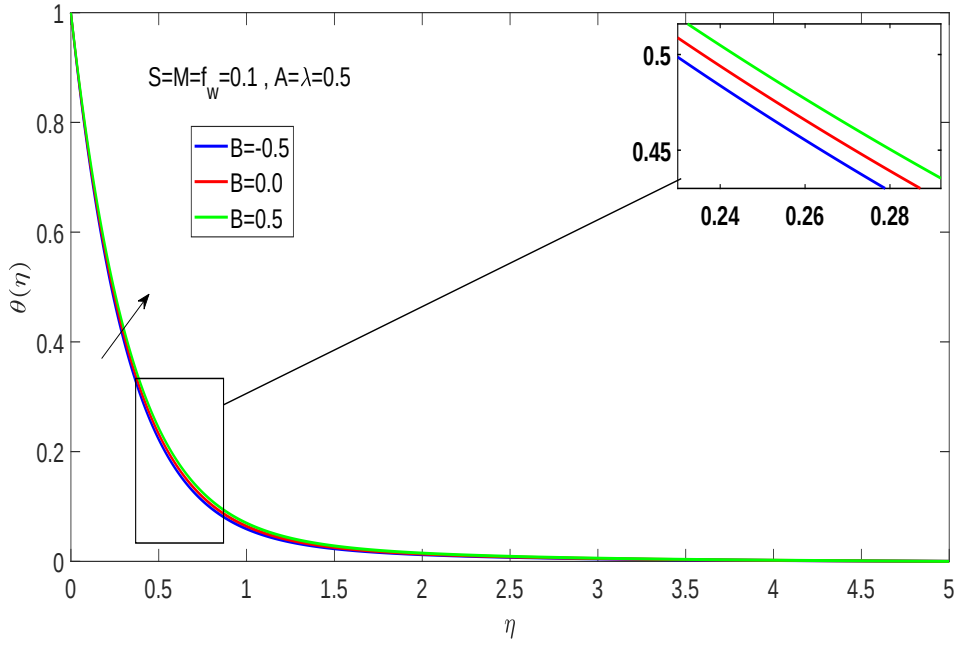

FIGURE 3.19: Effects of B on temperature distribution for Al_2O_3-water

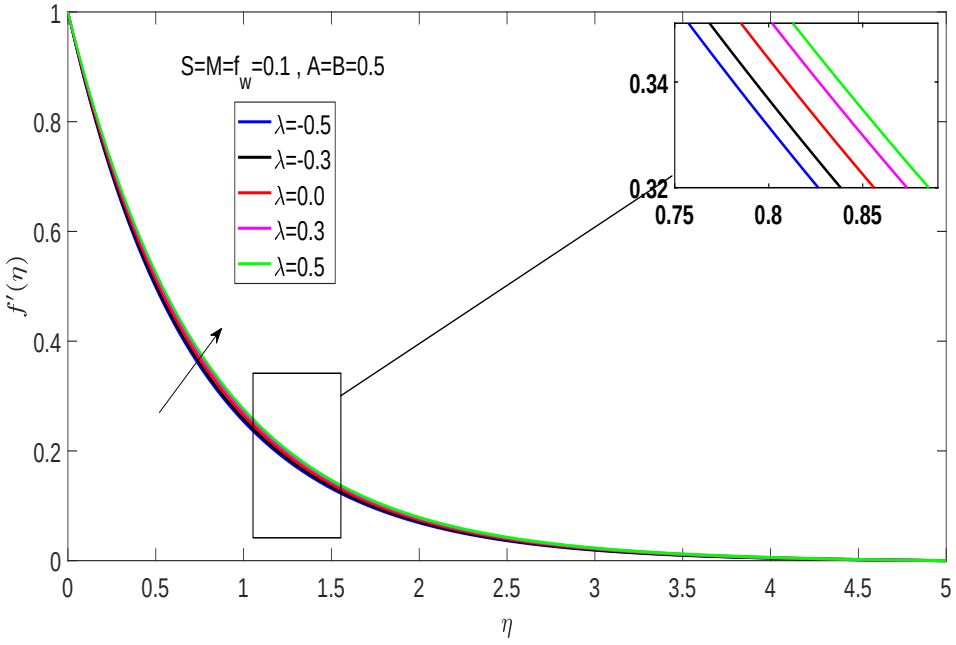

FIGURE 3.20: Effects of λ on velocity distribution for Cu-water

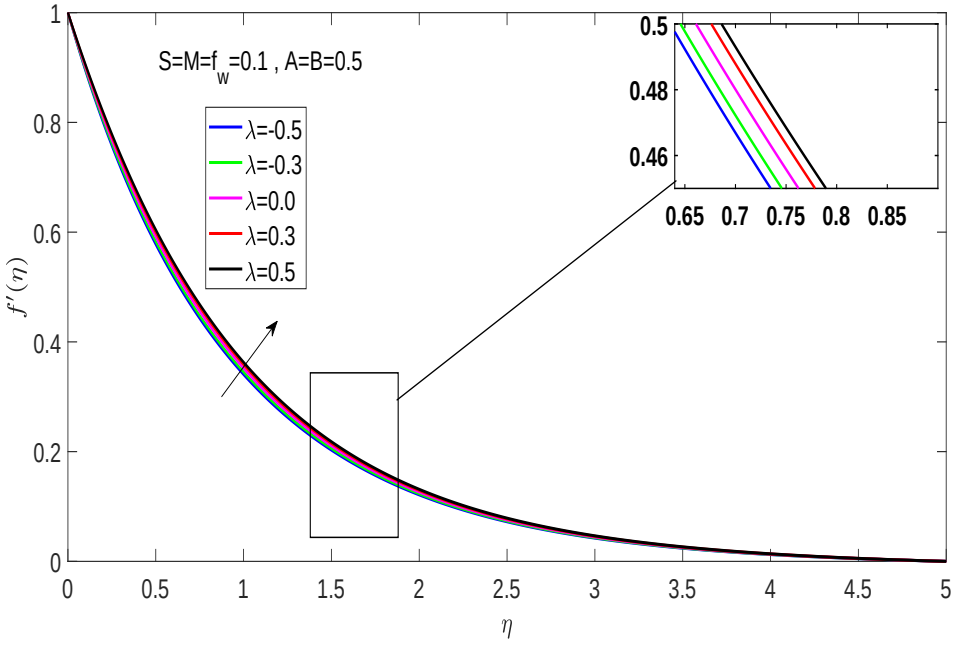

FIGURE 3.21: Effects of λ on velocity distribution for Al_2O_3-water

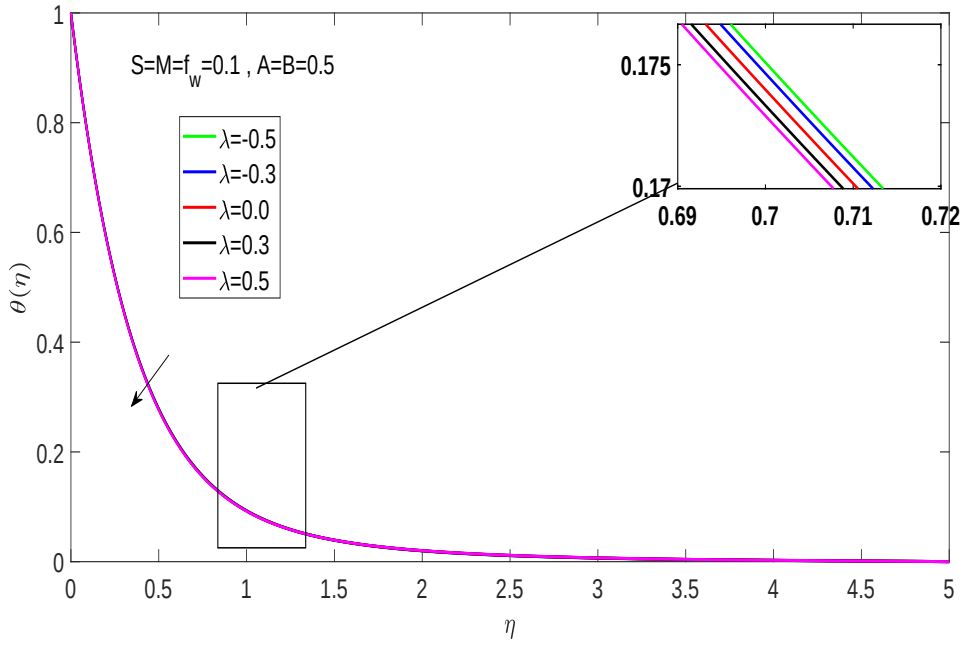

FIGURE 3.22: Effects of λ on temperature distribution for Cu-water

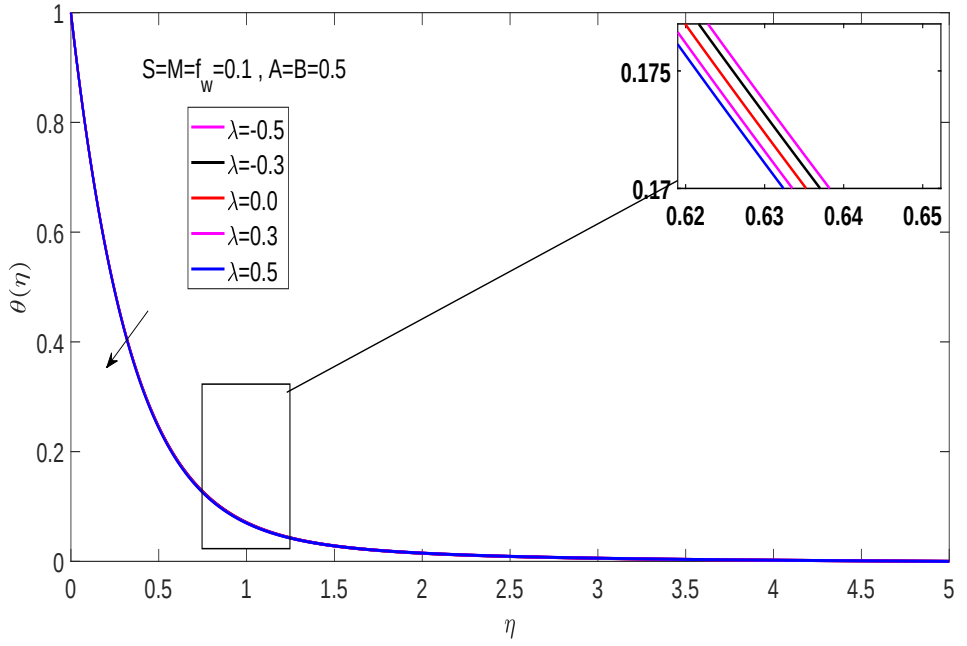

FIGURE 3.23: Effects of λ on temperature distribution for Al_2O_3-water

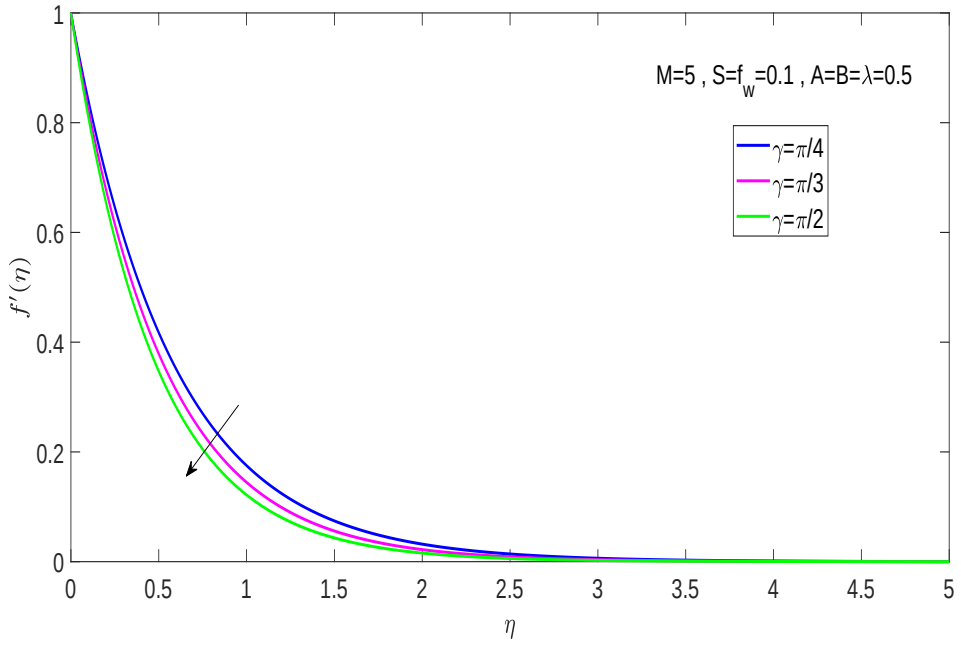

FIGURE 3.24: Effects of γ on velocity profile for Cu-water

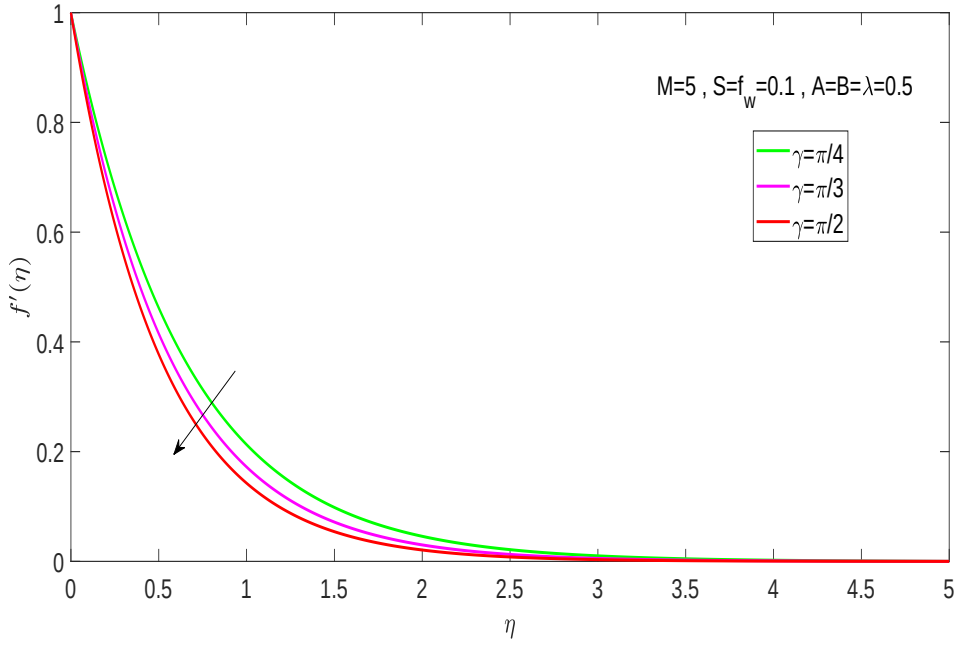

FIGURE 3.25: Effects of γ on velocity profile for Al_2O_3-water

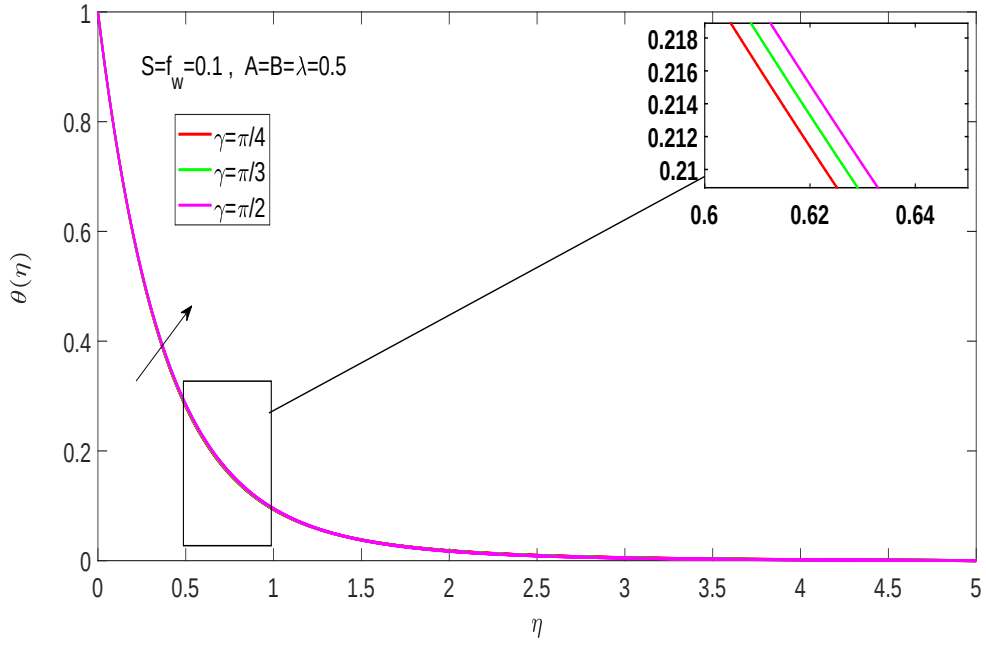

FIGURE 3.26: Effects of γ on temperature distribution for Cu-water

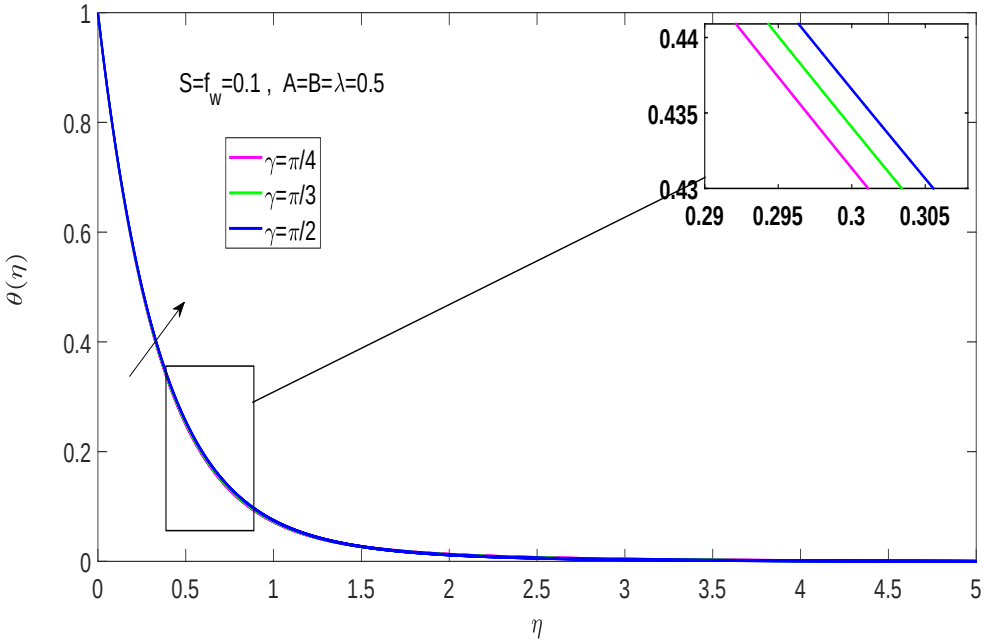

FIGURE 3.27: Effects of γ on temperature for Al_2O_3-water

Chapter 4

Unsteady Nanofluids Flow through Joule Heating, Thermal Radiation and Porous Medium in the Presence of Magnetic Field

4.1 Introduction

In this chapter, the work of Elgazery [40] is extended by considering nanofluids flow over a permeable unsteady stretching surface with non-uniform heat source/sink in the presence of inclined magnetic field over porous medium, viscous dissipation and Joule heating. The non-linear partial differential equations of velocity and temperature profiles are transformed into a set of ordinary differential equations utilizing suitable similarity transformations. By performing the shooting technique, the numerical solution of transformed governing ordinary differential equations is obtained. Utilizing MATLAB tool, the temperature are analyzed for pertinent variables. Through graphs the dynamics of various variables of suction parameter, stretching parameter, species diffusivity coefficient and chemical reaction parameter are displayed.

4.2 Mathematical Modeling

Consider an unsteady, two-dimensional stretched surface with a non-uniform heat source/sink, viscous dissipation, and Joule heating in the presence of an inclined magnetic field over a porous medium. The surface velocity has been represented by

$$U_w(x,t) = \frac{ax}{1-ct}.$$

The basic mathematical model describing the flow has been shown, which contains the PDEs of continuity equation, momentum, and energy transfer.

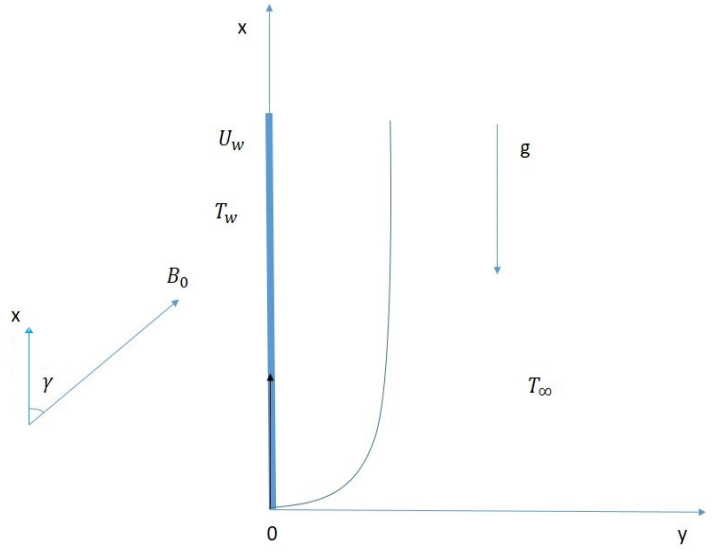

FIGURE 4.1: The physical model and coordinate system

Continuity Equation:

$$\frac{\partial u}{\partial x} + \frac{\partial v}{\partial y} = 0 \tag{4.1}$$

Momentum Equation:

$$\frac{\partial u}{\partial t} + u\frac{\partial u}{\partial x} + v\frac{\partial u}{\partial y} = \frac{\mu_{nf}}{\rho_{nf}}\frac{\partial^2 u}{\partial y^2} + g\frac{(\rho\beta)_{nf}}{\rho_{nf}}(T - T_\infty) - \frac{\sigma_{nf}}{\rho_{nf}}B_0^2 \sin^2\gamma u - \frac{1}{k}\frac{\mu_{nf}}{\rho_{nf}}u \tag{4.2}$$

Energy Equation:

$$\left.\begin{aligned}\frac{\partial T}{\partial t}+u\frac{\partial T}{\partial x}+v\frac{\partial T}{\partial y}=\alpha_{nf}\frac{\partial^2 T}{\partial y^2}+\frac{q'''}{(\rho C_P)_{nf}}+\frac{\mu_{nf}}{(\rho C_p)_{nf}}(\frac{\partial u}{\partial y})^2\\ +\frac{1}{(\rho C_p)_{nf}}(\frac{\partial q_r}{\partial y})+\frac{\sigma_{nf}}{(\rho C_p)_{nf}}B_0^2u^2\sin^2\gamma\end{aligned}\right\} \tag{4.3}$$

The boundary conditions for the above equations are:

$$\left.\begin{aligned}u=u_w(x,t)=\frac{ax}{1-ct},\\ v=v_w(t)=-\sqrt{\frac{av_f}{1-ct}}f_w,\\ T=T_{w(x,t)}=T_\infty+\frac{bx}{(1-ct)^2},\quad at\qquad y=0,\\ u=0,\quad T=T_\infty,\qquad\qquad as\quad y\to\infty\end{aligned}\right\} \tag{4.4}$$

Here, u and v are components of velocity in the direction of x and y respectively, t is the time, the fluid parameter is T, the fluid density is ρ, the fluid kinematic viscosity is ν, the fluid thermal diffusivity is α and the specific heat is C_p.
Following similarity transformations are used to convert the energy equation (4.2) and concentration equation (4.3) into dimensionless form

$$\eta=\sqrt{\frac{a}{v_f(1-ct)}}y, \qquad \psi(x,y,t)=\sqrt{\frac{av_f}{1-ct}}xf(\eta),$$
$$\theta(\eta)=\frac{T-T_\infty}{T_w-T_\infty}, \qquad u=\frac{\partial\psi}{\partial y}=\frac{a}{(1-ct)}xf'(\eta),$$
$$v=-\frac{\partial\psi}{\partial x}=-\sqrt{\frac{av_f}{1-ct}}f(\eta),$$

The detailed conversion of continuity equation (4.1) is already discussed in chapter 3. The conversion of (4.2) is presented below.To achieve this goal first of L.H.S of (4.2) is transformed as follows:

$$\frac{\partial u}{\partial t}+u\frac{\partial u}{\partial x}+v\frac{\partial u}{\partial y}=\frac{acxf'}{(1-ct)^2}+\frac{acxy}{2(1-ct)^{\frac{5}{2}}}\sqrt{\frac{a}{v_f}}f''+\frac{a^2x}{(1-ct)^2}(f')^2-\frac{xa^2}{(1-ct)^2}ff'',$$

$$\Rightarrow\quad \frac{\partial u}{\partial t}+u\frac{\partial u}{\partial x}+v\frac{\partial u}{\partial y}=\frac{xa}{(1-ct)^2}\left[cf'+\frac{c\eta}{2}f''+a(f')^2-aff''\right]. \tag{4.5}$$

The R.H.S of (4.2) is formulated as:

$$\frac{\mu_{nf}}{\rho_{nf}}\frac{\partial^2 u}{\partial y^2}+g\frac{(\rho\beta)_{nf}}{\rho_{nf}}(T-T_\infty)-\frac{\sigma_{nf}}{\rho_{nf}}B_0^2 u\sin^2\gamma-\frac{\mu_{nf}}{\rho_{nf}}\frac{1}{K}u=\frac{\mu_{nf}}{\rho_{nf}}\frac{a^2x}{v_f(1-ct)^2}f'''$$

$$+g\frac{(\rho\beta)_{nf}}{\rho_{nf}}\theta(T-T_\infty)-\frac{\sigma_{nf}}{\rho_{nf}}B_0^2\sin^2\gamma\frac{ax}{(1-ct)}f'-\frac{\mu_{nf}}{\rho_{nf}}\frac{1}{K}\frac{ax}{(1-ct)}f',$$

$$\Rightarrow \quad =\frac{\mu_{nf}}{\rho_{nf}}\frac{a^2x}{v_f(1-ct)^2}f'''+\frac{(\rho\beta)_{nf}}{\rho_{nf}}\frac{bxg}{(1-ct)^2}\theta-\frac{\sigma_{nf}}{\rho_{nf}}\frac{axB_0^2}{(1-ct)}\sin^2\gamma f' \qquad (4.6)$$

$$-\frac{\mu_{nf}}{\rho_{nf}}\frac{1}{K}\frac{ax}{(1-ct)}f'.$$

Combining (4.5) and (4.6) we get

$$\frac{a^2x}{(1-ct)^2}\left[\frac{\mu_{nf}}{\rho_{nf}v_f}f'''+\frac{(\rho\beta)_{nf}}{a^2\rho_{nf}}gb\theta-\frac{\sigma_{nf}}{a\rho_{nf}}B_0^2(1-ct)f'\sin^2\gamma\right]$$

$$-\frac{\mu_{nf}}{\rho_{nf}}\frac{1}{K}\frac{ax}{(1-ct)}f'=\frac{ax}{(1-ct)^2}\left[cf'+\frac{c}{2}\eta f''+a(f')^2-aff''\right],$$

$$\Rightarrow \quad \frac{\rho_{nf}v_f}{\mu_{nf}}\left[s(f'+\frac{\eta}{2}f'')+(f')^2-ff''\right]+\frac{\rho_{nf}\nu_f}{\mu_{nf}}\frac{\mu_{nf}}{\rho_{nf}}\frac{(1-ct)}{aK}f'$$

$$=f'''+\frac{(\rho\beta)_{nf}v_f}{a^2\mu_{nf}}gb\theta-\frac{\sigma_{nf}v_f}{a\mu_{nf}}B_0^2(1-ct)f'\sin^2\gamma,$$

$$\Rightarrow \quad f'''+(1-\phi)^{2.5}\left[\frac{((1-\phi)\rho_f+\phi\rho_p)\,v_f}{\mu_f}ff''-\frac{((1-\phi)\rho_f+\phi\rho_p)\,v_f}{\mu_f}(f')^2\right.$$

$$-\frac{((1-\phi)\rho_f+\phi\rho_p)\,v_f}{\mu_f}s\left(f'+\frac{\eta}{2}f''\right)+\frac{((1-\phi)(\rho\beta)_f+\phi(\rho\beta)_p)\,gbv_f}{a^2\mu_f}\theta$$

$$\left.-\frac{((1-\phi)\sigma_f+\phi\sigma_p)\,v_f}{a\mu_f}B_0^2(1-ct)f'\sin^2\gamma\right]-\frac{\nu_f(1-ct)}{aK}f'=0,$$

$$\Rightarrow \quad f'''+(1-\phi)^{2.5}\left[\left((1-\phi)+\phi\frac{\rho_p}{\rho_f}\right)ff''-\left((1-\phi)+\phi\frac{\rho_p}{\rho_f}\right)(f')^2\right.$$

$$-\left((1-\phi)+\phi\frac{\rho_p}{\rho_f}\right)s\left(f'+\frac{\eta}{2}f''\right)+\frac{((1-\phi)(\rho\beta)_f+\phi(\rho\beta)_p)}{a^2\rho_f}gb\theta$$

$$\left.-\frac{\sigma_{nf}}{a\rho_f}B_0^2(1-ct)f'\sin^2\gamma\right]-\frac{\nu_f(1-ct)}{a(1-ct)k_1}f'=0,$$

$$\Rightarrow \quad f'''+(1-\phi)^{2.5}\left[D_1ff''-D_1(f')^2-D_1s\left(f'+\frac{\eta}{2}f''\right)+(\rho\beta)_f\left((1-\phi)\right.\right.$$

$$\left.\left.+\phi\frac{(\rho\beta)_p}{(\rho\beta)_f}\right)\frac{gb}{a_2\rho_f}\theta\frac{\sigma_{nf}}{a\rho_f}B_0^2(1-ct)f'\sin^2\gamma\right]-\frac{1}{D}f'=0,$$

$$\Rightarrow \quad f'''+(1-\phi)^{2.5}\left[D_1\left(ff''-\left(f'\right)^2-s\left(f'+\tfrac{\eta}{2}f''\right)\right)+\lambda D_2\theta\right.$$

$$\left.-Mf'\sin^2\gamma\right]-df'=0$$

The necessary step to convert the energy equation (4.3) into dimensionless form are as follows.The detailed conversion of L.H.S of energy equation is already discussed in Chapter 3.

$$\frac{\partial T}{\partial t}+u\frac{\partial T}{\partial x}+v\frac{\partial T}{\partial y}=\frac{bx}{(1-ct)^3}\left[c(2\theta+\frac{\eta}{2}\theta')+a(f'\theta-f\theta')\right].$$

Furthermore, the R.H.S of (4.3) have been transformed into dimensionless form as shown below. The Rosseland approximation can be considered for radiative heat flux. Using Taylor series, we might expand the temperature difference T^4 about T_∞, for smaller values of temperature constant. The formula for radiative heat flux is as follows:

$$
\begin{aligned}
q_r &= -\frac{4\sigma^*}{3k^*}\frac{\partial T^4}{\partial y},\\
T^4 &= 4T_\infty^3 T - 3T_\infty^4,\\
\Rightarrow \quad T &= T_\infty + (T_w - T_\infty)\theta,\\
\Rightarrow \quad T^4 &= 4T_\infty^3[T_\infty + (T_w - T_\infty)\theta] - 3T_\infty^4,\\
\frac{\partial T^4}{\partial y} &= 4T_\infty^3(T_w - T_\infty)\theta^{'}\sqrt{\frac{a}{\nu_f(1-ct)}},\\
q_r &= -\frac{4\sigma^*}{3k^*}4T_\infty^3\theta^{'}\sqrt{\frac{a}{\nu_f(1-ct)}}(T_w - T_\infty),\\
\frac{\partial q_r}{\partial y} &= -\frac{16\sigma^*}{3k^*}T_\infty^3\theta^{''}\frac{a}{\nu_f(1-ct)}(T_w - T_\infty),\\
(\frac{\partial u}{\partial y})^2 &= \frac{a^3x^2}{\nu_f(1-ct)^3}(f^{''})^2.
\end{aligned}
$$

Now considering the R.H.S of (4.3):

$$
\alpha_{nf}\frac{\partial^2 T}{\partial y^2} + \frac{q^{'''}}{(\rho C_P)_{nf}} + \frac{\mu_{nf}}{(\rho C_p)_{nf}}(\frac{\partial u}{\partial y})^2 + \frac{1}{(\rho C_p)_{nf}}(\frac{\partial q_r}{\partial y}) + \frac{\sigma_{nf}B_0^2u^2}{(\rho C_p)_{nf}}\sin^2\gamma
$$

$$
= \frac{\alpha_{nf}abx}{\nu_f(1-ct)^3}\theta^{''} + \frac{axk_{nf}}{x(1-ct)\nu_{nf}(\rho C_p)_{nf}}\left[A(T_w - T_\infty)f^{'} + B(T - T_\infty)\right]
$$

$$
+\frac{1}{(\rho C_p)_{nf}}\left[\frac{a^3x^2\mu_f}{\nu_f(1-ct)^3}(f^{''})^2 + \frac{a^2x^2\sigma_{nf}B_0^2}{(1-ct)^2}(f^{'})^2\sin^2\gamma - \frac{16\sigma^*abxT_\infty^3}{3k^*\nu_f(1-ct)^3}\theta^{''}\right].
$$

Combining L.H.S and R.H.S of energy equation (4.3) we get:

$$
\frac{bx}{(1-ct)^3}\left[c(2\theta + \frac{\eta}{2}\theta') + a(f'\theta - f\theta')\right] = \frac{abx\alpha_{nf}}{(1-ct)^3\nu_f}\left[\theta'' + \frac{bx(1-ct)^2k_{nf}}{x(1-ct)^2\nu_{nf}}(Af'\right.
$$

$$
\left.+B\theta)\frac{\nu_f}{b\alpha_{nf}(\rho C_p)_{nf}}\right] + \frac{ax}{(\rho C_p)_{nf}(1-ct)^3}\left[\sigma_{nf}B_0^2ax(1-ct)(f^{'})^2\sin^2\gamma\right.
$$

$$+\rho_f a^2 x(f^{''})^2 - \frac{16\sigma^* b}{3k^*\nu_f}T_\infty^3\theta^{''}\Big],$$

$$\Rightarrow \quad \frac{\nu_f}{\alpha_{nf}}\left[\frac{c}{a}(2\theta+\frac{\eta}{2}\theta^{'})+f^{'}\theta-f\theta^{'}\right]=\theta^{''}+\frac{k_{nf}\nu_f}{\nu_{nf}\alpha_{nf}(\rho C_p)_{nf}}\left(Af^{'}+B\theta\right)$$

$$+\frac{\nu_f}{b\alpha_{nf}(\rho C_p)_{nf}}\left[Ma^2x\rho_f f^{'}\sin^2\gamma+a^2x\rho_f(f^{''})^2-\frac{16\sigma^* b}{3k^*\nu_f}T_\infty^3\theta^{''}\right],$$

$$\Rightarrow \quad \frac{P_r D_2}{D_3}\left[s\left(2\theta+\frac{\eta}{2}\theta^{'}\right)+f^{'}\theta-f\theta^{'}\right]=\theta^{''}+\frac{\alpha_{nf}(\rho C_p)_{nf}\nu_f}{\nu_{nf}\alpha_{nf}(\rho C_p)_{nf}}\left(Af^{'}+B\theta\right)$$

$$+\frac{P_r D_2}{D_3}\left[\frac{a^2x\rho_f}{b(\rho C_p)_{nf}}\left(M(f^{'})^2\sin^2\gamma+(f^{''})^2\right)-\frac{16\sigma^* b}{3k^* b\nu_f\rho(C_p)_{nf}}T_\infty^3\theta^{''}\right],$$

$$\Rightarrow \quad \theta^{''}+D_1(1-\phi)^{2.5}(Af^{'}+B\theta)+\frac{P_r D_2}{D_3}\left[f\theta^{'}-f^{'}\theta-s\left(2\theta+\frac{\eta}{2}\theta^{'}\right)\right]$$

$$+\frac{P_r D_2}{D_3}\left[\frac{gx(\rho\beta)_f}{\lambda(\rho C_p)_f\left((1-\phi)+\phi\dfrac{(\rho C_p)_p}{(\rho C_p)_f}\right)}(M(f^{'})^2\sin^2\gamma+(f^{''})^2)\right.$$

$$\left.-\frac{16\sigma^* T_\infty^3}{3k^*\nu_f(\rho C_p)_f[(1-\phi)+\phi\dfrac{(\rho C_p)_p}{(\rho C_p)_f}]}\theta^{''}\right]=0,$$

$$\Rightarrow \quad \theta^{''}+D_1(1-\phi)^{2.5}\left(Af^{'}+B\theta\right)+\frac{P_r D_2}{D_3}\left[f\theta^{'}-f^{'}\theta-s\left(2\theta+\frac{\eta}{2}\theta^{'}\right)\right]$$

$$+\frac{P_r D_2}{D_3}\frac{gx(\rho\beta)_f}{\lambda(\rho C_p)_f D_2}\left[M(f^{'})^2\sin^2\gamma+(f^{''})^2\right]-\frac{P_r D_2}{D_3}\frac{16\sigma^* T_\infty^3}{3k^*\nu_f(\rho C_p)_f D_2}\theta^{''}=0,$$

$$\Rightarrow \quad \theta^{''}+D_1(1-\phi)^{2.5}\left(Af^{'}+B\theta\right)+\frac{P_r D_2}{D_3}\left[f\theta^{'}-f^{'}\theta-s(2\theta+\frac{\eta}{2}\theta^{'})\right]$$

$$+\frac{P_r}{D_3}\frac{gx(\rho\beta)_f}{\lambda(\rho C_p)_f}\left[M(f^{'})^2\sin^2\gamma+(f^{''})^2\right]-\frac{P_r}{D_3}\frac{16\sigma^* T_\infty^3}{3k^* k_f P_r}\theta^{''}=0,$$

$$\Rightarrow \quad \theta^{''}+D_1(1-\phi)^{2.5}\left(Af^{'}+B\theta\right)+\frac{P_r D_2}{D_3}\left[f\theta^{'}-f^{'}\theta-s(2\theta+\frac{\eta}{2}\theta^{'})\right]$$

$$+\frac{P_r}{D_3}\frac{gx(\rho\beta)_f}{\lambda(\rho C_p)_f}\left[M(f^{'})^2\sin^2\gamma+(f^{''})^2\right]-\frac{4R}{3D_3}\theta^{''}=0,$$

$$\Rightarrow\quad \theta^{''}+D_1(1-\phi)^{2.5}\left(Af^{'}+B\theta\right)+\frac{P_rD_2}{D_3}\left[f\theta^{'}-f^{'}\theta-s(2\theta+\frac{\eta}{2}\theta^{'})\right]$$

$$+\frac{a^2bgP_r\rho_fE_c(\rho\beta)_f}{a^2bD_3g\rho_f(\rho\beta)_f}\left[M(f^{'})^2\sin^2\gamma+(f^{''})^2\right]-\frac{4R}{3D_3}\theta^{''}=0,$$

$$\Rightarrow\quad \left(1-\frac{4R}{3D_3}\right)\theta^{''}+D_1(1-\phi)^{2.5}\left(Af^{'}+B\theta\right)+\frac{P_rD_2}{D_3}\left[f\theta^{'}-f^{'}\theta\right.$$

$$\left.-s(2\theta+\frac{\eta}{2}\theta^{'})\right]+\frac{P_rE_c}{D_3}\left[M(f^{'})^2\sin^2\gamma+(f^{''})^2\right]=0.$$

Different parameters used in the above equations have the following formulation:

- $R=\dfrac{4\sigma^*T_\infty^3}{k_fk_*}.$
- $\lambda=\dfrac{bg(\rho\beta)_f}{a^2\rho_f}.$
- $E_c=\dfrac{u^2}{(C_p)_f(T_w-T_\infty)},\qquad \Rightarrow\quad =\dfrac{a^2x^2(1-ct)^2}{bx(C_p)_f(1-ct)^2},$
  $\Rightarrow\quad E_c=\dfrac{a^2x}{b(C_p)_f},\qquad \Rightarrow\quad \dfrac{b}{a^2}E_c=\dfrac{x}{(C_p)_f}.$
- $D=\dfrac{ak_1}{\nu_f},\qquad \Rightarrow\dfrac{1}{D}=d,$
- $D_{ax}=\dfrac{(1-ct)k_1}{x^2},\qquad \Rightarrow=\dfrac{K}{x^2},\qquad$ where $\quad K=k_1(1-ct).$

  The detailed procedure for the conversion of boundary conditions into the dimensionless form is similar to that discussed in chapter 3.

  The model's final dimensionless form is:

$$\left.\begin{aligned} f^{'''}+(1-\phi)^{2.5}\Big[D_1\left(ff^{''}-(f^{'})^2-s(f^{'}+\frac{\eta}{2}f^{''})\right)+\lambda D_2\theta\\ -Mf^{'}\sin^2\gamma\Big]-df^{'}=0.\end{aligned}\right\} \tag{4.7}$$

$$\left.\begin{aligned} \left(1-\frac{4R}{3D_3}\right)\theta^{''}+D_1(1-\phi)^{2.5}\left(Af^{'}+B\theta\right)+\frac{P_rD_2}{D_3}\left[f\theta^{'}-f^{'}\theta\right.\\ \left.-s(2\theta+\frac{\eta}{2}\theta^{'})\right]+\frac{P_rE_c}{D_3}\left[M(f^{'})^2\sin^2\gamma+(f^{''})^2\right]=0.\end{aligned}\right\} \tag{4.8}$$

The transformed boundary conditions are stated below:

$$\left.\begin{array}{llll} f^{'}=1, & f=f_w, \quad \theta=1, & at & \eta=0, \\ f^{'}=0, & \theta=0, & at & \eta\to\infty \end{array}\right\}. \tag{4.9}$$

4.3 Solution Methodology

This section is focused on the implementation of the shooting method to solve the transformed ODEs (4.7) and (4.8) depending on the boundary conditions (4.9). For this purpose, we first convert the system of ODEs into first order ODEs, by using the following notations:

$$f=y_1, \quad f^{'}=y_1^{'}, \quad f^{'''}=y_3^{'}, \quad \theta=y_4, \quad \theta^{''}=y_5^{'},$$

Further denote

$$f=y_1, \quad y_1^{'}=y_2, \quad y_2^{'}=y_3, \quad f^{'''}=y_3^{'}, \quad \theta=y_4, \quad y_4^{'}=y_5, \quad \theta^{''}=y_5^{'}.$$

Using the notations, (4.7) and (4.8) can be converted into system of following five first order ordinary differential equations:

$$\left.\begin{array}{ll} y_1^{'}=y_2, & y_1(0)=f_w, \\ y_2^{'}=y_3, & y_2(0)=1, \\ y_3^{'}=-(1-\phi)^{2.5}\left[D_1\left(y_1y_3-y_2^2-s(y_2+\dfrac{\eta}{2}y_3)\right)+D_2\lambda y_4\right. & \\ \quad \left.-M\sin^2\gamma y_2\right]-dy_2, & y_3(0)=p, \\ y_4^{'}=y_5, & y_4(0)=1, \\ y_5^{'}=\left(\dfrac{3D_3}{3D_3-4R}\right)\left[-(1-\phi)^{2.5}D_1(Ay_2+By_4)-\dfrac{p_rD_2}{D_3}\,(y_1y_5\right. & \\ \quad \left.-y_2y_4-s(\dfrac{\eta}{2}y_5+2y_4)\right)-\dfrac{P_rE_c}{D_3}\left(My_2^2\sin^2\gamma+y_3^2\right)\Bigg], & y_5(0)=q, \end{array}\right\}$$

The RK-4 method will be used to solve the above initial value problem. To obtain an approximate result, problem's domain has been defined as $[0,\eta_\infty]$ instead of $[0,\infty]$, where η_∞ is an appropriate positive real number that is finite. In the

equations listed above, the missing conditions p and q are to be chosen such that

$$\left.\begin{aligned} y_2(\eta_\infty, p, q) &= 0 \\ y_4(\eta_\infty, p, q) &= 0. \end{aligned}\right\} \tag{4.10}$$

To solve the above algebraic equations, the Newton's method is used which is governed by the following iterative scheme:

$$\begin{bmatrix} p_{n+1} \\ q_{n+1} \end{bmatrix} = \begin{bmatrix} p_n \\ q_n \end{bmatrix} - \begin{bmatrix} \frac{\partial y_2}{\partial p} & \frac{\partial y_2}{\partial q} \\ \frac{\partial y_4}{\partial p} & \frac{\partial y_4}{\partial q} \end{bmatrix}^{-1}_{(p_n, q_n)} \begin{bmatrix} y_2(\eta_\infty, p_n, q_n) \\ y_4(\eta_\infty, p_n, q_n) \end{bmatrix} \tag{4.11}$$

Now use the following notations:

$$\left.\begin{aligned} &\frac{\partial y_1}{\partial p} = y_6, && \frac{\partial y_2}{\partial p} = y_7, && \frac{\partial y_3}{\partial p} = y_8, \\ &\frac{\partial y_4}{\partial p} = y_9, && \frac{\partial y_5}{\partial p} = y_{10}, && \\ &\frac{\partial y_1}{\partial q} = y_{11}, && \frac{\partial y_2}{\partial q} = y_{12}, && \frac{\partial y_3}{\partial q} = y_{13}, \\ &\frac{\partial y_4}{\partial q} = y_{14}, && \frac{\partial y_5}{\partial q} = y_{15}, && \end{aligned}\right\} \tag{4.12}$$

As a result of these new notations, the Newton's iterative scheme gets the form with $(p, q) = (p_0, q_0)$:

$$\begin{bmatrix} p_{n+1} \\ q_{n+1} \end{bmatrix} = \begin{bmatrix} p_n \\ q_n \end{bmatrix} - \begin{bmatrix} y_7 & y_{12} \\ y_9 & y_{14} \end{bmatrix}^{-1}_{(p_n, q_n)} \begin{bmatrix} y_2(\eta_\infty, p_n, q_n) \\ y_4(\eta_\infty, p_n, q_n) \end{bmatrix} \tag{4.13}$$

Now differentiate the above system of five first order ODEs with respect to each of the variables p and q to have another system of ten ODEs. Writing all these ten ordinary differential equations together, we have the following IVP:

$$\begin{aligned} y_6^{'} &= y_7, && y_6(0) = 0, \\ y_7^{'} &= y_8, && y_7(0) = 0, \\ y_8^{'} &= -(1-\phi)^{2.5}\,[D_1(y_1 y_8 + y_3 y_6 - 2y_2 y_7 \\ &\quad -s(y_7 + \frac{\eta}{2} y_8)) + D_2 \lambda y_9 - M \sin^2 \gamma y_7\Big] + d y_7, && y_8(0) = 1, \end{aligned}$$

$$
\begin{aligned}
y_9^{'} &= y_{10}, && y_9(0) = 0,\\
y_{10}^{'} &= \left(\frac{3D_3}{3D_3 - 4R}\right)\Big[-(1-\phi)^{2.5}D_1(Ay_7 + By_9)\\
&\quad - \frac{P_r D_2}{D_3}\left(y_1 y_{10} + y_5 y_6 - y_2 y_9 - y_4 y_7\right.\\
&\quad \left. -s(2y_9 + \frac{\eta}{2}y_{10})\right) - \frac{P_r E_c}{D_3}(2My_2 y_7 \sin^2\gamma + 2y_3 y_8)\Big], && y_{10}(0) = 0,\\
y_{11}^{'} &= y_{12}, && y_{11}(0) = 0,\\
y_{12}^{'} &= y_{13}, && y_{12}(0) = 0,\\
y_{13}^{'} &= -(1-\phi)^{2.5}[D_1(y_1 y_{13} + y_3 y_{11} - 2y_2 y_{12} - s(y_{12} + \frac{\eta}{2}y_{13}))\\
&\quad + D_2\lambda y_{14} - M\sin^2\gamma y_{12}] + dy_{12}, && y_{13}(0) = 0,\\
y_{14}^{'} &= y_{15}, && y_{14}(0) = 0,\\
y_{15}^{'} &= \left(\frac{3D_3}{3D_3 - 4R}\right)\Big[-(1-\phi)^{2.5}D_1(Ay_{12} + By_{14})\\
&\quad - \frac{P_r D_2}{D_3}\left(y_1 y_{15} + y_5 y_{11} - y_2 y_{14} - y_4 y_{12} - s(2y_{14} + \frac{\eta}{2}y_{15})\right)\\
&\quad - \frac{P_r E_c}{D_3}(2My_2 y_{12}\sin^2\gamma + 2y_3 y_{13})\Big], && y_{15}(0) = 1.
\end{aligned}
$$

The RK-4 method is used to solve the above system of fifteen equations with initial guesses p and q. The missing conditions p and q are updated by using Newton's scheme. The iterative procedure is stopped when the following condition is met:

$$\max\{|y_2(\eta_\infty, p_n, q_n)|, |y_4(\eta_\infty, p_n, q_n)|\} < \varepsilon^*$$

where ε^* is an arbitrarily small positive number. Here ε^* is taken as 10^{-10}.

4.4 Representation of Graphs and Tables

A thorough discussion on the graphs and tables has been conducted which contains the impact of velocity and temperature distribution. The impact of different factors like thermal radiation R, Prandtle number P_r, Casson parameter β and Eckert number E_c is observed graphically. Numerical results of the skin friction coefficient and Nusselt number for the distinct values of some fixed parameters are

shown in Table 4.1 and 4.2.

TABLE 4.1: Value of $-f''(0)$ for various A, B, and ϕ with $\gamma = \frac{\pi}{3}$,$\lambda = 0.5$, $P_r = 6.785$, $M = S = f_w = 0.1$, $d = 0.1$, $E_c = 0.3$ and $R = 0$.

A	**B**	ϕ	**Cu**	Al_2O_3
-0.5	-0.5	0.05	1.33780	1.20980
-0.5	-0.5	0.15	1.95248	1.57769
-0.5	0.0	0.05	1.33457	1.20707
-0.5	0.0	0.15	1.94702	1.57397
-0.5	0.5	0.05	1.33113	1.20418
-0.5	0.5	0.15	1.93645	1.56997
0.0	-0.5	0.05	1.34134	3.26667
0.0	-0.5	0.15	1.14266	1.21456
0.0	0.0	0.05	1.33810	1.21193
0.0	0.0	0.15	1.94735	1.57740
0.0	0.5	0.05	1.33449	1.20909
0.0	0.5	0.15	2.02049	1.57326
0.5	-0.5	0.05	2.84204	1.22255
0.5	-0.5	0.15	1.95959	1.58886
0.5	0.0	0.05	1.34638	1.22060
0.5	0.0	0.15	1.95522	1.58611
0.5	0.5	0.05	1.88916	1.21852
0.5	0.5	0.15	1.95017	1.58309

4.5 Results and Discussion

Graphs are used to display the numerical results. In this section for numerical calculation physical properties of copper and alumina are considered. The computations for various values of volume fraction ϕ, the Prandtl number P_r, chemical reaction γ, Eckert number E_c, Magnetic parameter M are performed, and hence the effect of these parameters on heat transfer are discussed.

FIGURE 4.2 and 4.3 explain how different types of nanofluids behave in terms of velocity and temperature profiles. Thermal boundary layer thickness and momentum are observed to alter as the type of nanoparticle changes. It is observed that the lower velocity is attained for Ag-water fluid while the highest velocity profile can be seen for alumina oxide.

In the FIGURE 4.4, 4.5, 4.6 and 4.7 the velocity profile and temperature profile

TABLE 4.2: Value of $-\theta^{'}(0)$ for various A, B, and ϕ with $\gamma = \frac{\pi}{3}$,$\lambda = 0.5$, $\mathrm{P}_r = 6.785$, $M = S = f_w = 0.1$, $d = 0.1$, $E_c = 0.3$ and $R = 0$.

A	**B**	ϕ	**Cu**	Al_2O_3
-0.5	-0.5	0.05	2.16355	2.21572
-0.5	-0.5	0.15	2.46836	2.51924
-0.5	0.0	0.05	1.96346	2.05386
-0.5	0.0	0.15	2.11019	2.29231
-0.5	0.5	0.05	1.75225	1.88450
-0.5	0.5	0.15	2.35127	2.05172
0.0	-0.5	0.05	3.18932	3.26666
0.0	-0.5	0.15	3.13890	3.60544
0.0	0.0	0.05	3.03071	3.13986
0.0	0.0	0.15	3.17388	3.42430
0.0	0.5	0.05	2.86349	3.00769
0.0	0.5	0.15	1.38608	3.23280
0.5	-0.5	0.05	2.89283	4.16635
0.5	-0.5	0.15	4.37272	4.55925
0.5	0.0	0.05	3.95651	4.06780
0.5	0.0	0.15	4.14634	4.41811
0.5	0.5	0.05	3.18719	3.96663
0.5	0.5	0.15	3.90661	4.27199

for the copper water and alumina water are depicted for different values of M, when $S = d = f_w = 0.1$, $A = B = \lambda = 0.5$ and $E_c = 0.3$. It has been noted that with the increase of M the velocity boundary layer thickness decreases and temperature profile increases.

FIGURE 4.8, 4.9, 4.10 and 4.11 depict the dimensionless velocity and temperature profile for various values of suction parameter f_w when $S = M = d = 0.1$, $A = B = \lambda = 0.5$ and $E_c = 0.3$. It can be seen that with the increase of suction parameter f_w of the fluid, velocity profile and temperature profile decreases. The physical reason for fact that told fluid particles are injected into the micro-porous channel while the fluid particles that are heated on the hot wall of the micro-porous channel are removed out. This decreases the temperature by weakening the convection which results to a decrease in velocity.

FIGURE 4.12, 4.13, 4.14, 4.15, 4.16, 4.17, 4.18 and 4.19 present the impact of the various value of heat generation source ($A > 0$ and $B > 0$) and heat absorption sink ($A < 0$ and $B < 0$) on the velocity and temperature distribution when

$S = M = d = 0.1$, $\lambda = 0.5$ and $E_c = 0.3$. An increase in heat source results the increase in velocity and temperature profile. Figures 4.12, 4.13, 4.16 and 4.17 depicts that velocity profile increases with the increases in heat source parameter A for all the nanofluids.

FIGURE 4.20, 4.21, 4.22 and 4.23 demonstrates the velocity and temperature behaviors in both situations of copper and Alumina water for various values of λ when $S = M = d = f_w = 0.1$, $A = B = 0.5$ and $E_c = 0.3$. It is noted that when convection parameter is increased for both nanofluids whereas temperature profile is decreased. This is due to the fact that heat transfer through a fluid increases the fluid motion.

FIGURE 4.24, 4.25, 4.26 and 4.27 are delineating the impact of the magnetic field inclination angle γ, while other parameters are fixed for both Cu-water and Al_2O_3 water. Figures 4.24 and 4.25 disposes the consequence of the magnetic field inclination angle γ on the velocity profiles. It is self-evident that increasing the angle of inclination γ decreases the velocity profile. The reason for this is that as the angle of inclination increases, the magnetic field becomes stronger. From these figures the fact that an opposing force is generated by the magnetic field, generally referred as the Lorentz force, which opposes the motion of the fluid resulting a decrements in the momentum boundary layer thickness and increment in the thermal and boundary layer thickness.

FIGURE 4.28, 4.29, 4.30 and 4.31 are sketched to show the impact of permeability parameter d on the velocity and temperature distributions when $S = M = f_w = 0.1$, $A = B = \lambda = 0.5$ and $E_c = 0.3$. It is obvious that presence of porous medium causes higher restriction to fluid flow which causes the fluid decelerate. The effect of increases value of permeability parameter contributes to thickness of thermal boundary layer which is shown in figure 4.30.

In FIGURE 4.32, 4.33, 4.34 and 4.35 the effect of Eckert number E_c on velocity and temperature profile when $S = M = d = f_w = 0.1$ and $A = B = \lambda = 0.5$ are plotted. It can be seen that for larger values of the Eckert number intensifies the momentum and thermal boundary layer thickness. Generally, the rising value of E_c encourage the diffusion of particle due to this cause we saw improvement in momentum and thermal boundary layers.

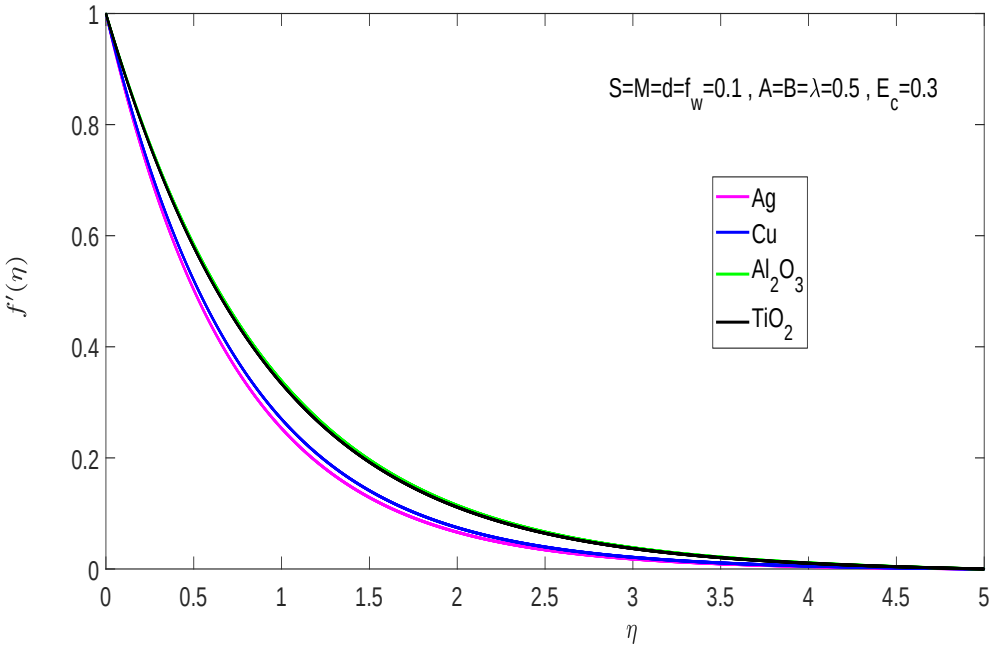

FIGURE 4.2: Velocity profile for different types of nanofluids

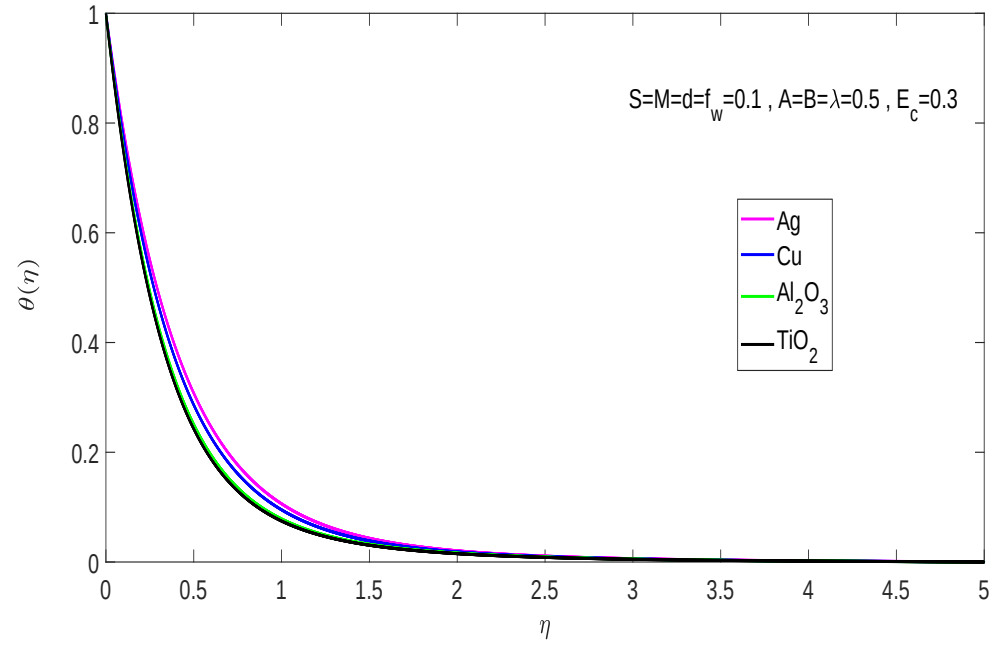

FIGURE 4.3: Temperature profile for different types of nanofluids

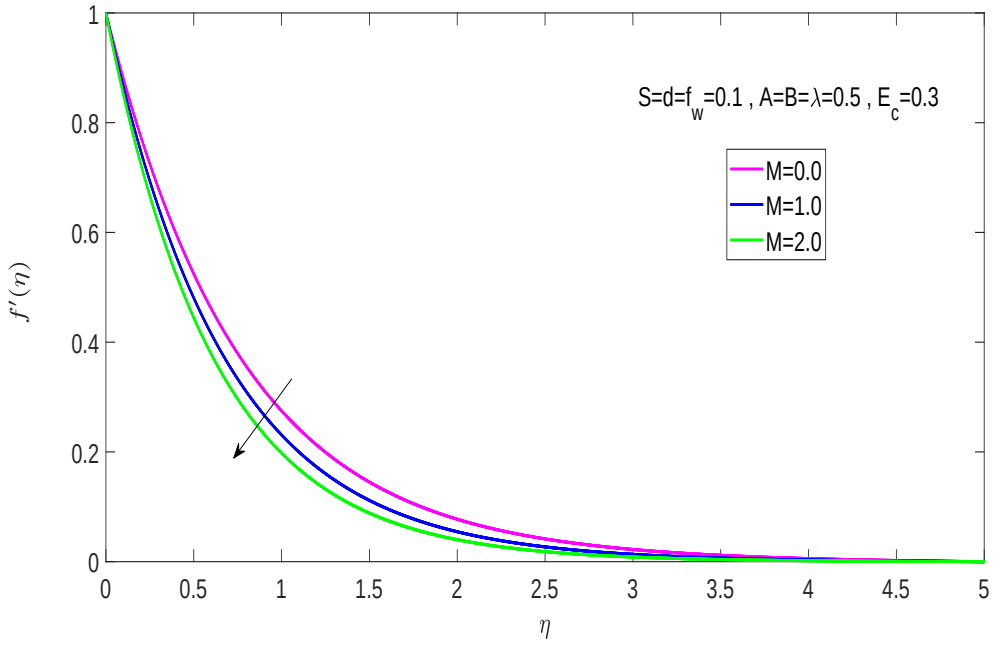

FIGURE 4.4: Effects of M on velocity distribution for Cu-water

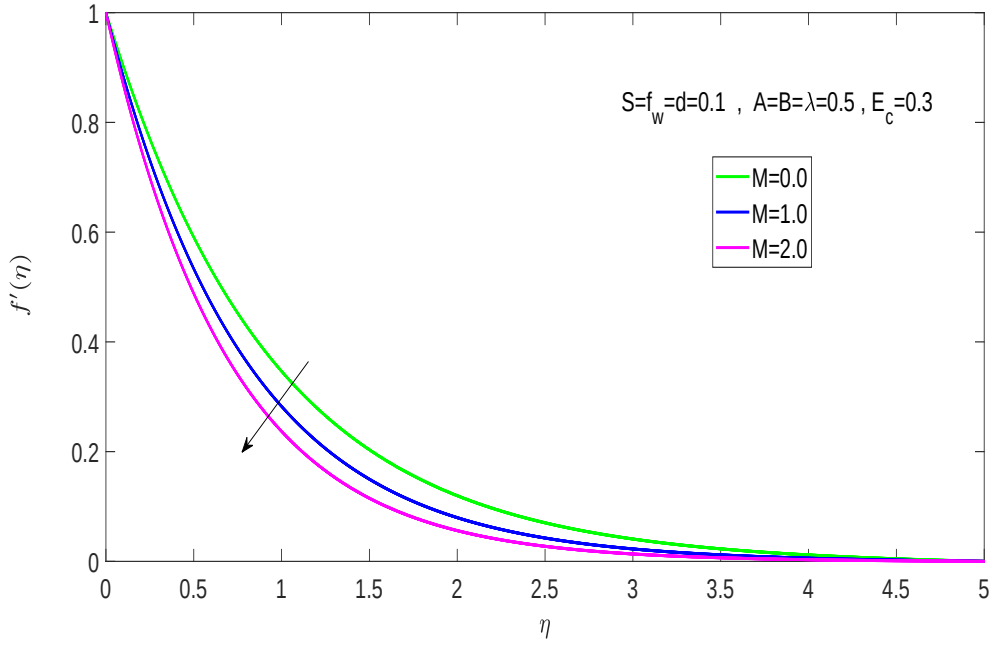

FIGURE 4.5: Effects of M on velocity profile for Al_2O_3-water

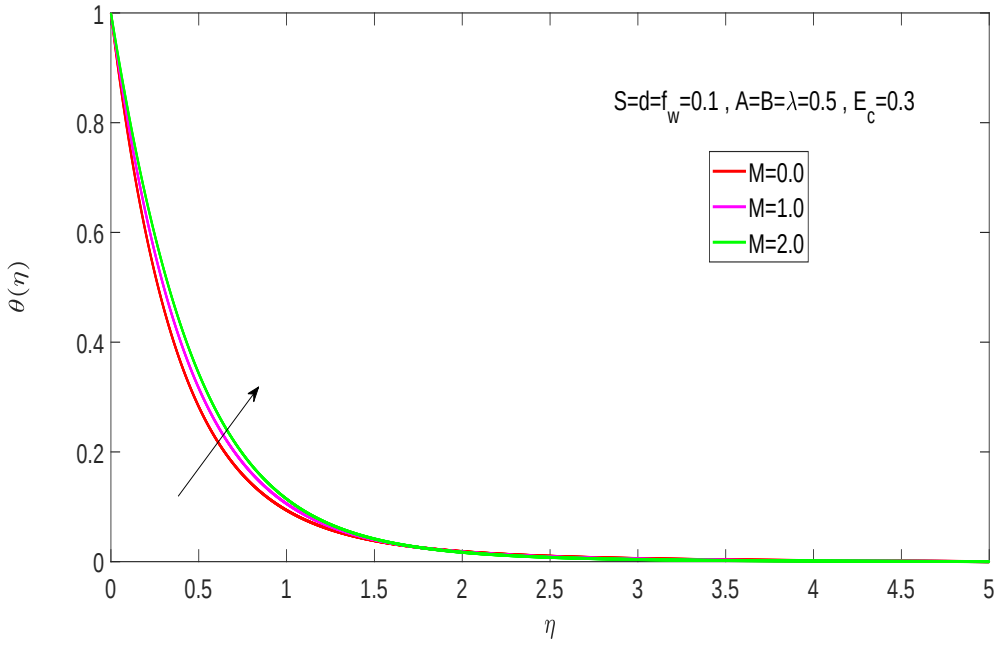

FIGURE 4.6: Effects of M on temperature profile for Cu-water

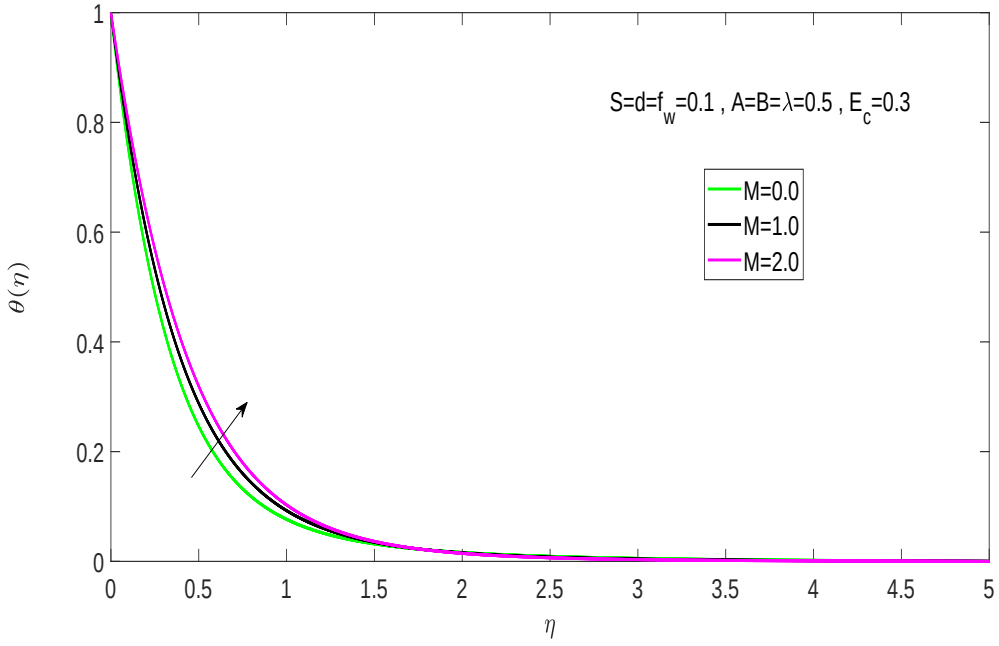

FIGURE 4.7: Effects of M on temperature distribution for Al_2O_3-water

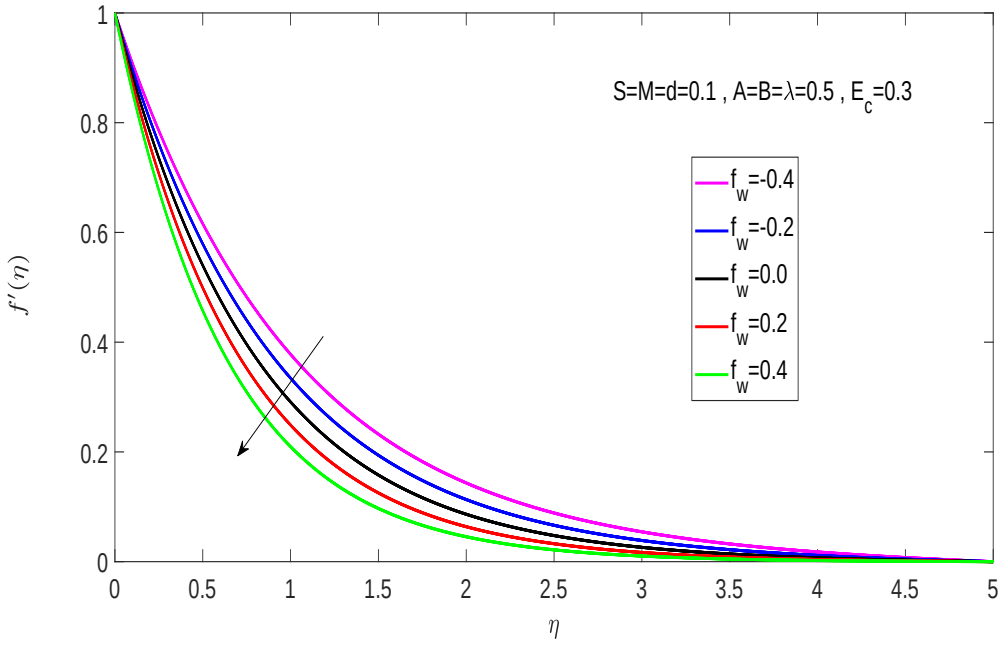

FIGURE 4.8: Effects of f_w on velocity profile for Cu-water

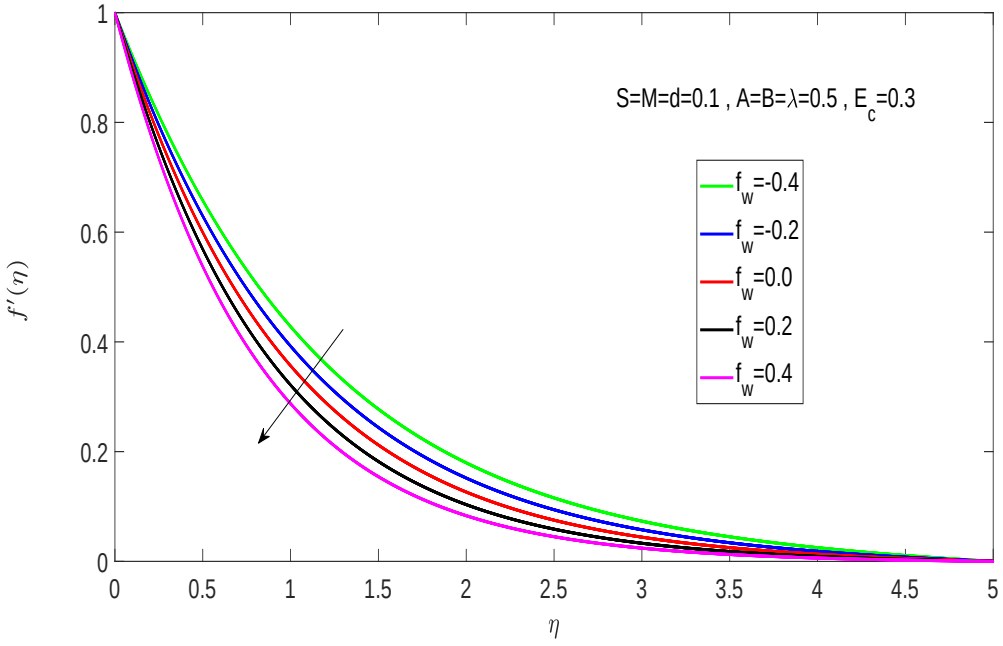

FIGURE 4.9: Effects of f_w on velocity distribution for Al_2O_3-water

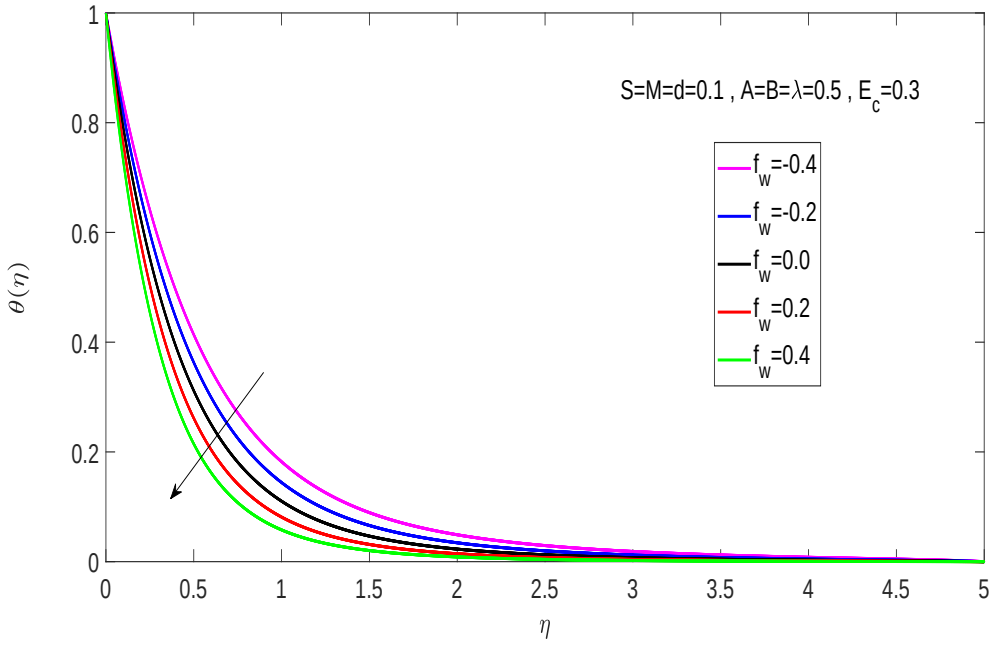

FIGURE 4.10: Effects of f_w on temperature distribution for Cu-water

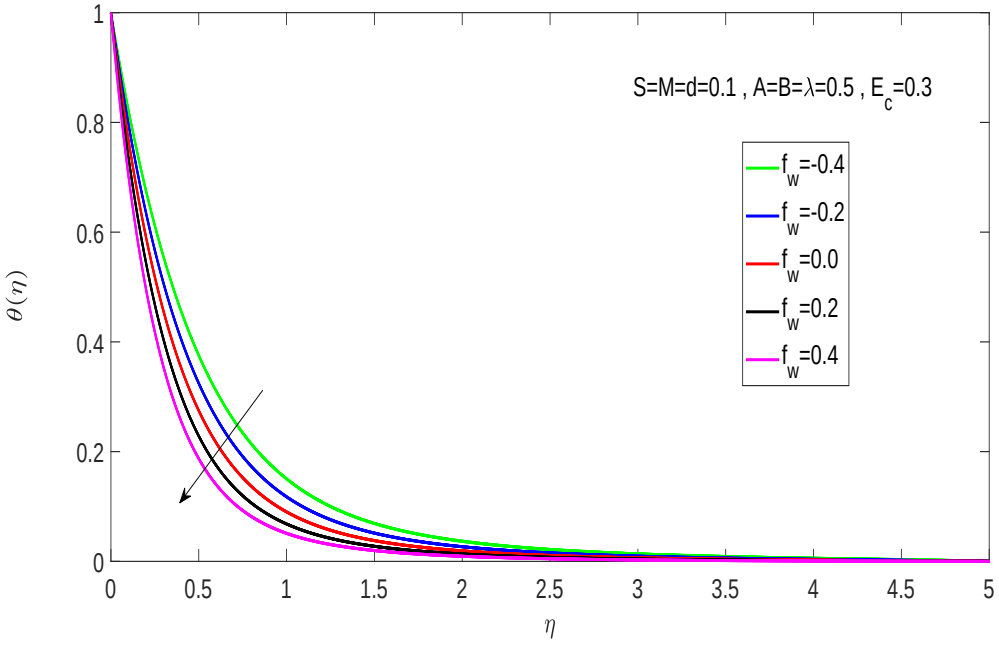

FIGURE 4.11: Effects of f_w on temperature distribution for Al_2O_3-water

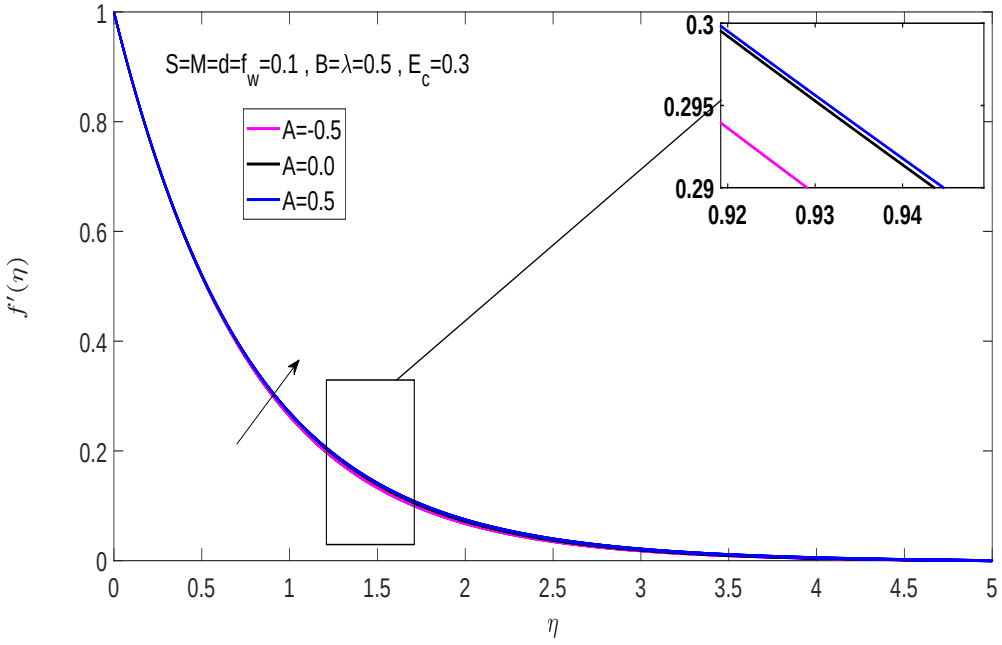

FIGURE 4.12: Effects of A on velocity distribution for Cu-water

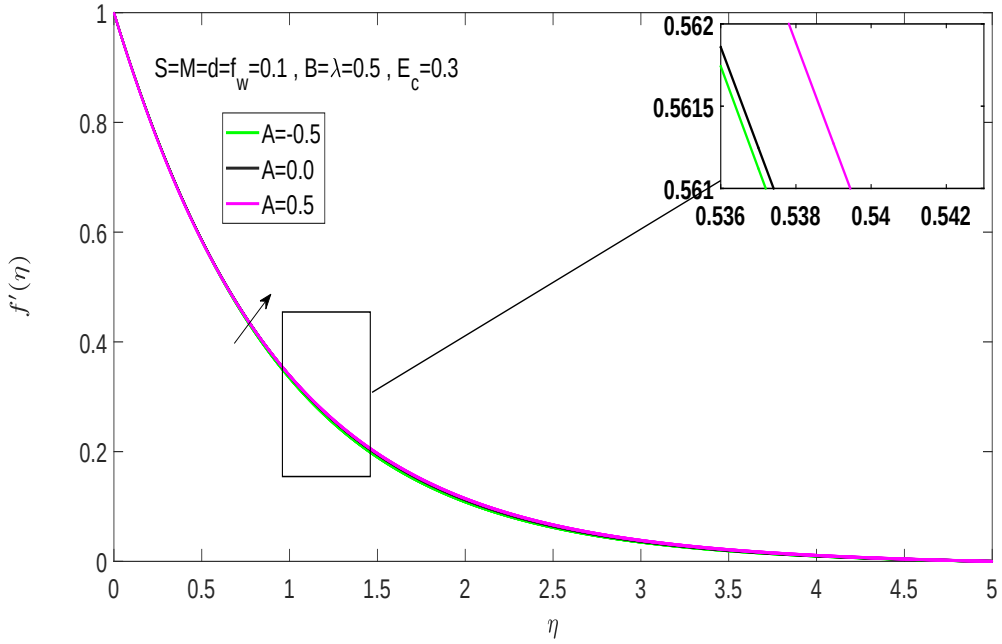

FIGURE 4.13: Effects of A on velocity distribution for Al_2O_3-water

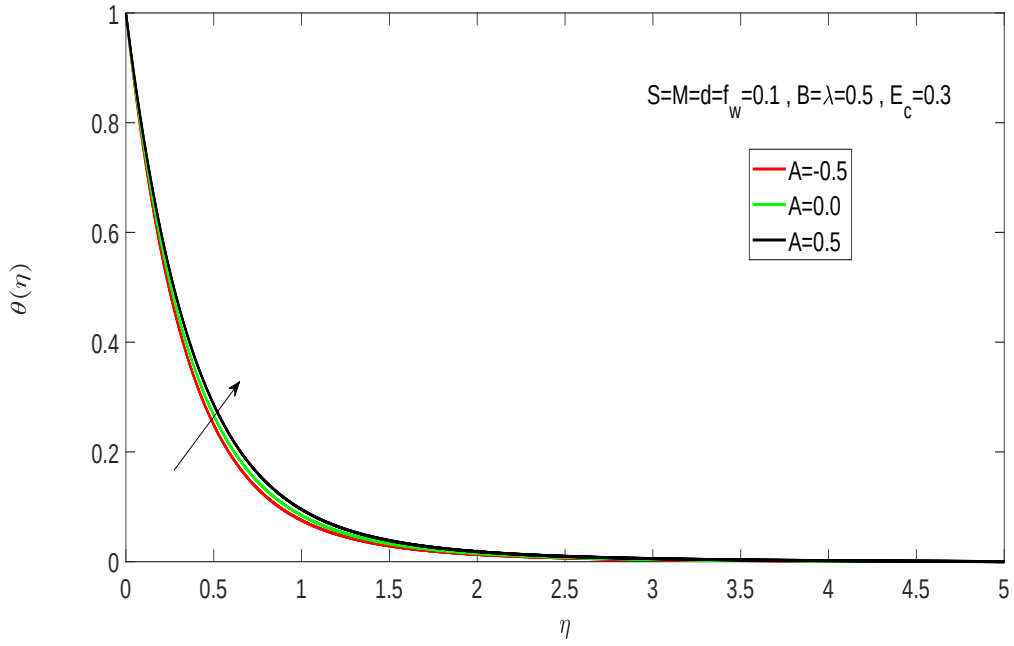

FIGURE 4.14: Effects of A on temperature distribution for Cu-water

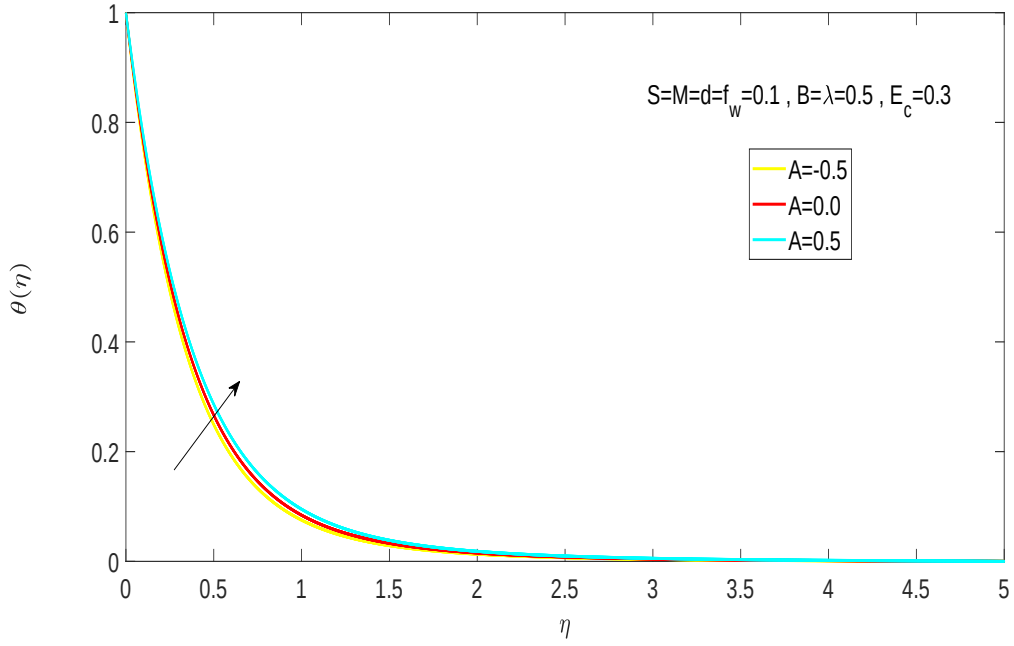

FIGURE 4.15: Effects of A on temperature distribution for Al_2O_3-water

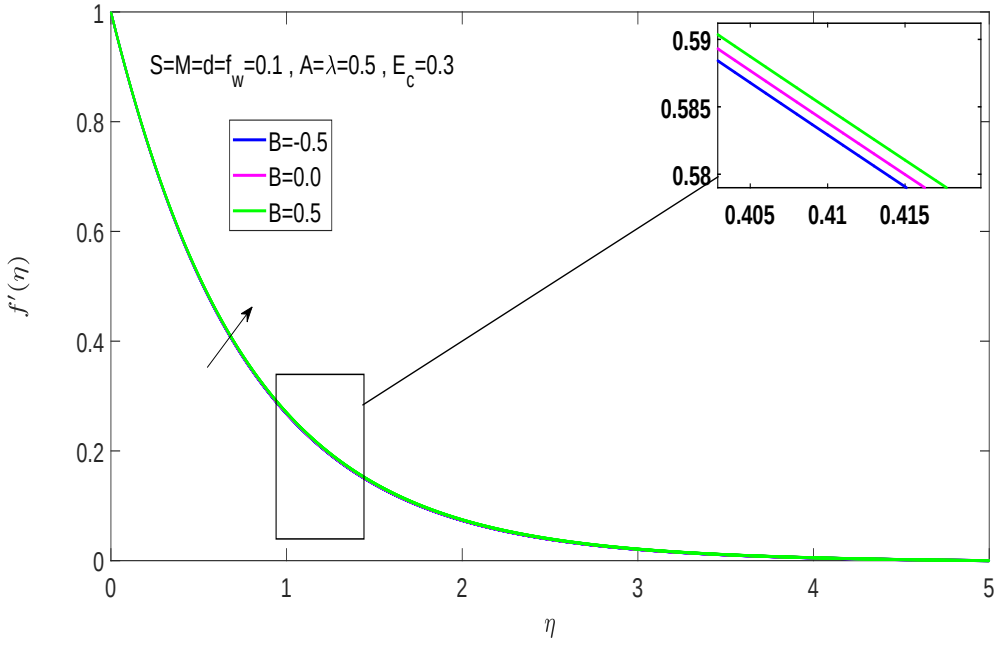

FIGURE 4.16: Effects of B on velocity distribution for Cu-water

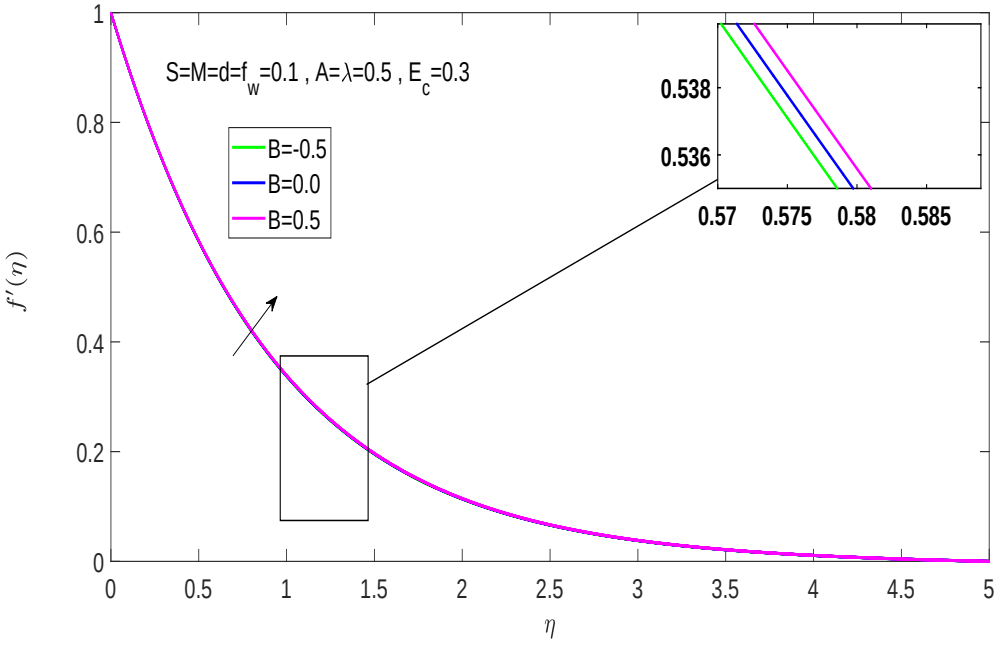

FIGURE 4.17: Effects of B on velocity distribution for Al_2O_3-water

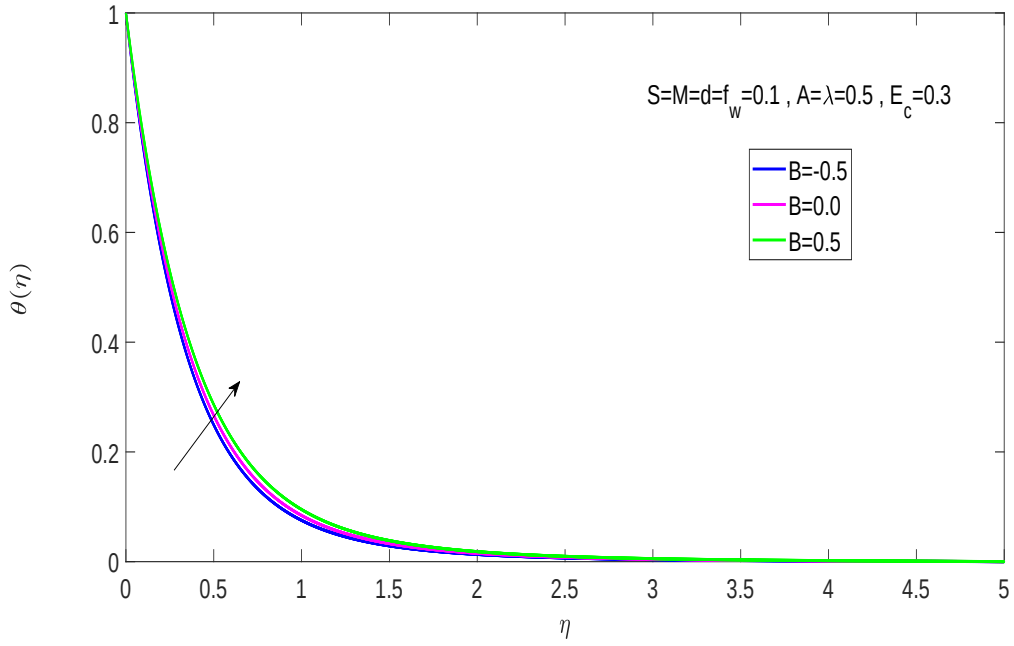

FIGURE 4.18: Effects of B on temperature distribution for Cu-water

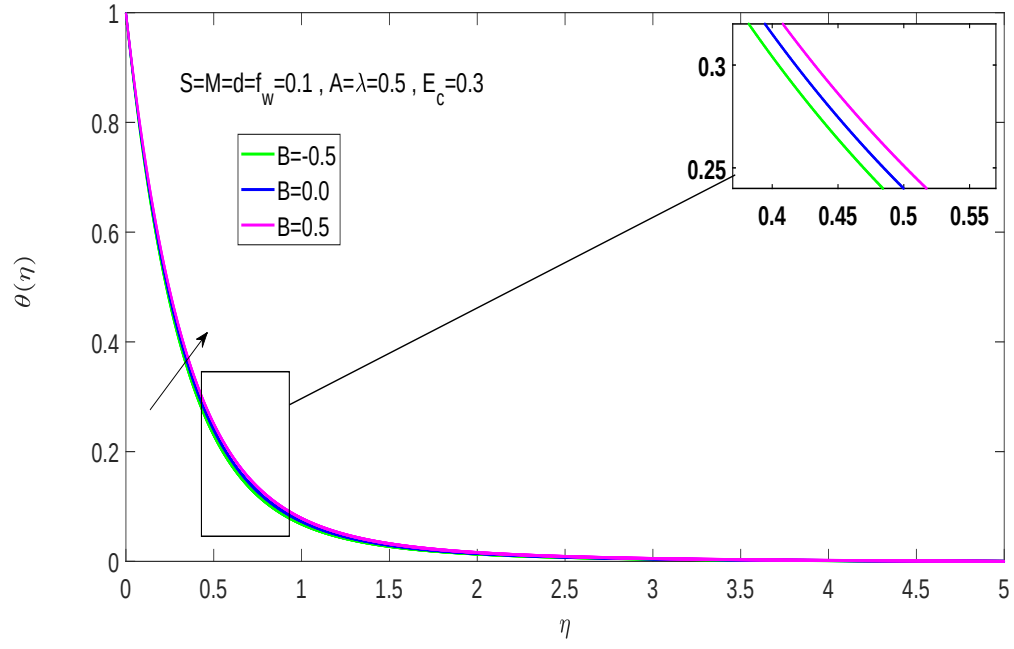

FIGURE 4.19: Effects of B on temperature distribution for Al_2O_3-water

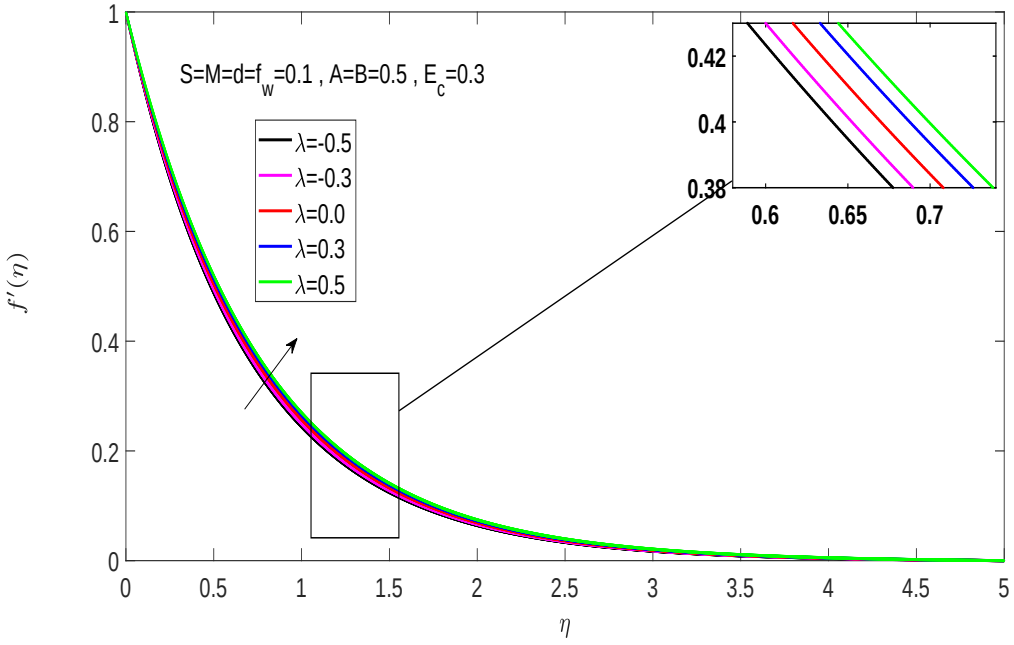

FIGURE 4.20: Effects of λ on velocity distribution for Cu-water

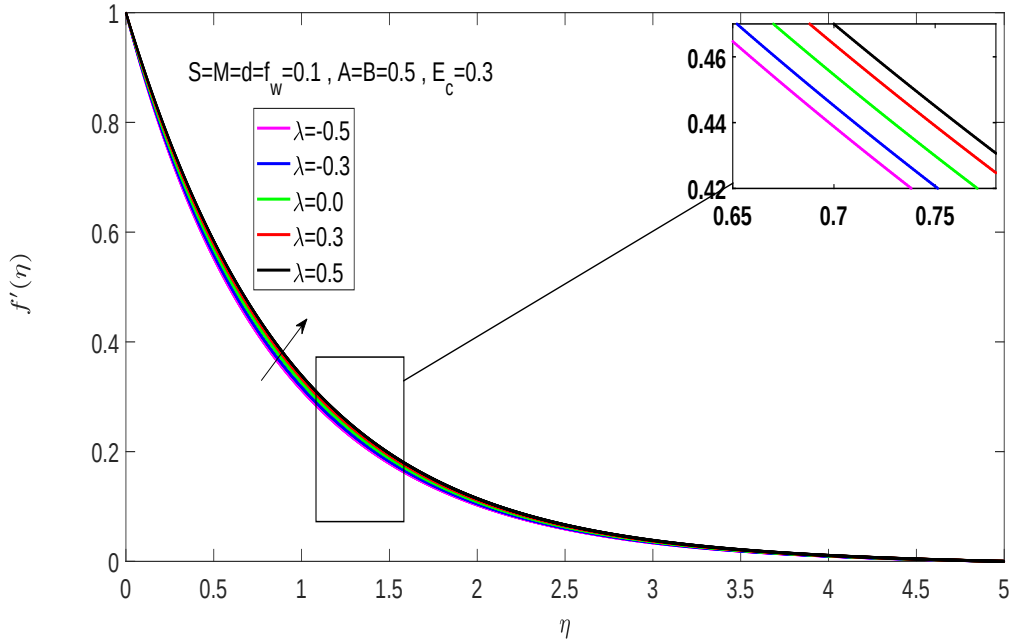

FIGURE 4.21: Effects of λ on velocity distribution for Al_2O_3-water

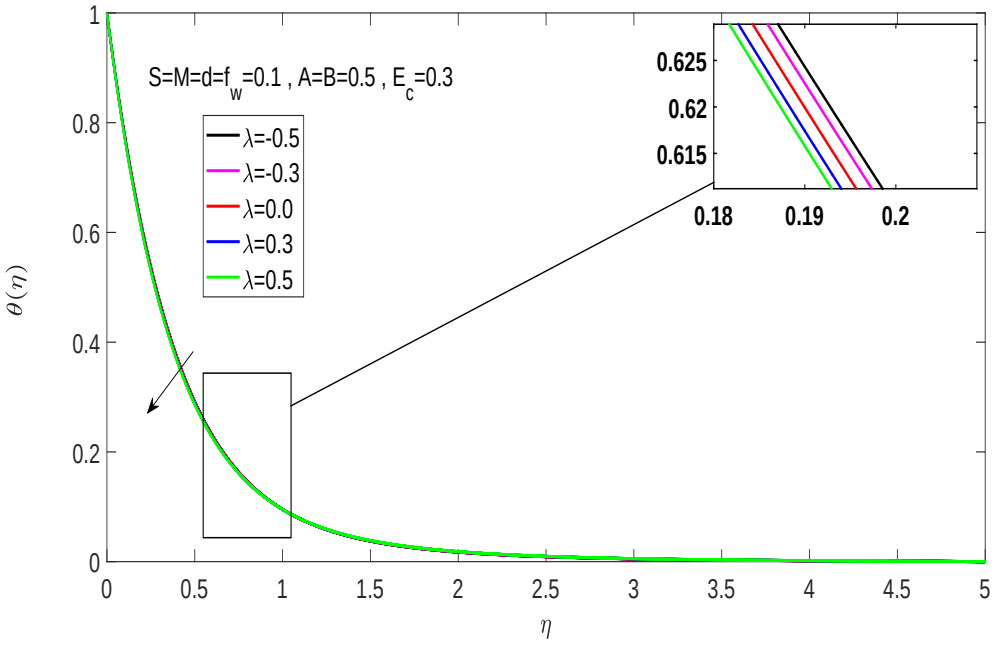

FIGURE 4.22: Effects of λ on temperature distribution for Cu-water

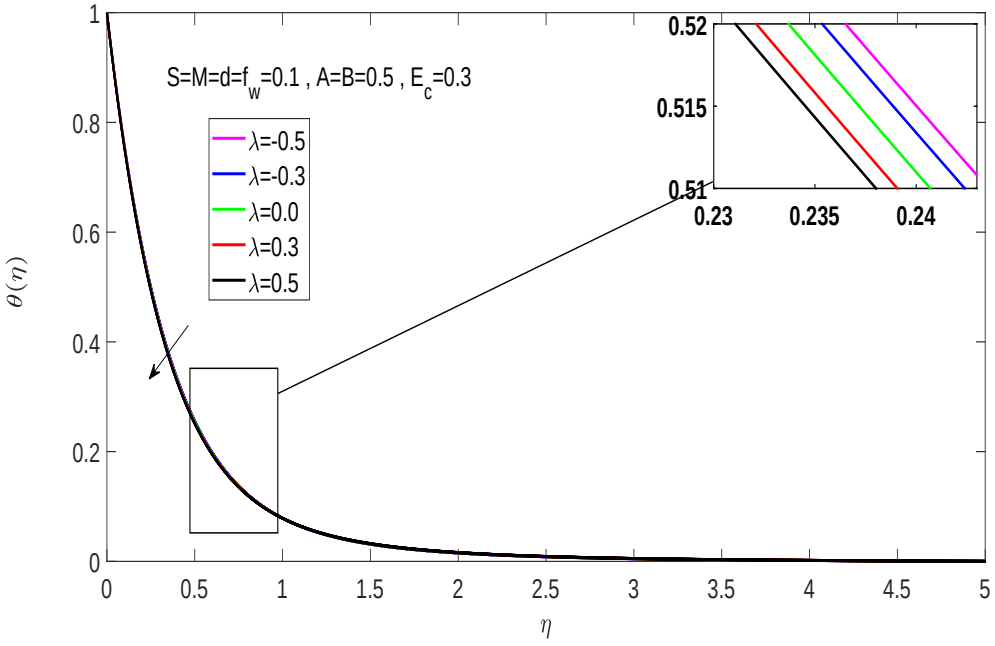

FIGURE 4.23: Effects of λ on temperature distribution for Al_2O_3-water

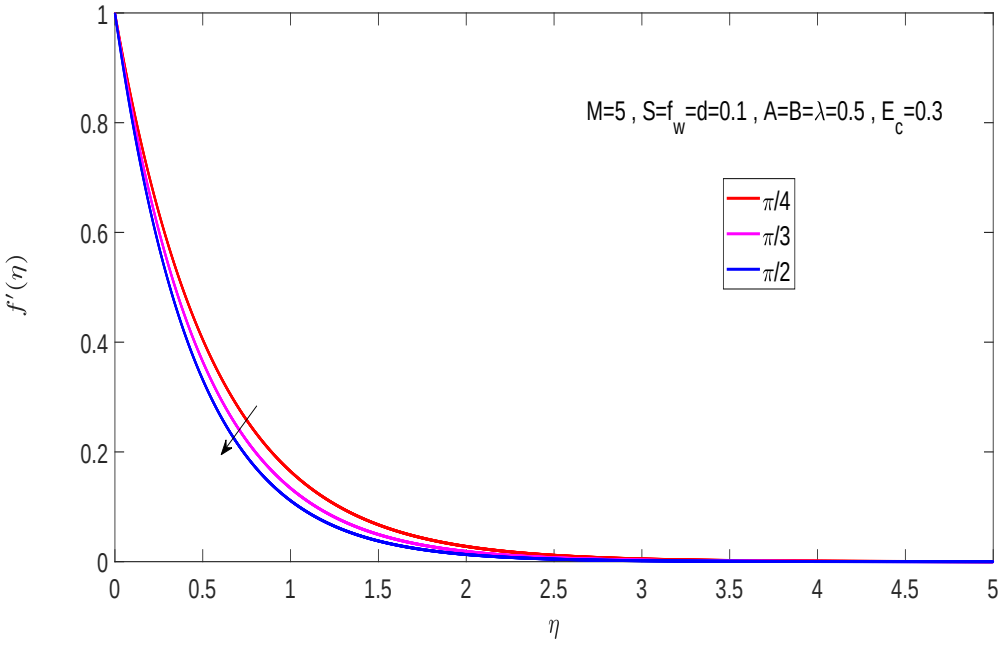

FIGURE 4.24: Effects of γ on velocity profile for Cu-water

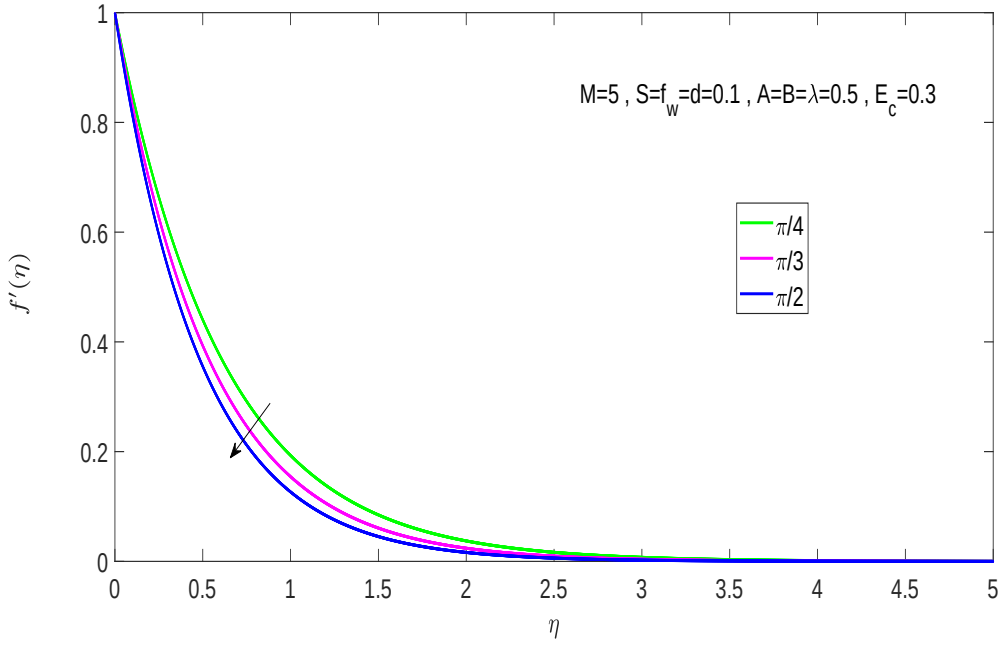

FIGURE 4.25: Effects of γ on velocity profile for Al_2O_3-water

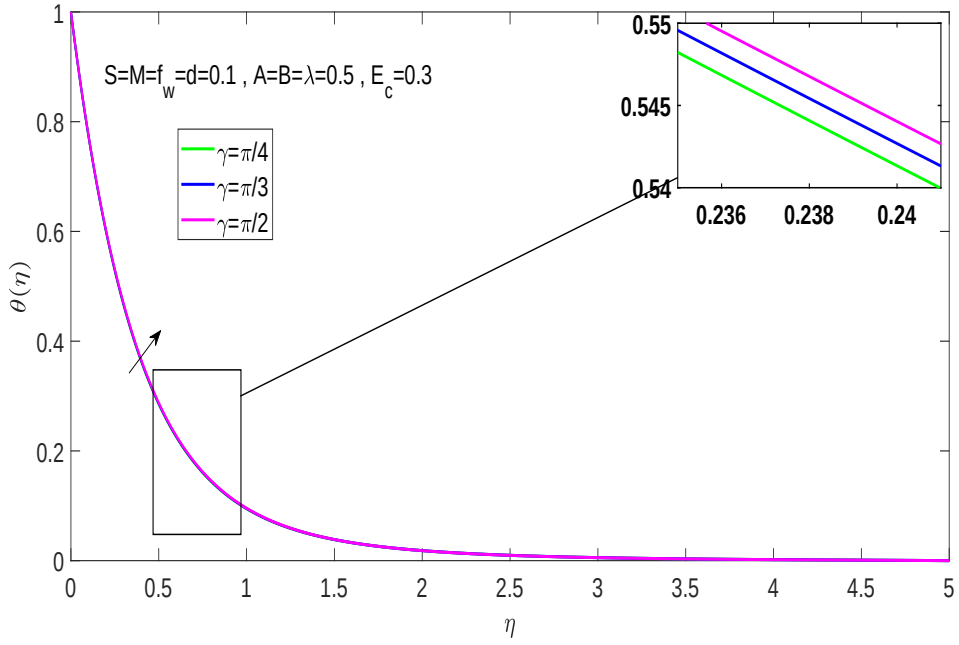

FIGURE 4.26: Effects of γ on temperature profile for Cu-water

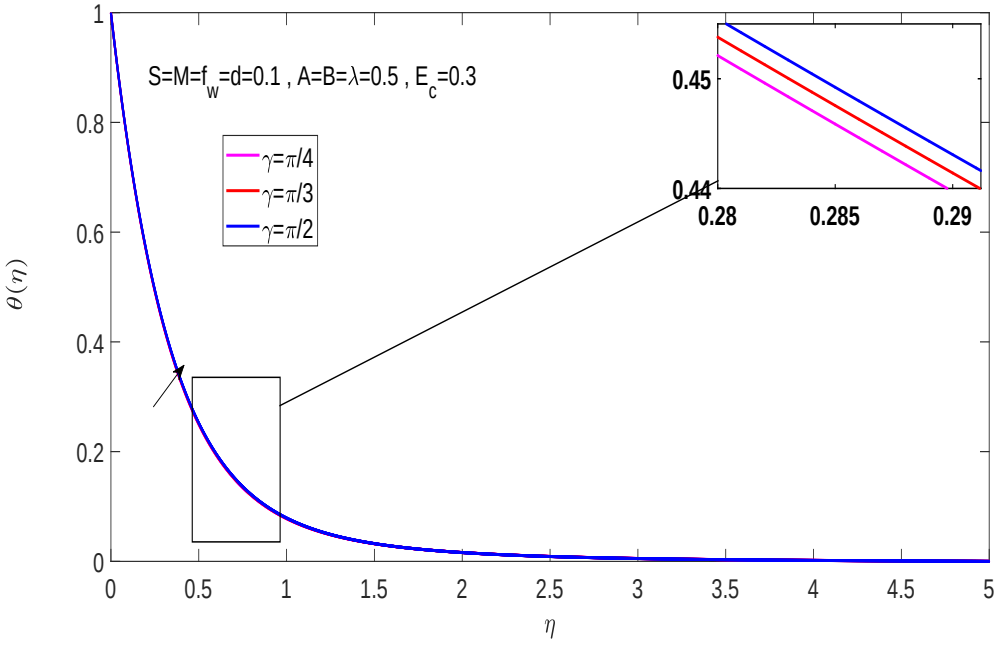

FIGURE 4.27: Effects of γ on temperature distribution for Al_2O_3-water

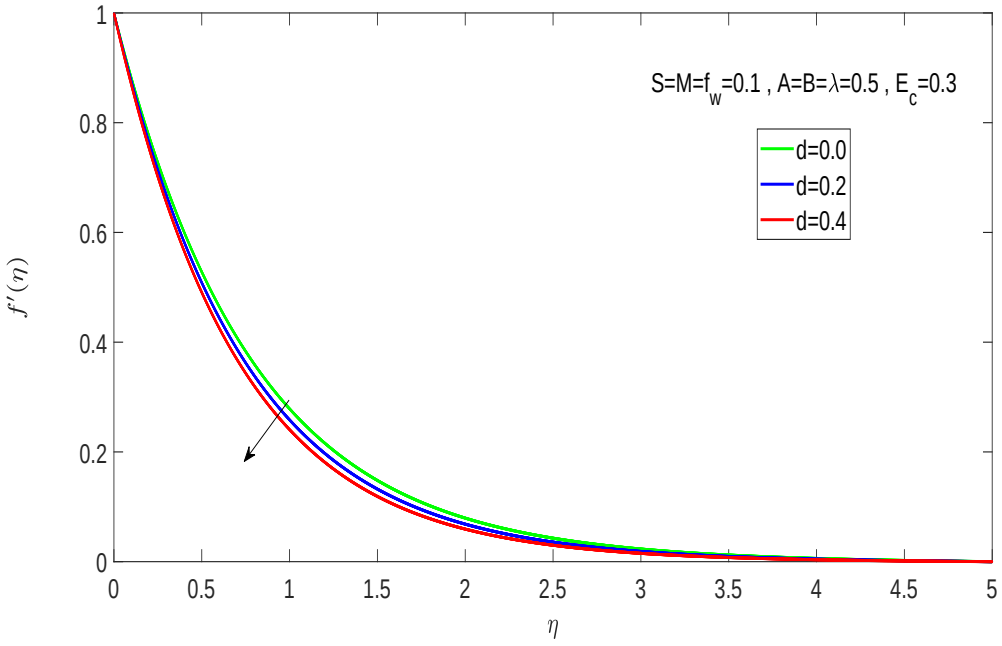

FIGURE 4.28: Effects of d on velocity distribution for Cu-water

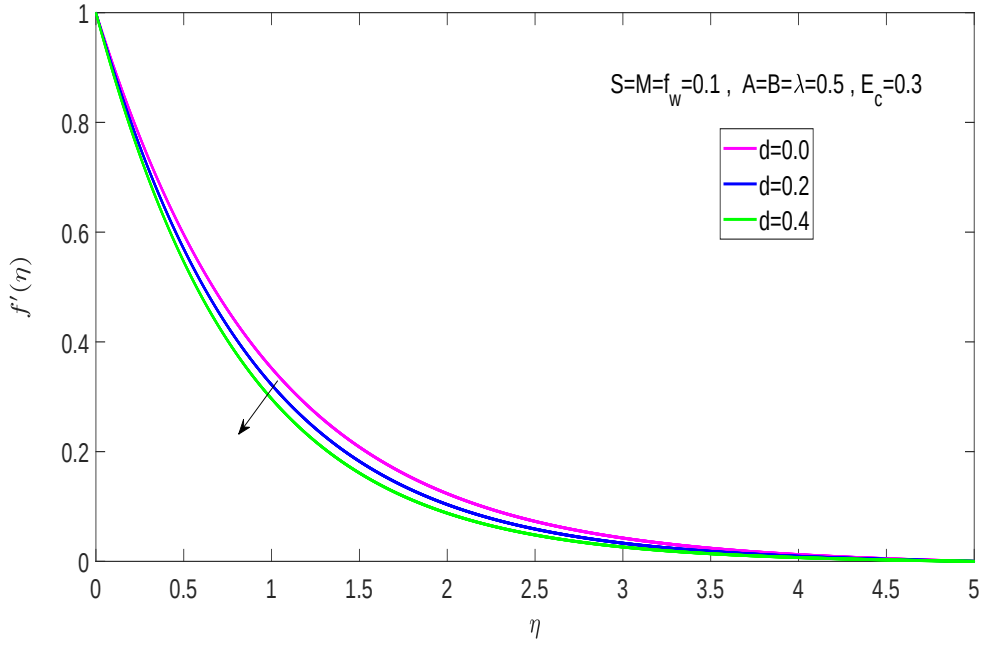

FIGURE 4.29: Effects of d on velocity distribution for Al_2O_3-water

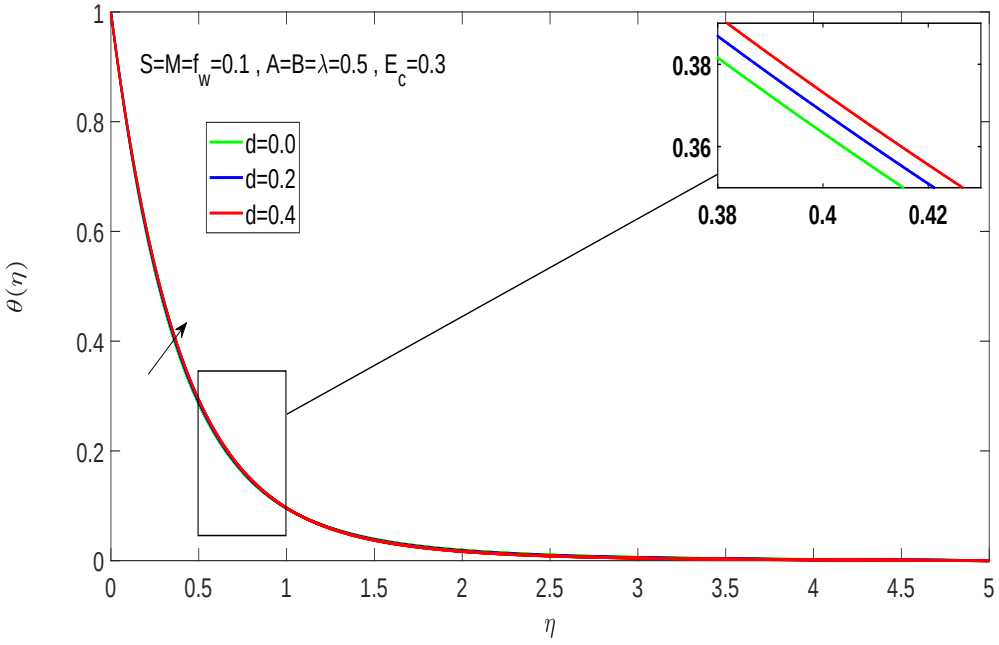

FIGURE 4.30: Effects of d on temperature distribution for Cu-water

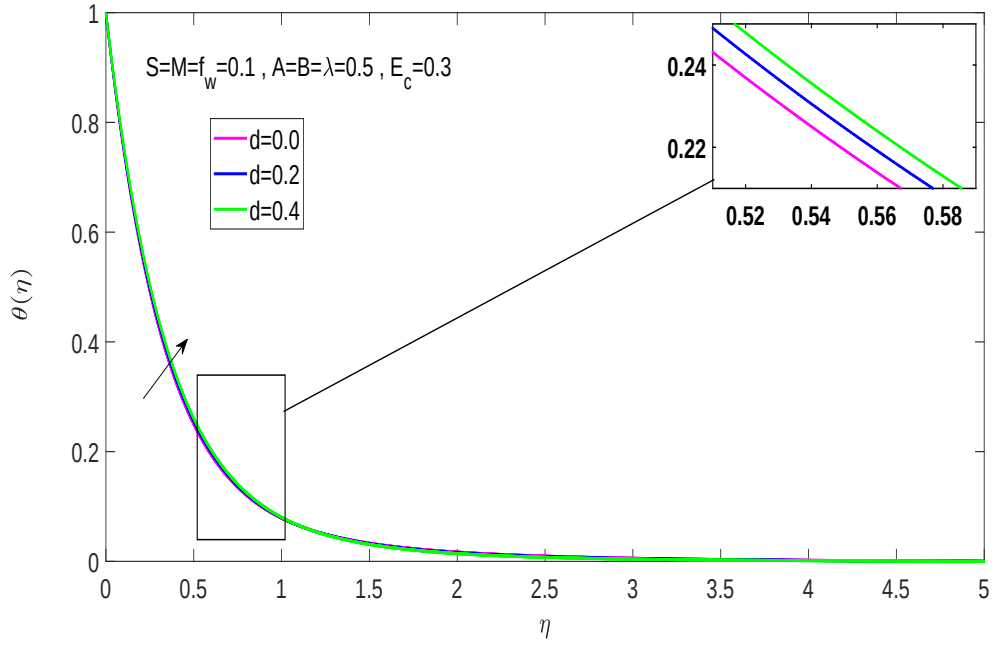

FIGURE 4.31: Effects of d on temperature distribution for Al_2O_3-water

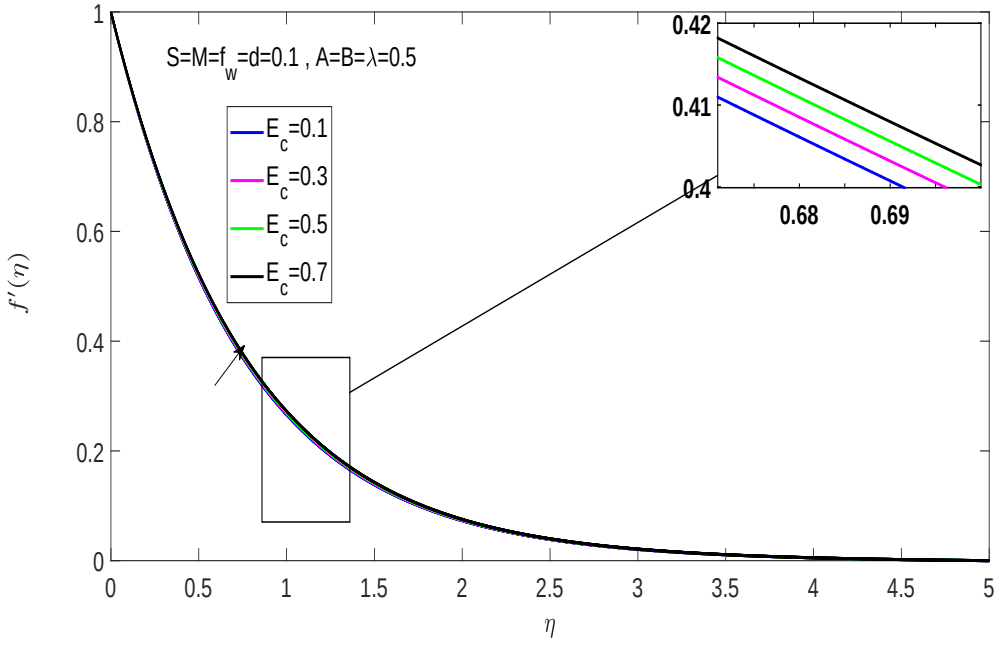

FIGURE 4.32: Effects of E_c on velocity profile for Cu-water

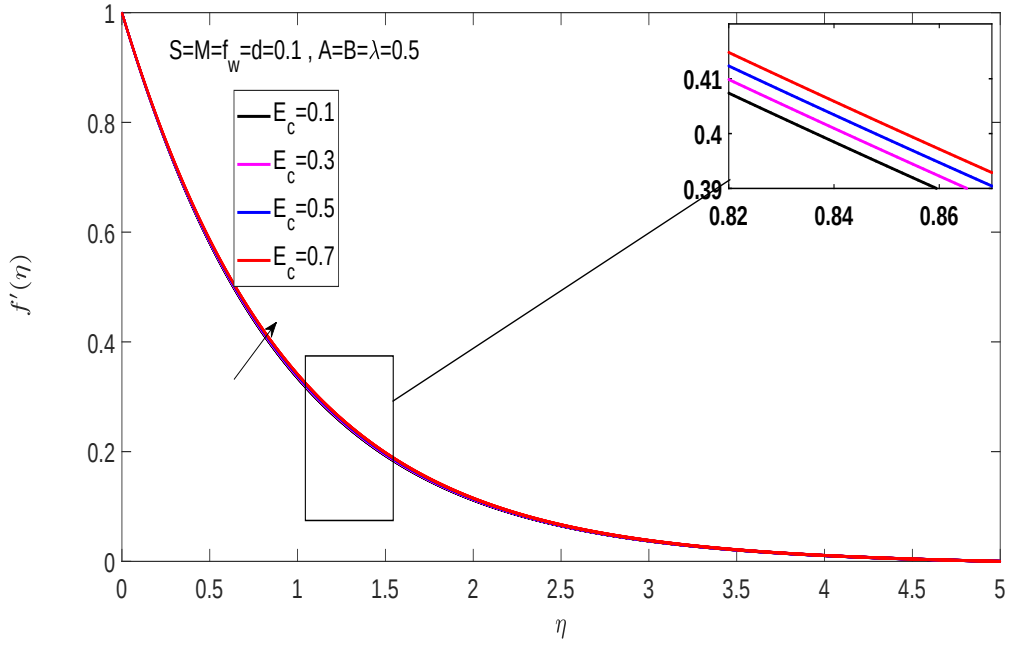

FIGURE 4.33: Effects of E_c on velocity profile for Al_2O_3-water

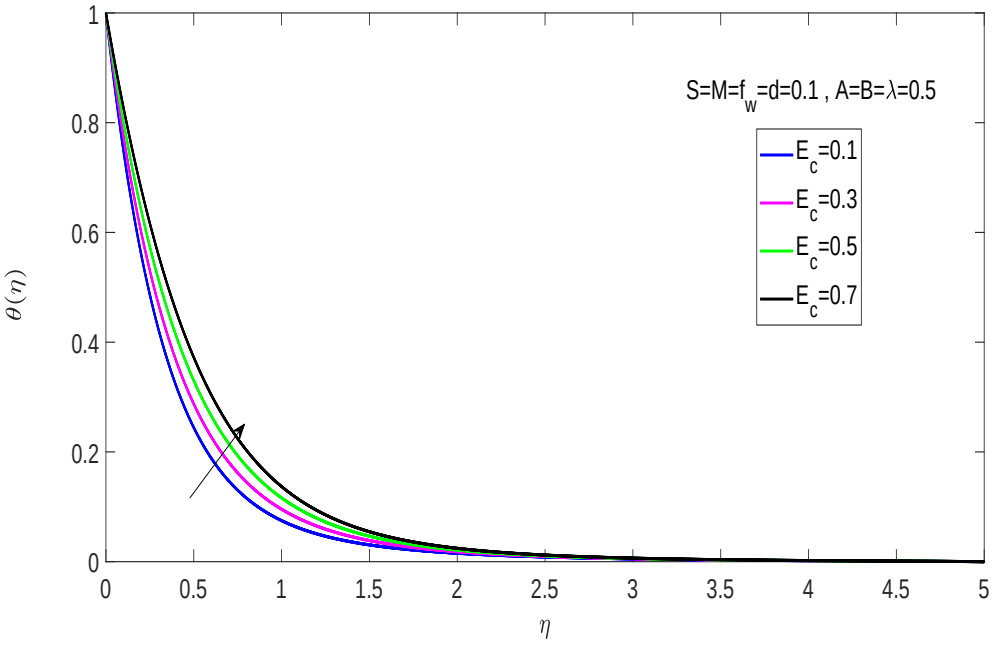

FIGURE 4.34: Effects of E_c on temperature distribution for Cu-water

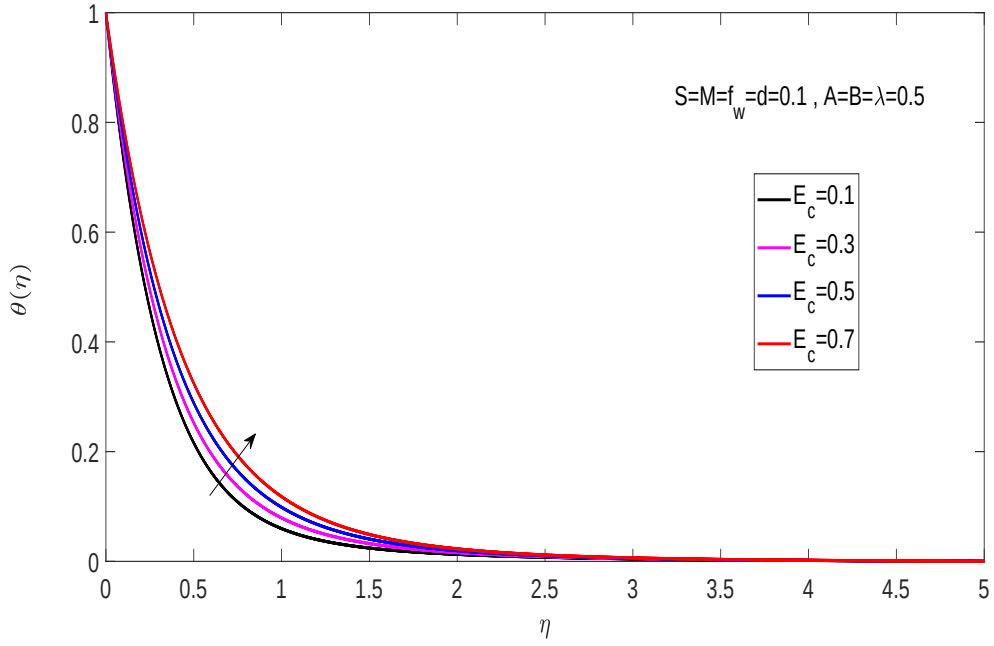

FIGURE 4.35: Effects of E_c on temperature distribution for Al_2O_3-water

Chapter 5

Conclusion

In this research work, we first analyzed the two-dimensional, unsteady stretching surface with non-uniform heat source/sink in the presence of inclined magnetic field. The set of continuity equation, momentum and energy equations are transformed into the dimensionless ODEs by an appropriate transformation. Numerical solutions are obtained by using the shooting technique. The influence of distinct physical parameters such as, Eckert number E_c, magnetic field parameter M, Prandtl number P_r, unsteadiness parameter S and buoyancy or convection parameter λ on the velocity profile and temperature profile are elaborated in the graphical and tabular form. Some interesting findings have been listed below:

The magnetic field is strengthened by the inclined angle, which also reduces the velocity profile of the flow and the local Nusselt number while improving the skin friction coefficient.

At $\gamma = \frac{\pi}{2}$ the magnetic field acts like a transverse magnetic field.

The velocity and temperature of various types of nanofluids alter, implying that nanofluids in the presence of a magnetic field and a heat source/sink are significant in the cooling and heating processes.

For all forms of nanofluids, the heat transfer rate increases with the heat sink $A < 0$and $B < 0$, but the opposite is true with the heat source $A > 0$ and $B > 0$.

For both pure fluid and nanofluids, increasing the suction parameter $f_w > 0$ increases the skin friction coefficient and local Nusselt number, whereas increasing

the injection parameter $f_w < 0$ has the reverse effect.

In both pure fluid and nanofluids, increasing the unsteadiness parameter S increases the skin friction coefficient and the local Nusselt number.

The skin friction coefficient decreases as the convection parameter λ is increased, whereas the local Nusselt number has the reverse effect in both pure fluid and nanofluid scenarios.

Bibliography

[1] B. Sakiadis, "Boundary-layer behavior on continuous solid surfaces: Ii. the boundary layer on a continuous flat surface," *AiChE journal*, vol. 7, no. 2, pp. 221–225, 1961.

[2] L. Erickson, L. Fan, and V. Fox, "Heat and mass transfer on moving continuous flat plate with suction or injection," *Industrial & Engineering Chemistry Fundamentals*, vol. 5, no. 1, pp. 19–25, 1966.

[3] F. Tsou, E. M. Sparrow, and R. J. Goldstein, "Flow and heat transfer in the boundary layer on a continuous moving surface," *International Journal of Heat and Mass Transfer*, vol. 10, no. 2, pp. 219–235, 1967.

[4] L. J. Crane, "Flow past a stretching plate," *Zeitschrift für angewandte Mathematik und Physik ZAMP*, vol. 21, no. 4, pp. 645–647, 1970.

[5] T. Hayat, S. Saif, and Z. Abbas, "The influence of heat transfer in an MHD second grade fluid film over an unsteady stretching sheet," *Physics letters A*, vol. 372, no. 30, pp. 5037–5045.

[6] K. Prasad and K. Vajravelu, "Heat transfer in the MHD flow of a power law fluid over a non-isothermal stretching sheet," *International Journal of Heat and Mass Transfer*, vol. 52, no. 21-22, pp. 4956–4965, 2009.

[7] V. Kumaran, A. V. Kumar, and I. Pop, "Transition of MHD boundary layer flow past a stretching sheet," *Communications in Nonlinear Science and Numerical Simulation*, vol. 15, no. 2, pp. 300–311, 2010.

[8] S. Mukhopadhyay, "Heat transfer analysis for unsteady MHD flow past a non-isothermal stretching surface," *Nuclear engineering and design*, vol. 241, no. 12, pp. 4835–4839, 2011.

[9] C. W. W. Ostwald, *An Introduction to Theoretical and Applied Colloid Chemistry," the World of Neglected Dimensions,"*. John Wiley & Sons, Incorporated, 1922.

[10] J. A. Eastman, S. Choi, S. Li, W. Yu, and L. Thompson, "Anomalously increased effective thermal conductivities of ethylene glycol-based nanofluids containing copper nanoparticles," *Applied physics letters*, vol. 78, no. 6, pp. 718–720, 2001.

[11] M.-S. Liu, M. C.-C. Lin, C. Tsai, and C.-C. Wang, "Enhancement of thermal conductivity with cu for nanofluids using chemical reduction method," *International Journal of Heat and Mass Transfer*, vol. 49, no. 17-18, pp. 3028–3033, 2006.

[12] J. Garg, B. Poudel, M. Chiesa, J. Gordon, J. Ma, J. Wang, Z. Ren, Y. T. Kang, H. Ohtani, J. Nanda *et al.*, "Enhanced thermal conductivity and viscosity of copper nanoparticles in ethylene glycol nanofluid," *Journal of Applied Physics*, vol. 103, no. 7, p. 074301, 2008.

[13] S. U. Choi and J. A. Eastman, "Enhancing thermal conductivity of fluids with nanoparticles," Argonne National Lab., IL (United States), Tech. Rep., 1995.

[14] S. Choi, Z. G. Zhang, W. Yu, F. Lockwood, and E. Grulke, "Anomalous thermal conductivity enhancement in nanotube suspensions," *Applied physics letters*, vol. 79, no. 14, pp. 2252–2254, 2001.

[15] W. Yu, D. M. France, J. L. Routbort, and S. U. Choi, "Review and comparison of nanofluid thermal conductivity and heat transfer enhancements," *Heat transfer engineering*, vol. 29, no. 5, pp. 432–460, 2008.

[16] S. Kakaç and A. Pramuanjaroenkij, "Review of convective heat transfer enhancement with nanofluids," *International journal of heat and mass transfer*, vol. 52, no. 13-14, pp. 3187–3196, 2009.

[17] L. Godson, B. Raja, D. M. Lal, and S. e. a. Wongwises, "Enhancement of heat transfer using nanofluids an overview," *Renewable and sustainable energy reviews*, vol. 14, no. 2, pp. 629–641, 2010.

[18] S. Z. Heris, S. G. Etemad, and M. N. Esfahany, "Experimental investigation of oxide nanofluids laminar flow convective heat transfer," *International communications in heat and mass transfer*, vol. 33, no. 4, pp. 529–535, 2006.

[19] H. A. Mintsa, G. Roy, C. T. Nguyen, and D. Doucet, "New temperature dependent thermal conductivity data for water-based nanofluids," *International journal of thermal sciences*, vol. 48, no. 2, pp. 363–371, 2009.

[20] Y. S. Daniel, Z. A. Aziz, Z. Ismail, and F. Salah, "Double stratification effects on unsteady electrical MHD mixed convection flow of nanofluid with viscous dissipation and joule heating," *Journal of applied research and technology*, vol. 15, no. 5, pp. 464–476, 2017.

[21] P. S. Reddy, A. J. Chamkha, and A. Al-Mudhaf, "MHD heat and mass transfer flow of a nanofluid over an inclined vertical porous plate with radiation and heat generation/absorption," *Advanced Powder Technology*, vol. 28, no. 3, pp. 1008–1017, 2017.

[22] B. Prabhavathi, P. S. Reddy, R. B. Vijaya, A. Chamkha *et al.*, "MHD boundary layer heat and mass transfer flow over a vertical cone embedded in porous media filled with al2o3-water and cu-water nanofluid," *Journal of Nanofluids*, vol. 6, no. 5, pp. 883–891, 2017.

[23] P. Sreedevi, P. S. Reddy, K. Rao, and A. J. Chamkha, "Heat and mass transfer flow over a vertical cone through nanofluid saturated porous medium under convective boundary condition suction/injection," *Journal of Nanofluids*, vol. 6, no. 3, pp. 478–486, 2017.

[24] T. Hayat, M. I. Khan, M. Waqas, A. Alsaedi, and M. Farooq, "Numerical simulation for melting heat transfer and radiation effects in stagnation point flow of carbon–water nanofluid," *Computer methods in applied mechanics and engineering*, vol. 315, pp. 1011–1024, 2017.

[25] M. Madhu, N. Kishan, and A. J. Chamkha, "Unsteady flow of a maxwell nanofluid over a stretching surface in the presence of magnetohydrodynamic and thermal radiation effects," *Propulsion and Power research*, vol. 6, no. 1, pp. 31–40, 2017.

[26] T. Hayat, T. Muhammad, S. A. Shehzad, and A. Alsaedi, "An analytical solution for magnetohydrodynamic oldroyd-b nanofluid flow induced by a stretching sheet with heat generation/absorption," *International Journal of Thermal Sciences*, vol. 111, pp. 274–288, 2017.

[27] K.-L. Hsiao, "Micropolar nanofluid flow with MHD and viscous dissipation effects towards a stretching sheet with multimedia feature," *International Journal of Heat and Mass Transfer*, vol. 112, pp. 983–990, 2017.

[28] N. Eldabe and M. Abou-Zeid, "Homotopy perturbation method for MHD pulsatile non-newtonian nanofluid flow with heat transfer through a non-darcy porous medium," *Journal of the Egyptian Mathematical Society*, vol. 25, no. 4, pp. 375–381, 2017.

[29] P. S. Reddy, P. Sreedevi, and A. J. Chamkha, "Heat and mass transfer analysis of nanofluid flow over swirling cylinder with cattaneo–christov heat flux," *Journal of Thermal Analysis and Calorimetry*, pp. 1–16, 2021.

[30] P. Sreedevi, P. S. Reddy, and A. J. Chamkha, "Magneto-hydrodynamics heat and mass transfer analysis of single and multi-wall carbon nanotubes over vertical cone with convective boundary condition," *International journal of Mechanical sciences*, vol. 135, pp. 646–655, 2018.

[31] K. Jyothi, P. S. Reddy, and M. S. Reddy, "Influence of magnetic field and thermal radiation on convective flow of swcnts-water and mwcnts-water nanofluid between rotating stretchable disks with convective boundary conditions," *Powder Technology*, vol. 331, pp. 326–337, 2018.

[32] A. Zeeshan, N. Shehzad, and R. Ellahi, "Analysis of activation energy in couette-poiseuille flow of nanofluid in the presence of chemical reaction and convective boundary conditions," *Results in Physics*, vol. 8, pp. 502–512, 2018.

[33] R. K. Tiwari and M. K. Das, "Heat transfer augmentation in a two-sided lid-driven differentially heated square cavity utilizing nanofluids," *International Journal of heat and Mass transfer*, vol. 50, no. 9-10, pp. 2002–2018, 2007.

[34] E. Abu-Nada, "Application of nanofluids for heat transfer enhancement of separated flows encountered in a backward facing step," *International Journal of Heat and Fluid Flow*, vol. 29, no. 1, pp. 242–249, 2008.

[35] H. F. Oztop and E. Abu-Nada, "Numerical study of natural convection in partially heated rectangular enclosures filled with nanofluids," *International journal of heat and fluid flow*, vol. 29, no. 5, pp. 1326–1336, 2008.

[36] F. Hady, F. Ibrahim, S. Abdel-Gaied, and M. Eid, "Effect of heat generation/absorption on natural convective boundary-layer flow from a vertical cone embedded in a porous medium filled with a non-newtonian nanofluid," *International Communications in Heat and Mass Transfer*, vol. 38, no. 10, pp. 1414–1420, 2011.

[37] A. Ishak, R. Nazar, and I. Pop, "Heat transfer over an unsteady stretching permeable surface with prescribed wall temperature," *Nonlinear Analysis: Real World Applications*, vol. 10, no. 5, pp. 2909–2913, 2009.

[38] L. Grubka and K. Bobba, "Heat transfer characteristics of a continuous, stretching surface with variable temperature," 1985.

[39] M. E. Ali, "Heat transfer characteristics of a continuous stretching surface," *Wärme-und Stoffübertragung*, vol. 29, no. 4, pp. 227–234, 1994.

[40] N. Elgazery, "Nanofluids flow over a permeable unsteady stretching surface with non-uniform heat source/sink in the presence of inclined magnetic field," *Journal of the Egyptian Mathematical Society*, vol. 27, no. 1, pp. 1–26, 2019.

[41] F. M. White and I. Corfield, *Viscous fluid flow*. McGraw-Hill New York, 2006, vol. 3.

[42] W. M. Rohsenow, J. P. Hartnett, Y. I. Cho *et al.*, *Handbook of heat transfer*. McGraw-Hill New York, 1998, vol. 3.

[43] F. M. White, "Fluid mechanics, mcgraw-hill," *New York*, 1994.

[44] J. Kunes, *Dimensionless physical quantities in science and engineering.* Elsevier, 2012.

[45] J. N. Reddy and D. K. Gartling, *The finite element method in heat transfer and fluid dynamics.* CRC press, 2010.

[46] W. Rohsenow, J. Hartnett, and T. Cho, "Handbook of heat transfer mcgraw hill," *New York*, 1973.

[47] C. Raju, N. Sandeep, C. Sulochana, V. Sugunamma, and M. J. Babu, "Radiation, inclined magnetic field and cross-diffusion effects on flow over a stretching surface," *Journal of the Nigerian Mathematical Society*, vol. 34, no. 2, pp. 169–180, 2015.

[48] A. Ishak, R. Nazar, and I. Pop, "Boundary layer flow and heat transfer over an unsteady stretching vertical surface," *Meccanica*, vol. 44, no. 4, pp. 369–375, 2009.

[49] M. A. Mahmoud and A. M. Megahed, "Non-uniform heat generation effect on heat transfer of a non-newtonian power-law fluid over a non-linearly stretching sheet," *Meccanica*, vol. 47, no. 5, pp. 1131–1139, 2012.

[50] H. C. Brinkman, "The viscosity of concentrated suspensions and solutions," *The Journal of chemical physics*, vol. 20, no. 4, pp. 571–571, 1952.